The Radio Science Bulletin

ISSN 1024-4530

INTERNATIONAL
UNION OF
RADIO SCIENCE

UNION
RADIO-SCIENTIFIQUE
INTERNATIONALE

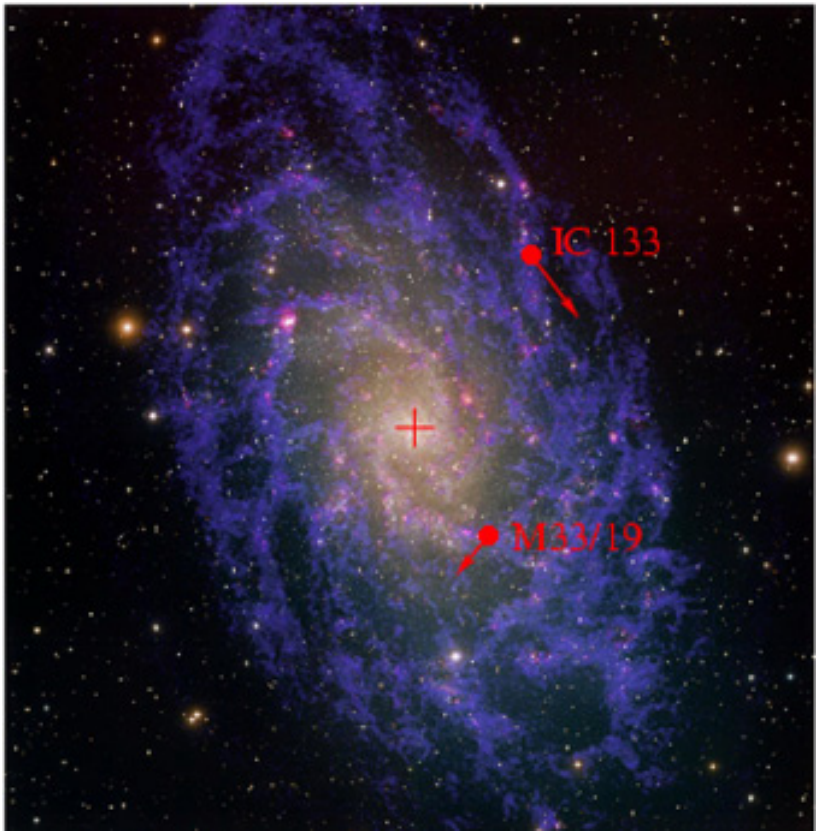

No 318
September 2006

Publié avec l'aide financière de l'ICSU
URSI, c/o Ghent University (INTEC)
St.-Pietersnieuwstraat 41, B-9000 Gent (Belgium)

Contents

Front cover: The relative motion of two maser sources in M33. See the paper by Fomalont and Kobayashi on pp. 13-29.

For information, please contact :
The URSI Secretariat
c/o Ghent University (INTEC)
Sint-Pietersnieuwstraat 41, B-9000 Gent, Belgium
Tel.: (32) 9-264 33 20, Fax: (32) 9-264 42 88
E-mail: info@ursi.org
http://www.ursi.org

Editorial

We have two *Reviews of Radio Science* in this issue, and two papers based on Commission Tutorial Lectures that were presented at the New Delhi General Assembly.

The paper by Dave Giri, Fred Tesche, and Carl Baum is based on their Commission E Tutorial Lecture. It deals with high-power electromagnetic (HPEM) systems, both conductive and radiative. These are systems primarily intended to disrupt or harm electronics and associated systems, or to have an effect directly on people. The understanding and analysis of the potential threats presented by such HPEM systems is important because of the tremendous dependence of modern society on electronic systems, and thus the substantial vulnerability of society's infrastructure to such systems. The authors discuss the classification of HPEM systems. They present a classification scheme based on the bandwidth of the system, and provide an extensive set of examples of HPEM systems in each category. These HPEM systems are primarily designed to interfere with or destroy electronics. They then conclude with a look at an HPEM system that is designed specifically as an anti-personnel system.

The efforts of Christos Christopoulos in bringing us this tutorial are greatly appreciated.

James Green and Scott Boardsen have provided us with a very interesting *Review* on the kilometric continuum radiation. The kilometric continuum radiation is part of the non-thermal continuum radiation. The non-thermal continuum is electromagnetic radiation in the frequency range from about 5 kHz to 800 kHz, which is generated within the Earth's magnetosphere, and which can be observed outside the influence of the Earth's magnetic field. The kilometric continuum is the portion of this radiation above about 100 kHz. Both the thermal and kilometric continuums have very interesting properties, including portions that are trapped between the plasmapause and the magnetopause; radiation in beams; complex frequency structures; and variations as a function of several magnetospheric parameters. This paper provides a very readable overview of both types of radiation, and presents a critical review of the various theories for the generation of the radiation. An interesting discussion of desirable future research directions is also included.

The *Bulletin* greatly appreciates Richard Horne's efforts in bringing us this *Review*.

The measurement of the positions and motions of celestial objects is the science of astrometry. E. B. Fomalont and H. Kobayashi have provided us with an up-to-date *Review* of this field. Absolute astrometry is the determination of the absolute positions of bodies. This requires a reference frame, and the determination of an accurate, non-rotating, non-accelerating celestial reference frame is a major challenge. The authors provide a fascinating review of the development of such reference frames, most of which now use quasars as the fundamental reference points. Relative astrometry is the determination of the relative positions and motions of bodies. There are a variety of techniques used in relative astrometry, and they are reviewed and analyzed in this paper. Both types of astrometry use very-long-baseline interferometry (VLBI) as the fundamental measurement technique, and thus the status of VLBI is also covered. A number of examples of astrometry results are presented, along with a discussion of what the future is likely to hold for this interesting field.

The efforts of Ray Norris in bringing us this Commission J *Review* are much appreciated.

The World Health Organization (WHO), the International Agency for Research on Cancer (IARC), and the International Commission on Non-Ionizing Radiation Protection (ICNIRP) are international bodies that are all concerned with the assessment of the health effects of electromagnetic radiation. The paper by Paolo Vecchia, which is based on the Commission K Tutorial presented at the New Delhi General Assembly, provides an overview of the status of the work of these three organizations in this field. Each organization has a different set of criteria for risk assessment, and each has different procedures for making assessments. The paper reviews all of these. It then provides a summary of the present risk assessments for static magnetic fields, for ELF electric and magnetic fields, and for RF fields. The paper concludes with a look at the impact of these risk assessments on protection policies.

The efforts of Guglielmo d'Inzeo in bringing us this Commission K Tutorial paper are gratefully acknowledged.

As always, Phil Wilkinson's leadership as Senior Associate Editor for the *Reviews of Radio Science* and his help with the Tutorials has been a key element in brining us these papers.

Jim Lin looks at a technique for doing heart surgery with microwaves in his Radio-Frequency Radiation Safety and Health column. One of the fascinating aspects of this technique is that it in part utilizes how the electrical properties

of tissue vary with both function in the body and with exposure to the heating effects of the microwave fields.

I wrote about the outstanding venue for the XIXth URSI General Assembly in Chicago, Illinois, in my last column. The first announcement for the General Assembly appears in this issue. Start your planning now!

The *Radio Science Bulletin* is always looking for good papers that are likely to be of interest to the radio-science community as a whole, particularly those that will appeal to workers in the area of more than one Commission of URSI. If you have such a paper, we can offer relatively rapid publication, no page charges, no fixed length limits, indexing and abstracting by INSPEC, and an audience of the leading radio scientists around the world. I strongly encourage you to submit your contributions.

W. Ross Stone

XXIX General Assembly of the International Union of Radio Science

Union Radio Scientifique Internationale

August 07-16, 2008
Hyatt Regency Chicago Hotel on the Riverwalk
151 East Wacker Drive, Chicago, Illinois 60601, USA

First Announcement

The XXIX General Assembly of the International Union of Radio Science (Union Radio Scientifique Internationale: URSI) will be held at the Hyatt Regency Chicago Hotel in downtown Chicago, Illinois, USA, August 07-16, 2008.

The General Assemblies of URSI are held at intervals of three years to review current research trends, present new discoveries, and make plans for future research and special projects in all areas of radio science, especially where international cooperation is desirable. The first Assembly was held in Brussels, Belgium, in 1922, and the latest in New Delhi, India, in 2005. Assemblies were held in the USA on three previous occasions: in Washington, DC, in 1927 and 1981, and in Boulder, Colorado in 1957.

The XXIX General Assembly will have a scientific program organized around the ten Commissions of URSI and consisting of plenary lectures, public lectures, tutorials, invited, and contributed papers. In addition, there will be workshops, short courses, special programs for young scientists and graduate students, and programs for accompanying persons. More than 1,500 scientists from more than fifty countries are expected to participate in the Assembly.

Call for Papers

The Call for Papers will be issued in mid-2007, will be published in the Radio *Science* Bulletin and in the IEEE Antennas and Propagation Magazine, and will be posted on the URSI Web site. It is expected that all contributions should be received by the end of January, 2008, and that authors will be notified of the disposition of their submissions by the end of March, 2008.

Organizing Committee

Chair	P. L. E. Uslenghi, *University of Illinois at Chicago*, uslenghi@uic.edu
Vice Chair	D. Erricolo, *University of Illinois at Chicago*, erricolo@ece.uic.edu
Technical program	J. E. Carlstrom, *University of Chicago*, jc@hyde.uchicago.edu
	A. Taflove, *Northwestern University*, taflove@ece.northwestern.edu
Poster sessions	D. Erricolo, *University of Illinois at Chicago*, erricolo@ece.uic.edu
Finance	S. R. Laxpati, *University of Illinois at Chicago*, laxpati@uic.edu
	T. T. Y. Wong, *Illinois Institute of Technology*, twong@ece.iit.edu
Publications	D. Erricolo, *University of Illinois at Chicago*, erricolo@ece.uic.edu
Young scientists	S. C. Hagness, *University of Wisconsin at Madison*, hagness@engr.wisc.edu
Graduate students	S. C. Reising, *Colorado State University*, steven.reising@colostate.edu
Workshops & short courses	Y. Rahmat-Samii, *University of California at Los Angeles*, rahmat@ee.ucla.edu
Exhibits	T. T. Y. Wong, *Illinois Institute of Technology*, twong@ece.iit.edu
Fundraising	A. Taflove, *Northwestern University*, taflove@ece.northwestern.edu
	P. L. E. Uslenghi, *University of Illinois at Chicago*, uslenghi@uic.edu
Registration	Three Dimensions Meeting Planners, mevegter@verizon.net
	or: mevegter@threedimensions.com
Social activities	Three Dimensions Meeting Planners, mevegter@verizon.net
	Marie Erricolo, Shelly Uslenghi
Contact with Intl. URSI	W. R. Stone, r.stone@ieee.org
Honorary member	S. K. Avery, *University of Colorado at Boulder*

International Scientific Program Committee

Coordinator	M. K. Goel (India)
Associate Coordinator	P. L. E. Uslenghi (U.S.A.)
Commission A	S. Pollit (U.K.), P. Banerjee (India)
Commission B	L. Shafai (Canada), K. J. Langenberg (Germany)
Commission C	A. F. Molisch (U.S.A.), T. Ohira (Japan)
Commission D	F. de Fornel (France), F. Kaertner (U.S.A.)
Commission E	F. G. Canavero (Italy), C. Christopoulos (U.K.)
Commission F	P. Sobieski (Belgium), M. Chandra (Germany)
Commission G	P. S. Cannon (U.K.), M. Rietveld (Norway)
Commission H	R. B. Horne (U.K.), Y. Omura (Japan)
Commission J	R. T. Schilizzi (The Netherlands), S. Ananthakrishnan (India)
Commission K	F. Prato (Canada), G. D'Inzeo (Italy)

An Overview of High-Power Electromagnetic (HPEM) Radiating and Conducting Systems

D.V. Giri
F.M. Tesche
Carl E. Baum

Abstract

Diverse activities of civilized societies, such as civil defense, air-traffic safety and control, police, ambulance, communications, and Internet commerce are becoming increasingly dependent on advances in computer and electronic systems. While this dependence results in enhanced quality of service, it comes at the price of increased vulnerability to a wide variety of threats to the society's infrastructure. One of the ways of ordering potential intentional electromagnetic environments (IEME) is based on the frequency of coverage of the threat environment. In this paper, we will outline this classification, which is also consistent with current and emerging technologies in HPEM (high-power electromagnetic) generation. Many examples of HPEM generators (from wall socket to radiated waves) are described here. In addition, there exists an HPEM system operating at ~100 GHz, designed to impair the functioning of people without causing serious physiological damage, for crowd-control applications.

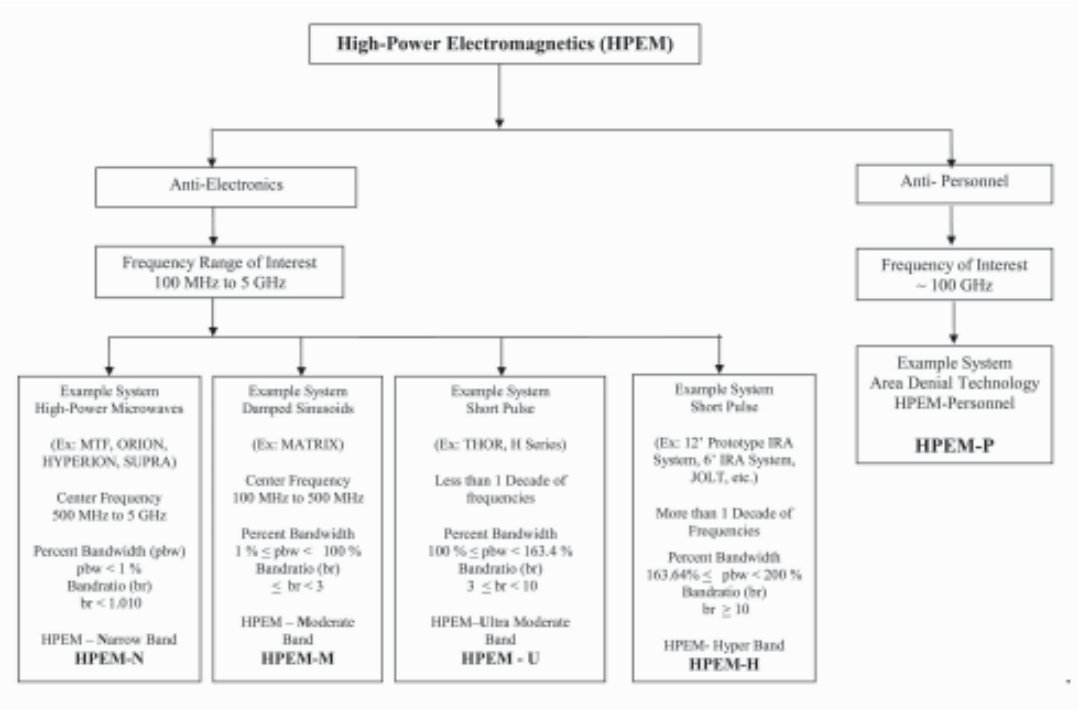

Figure 1. The classification of high-power electromagnetics (HPEM).

D. V. Giri is with Pro-Tech, 11-C Orchard Court, Alamo, CA 94507-1541, USA; e-mail: Giri@DVGiri.com; http://www.dvgiri.com.
F. M. Tesche is with the Department of ECE, Clemson University, Clemson, SC 29634-0915, USA; e-mail: Fred@Tesche.com; http://www.tesche.com.
Carl E. Baum is with the Department of ECE, University of New Mexico, Albuquerque, NM87131-0001, USA; e-mail: carl.e.baum@ieee.org; http://www.ece.unm.edu.

This paper is based on the invited Commission E Tutorial Lecture given at the XXVIIIth General Assembly of URSI, New Delhi, India, October 28, 2005.

Figure 2. The factorization of the transfer function from an HPEM source to a system.

1. Introduction

HPEM systems can be broadly classified into two groups:

1. **Anti-electronics:** designed to destroy or impair hardware, munitions, or electronics, with the intent to stop an enemy's systems from functioning.
2. **Anti-personnel:** designed to impair the functioning of people without causing serious physiological damage.

This classification and the various sub-classifications are shown in Figure 1.

1.1 Anti-Material Technologies

It is well established that sufficiently intense electromagnetic (EM) signals, in the frequency range of 200 MHz to 5 GHz, can cause upset or damage in electronic systems. This induced effect in an electronic system is commonly referred to as intentional electromagnetic interference (IEMI). Such intentional electromagnetic environments (IEME) could be radiated or conducted. One way of classifying the HPEM environments is based on the frequency content of their spectral densities: "narrowband," "moderate band," "ultra-moderate band," and "hyperband." To characterize these environments, we consider the *bandratio* of the EM spectrum, $br = (f_h / f_l)$. Using the inherent features of *br* in a manner consistent with the emerging EM field-production technologies, the definitions for bandwidth classification presented in Table 1 have been formalized [1, 2].

Note that this terminology is consistent with IEC Standard 61000-2-13, entitled "EMC, High-power Electromagnetic (HPEM) Environments – Radiated and Conducted." We observe that the definition of upper and lower significant frequencies as the 3 dB frequency points is not always feasible. For this reason, the lower and upper frequency points are defined by using weighted energy norms [3, 4], considering the range in which 90% of the energy is contained. Such weighted norms have the property of giving approximately equal weighting to the high- and low-frequency portions. One can provide examples of HPEM generators that employ current and emerging technologies for each category of the four-band classification. The above classification is useful in describing potential HPEM environments. In the case of HPEM waveforms, we stipulate the lower frequency limit to be 1 Hz if there is a large dc content in the spectrum (not applicable to radiating systems).

Band Type	Percent Bandwidth $pbw = 200\left(\frac{br-1}{br+1}\right)\%$	Bandratio br
Narrow (Hypo)	$<1\%$	<1.01
Moderate (Meso)	$1\% \le pbw < 100\%$	$1.01 < br < 3$
Ultra-Moderate (Ultra Meso or Subhyper)	$100\% \le pbw < 163.64\%$	$3 < br < 10$
Hyperband	$163.64\% \le pbw < 200\%$	$br \ge 10$

Table 1. IEME classification based on bandwidth.

There are various factors to be considered while considering the interaction between an electronic system and a high-power electromagnetic beam from a source at some distance away. Baum [5] has examined these factors, going from the source to the system, as illustrated in Figure 2. A maximum response is normally achieved by the use of highly resonant exciting waveforms (such as damped sinusoids). The factorization shown in Figure 2 is applicable primarily to narrowband and moderate-band HPEM.

Conducted HPEM environments are also a potential threat to electronic equipment connected to power and communication lines [6, 7]. In most modern buildings, there is a personal computer on nearly every desk, and these computers are typically connected to the power supply and to a telephone cable or local-area network (LAN), which make them vulnerable to conducted and interfering HPEM signals.

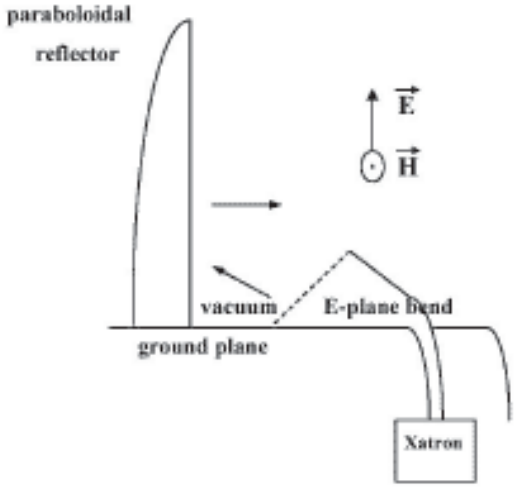

Figure 3. A half-reflector Phaser.

Feature	MTF Sweden	ORION UK	Hyperion France	Supra Germany
RF source	Conventional tubes	Relativistic magnetrons	Relativistic magnetron and reltrons	Reltrons
Frequency	1.3, 2.86, 5.71, 9.30, and 15 GHz	1-3 GHz	1.3-1.8 GHz (magnetron), 2.4-3.0 GHz (magnetron), 0.72-1.44 GHz (reltron)	0.675-1.44 GHz
Max. power	25, 20, 5, 1, 0.25 MW as function of frequency	350 MV microwave power; 5 GW pulse power; 500 kV, 50 Ω	–	400 MW-200 MW
Max. PRF	1000, 1000, 1000, 1000, and 2100 Hz	Single shot to 100 Hz	– (magnetron) 1 Hz (reltron)	10 Hz
Max. pulse duration	5, 5, 5, 3, 8, and 0.53 μs	500 ns	100 ns magnetron 200 ns reltron	>300 ns
Field level	–	–	40 kV/m (reltron) 60 kV/m (magnetron)	70 kV/m at 15 m

Table 2. Examples of high-power narrowband systems.

2. Narrowband Systems (*pbw* < 1%)

High-power microwave (HPM) ($\geq$100 MW) sources, operating in a single-shot mode or with tens or hundreds of Hz repetition rates, are being developed in various countries. This technology is reaching power levels in the GW range, and is frequency-agile. These sources can be used to create intense electromagnetic fields in the range of ~500 MHz to 3 GHz that can couple to targeted systems and cause electronic upset or damage. While several nations may not be interested in developing or deploying HPM weapon systems, they will be compelled to understand and protect their military assets against this potential threat. Several HPM facilities in the frequency range of 0.7 GHz to 3 GHz exist [8]. Examples are shown in Table 2. However, it is possible that some smaller-scale versions of such systems could be used for destructive purposes, if acquired by organizations or groups intent upon harming other societies. Therein lays the potential threat in the present context of civilian and military electronics systems and infrastructure.

Baum [9] has postulated that the narrowband systems can also be built with a half-reflector and a ground plane (Figure 3). Half a pyramidal horn can be bonded to the ground plane, with its phase center coincident with the focal point of the reflector. The pyramidal horn is fed from underneath the ground plane in an E-plane bend by the usual WR-975 rectangular waveguide for 1 GHz operation. The ground plane provides an electromagnetically shielded volume, in which the narrowband source and ancillary equipment can be housed. The RF source is typically a narrowband high-power microwave generator, such as a magnetron, reltron, or klystron. If space is a consideration, e.g., on an airborne platform, Baum [10] has suggested a high-power scanning waveguide array, illustrated in Figures 4a, 4b, and 4c. This system involves subdivision of rectangular waveguide to form an array, [$(N-1)$ sheets $\rightarrow N$ sub-guides $\rightarrow N$ sub-apertures], and avoids the use of small coupling holes/slots in a waveguide. Beam scanning is accomplished by varying the frequency.

3. Moderate-Band Systems (1% < *pbw* < 100 %)

Moderate-band systems (source and antenna) have been built in the range of 100 MHz to 700 MHz, and have been called the Dispatcher. The term Dispatcher stands for Damped Intensive Sinusoidal Pulsed Antenna, Thereby Creating Highly Energetic Radiation. Baum [11, 12] has described certain systems that integrate an oscillator into

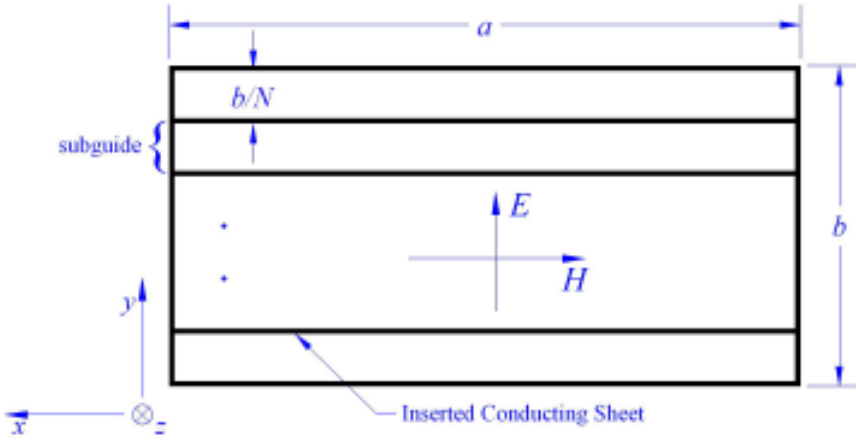

Figure 4a. A high-power split-waveguide antenna [10]: A cross section of a split waveguide.

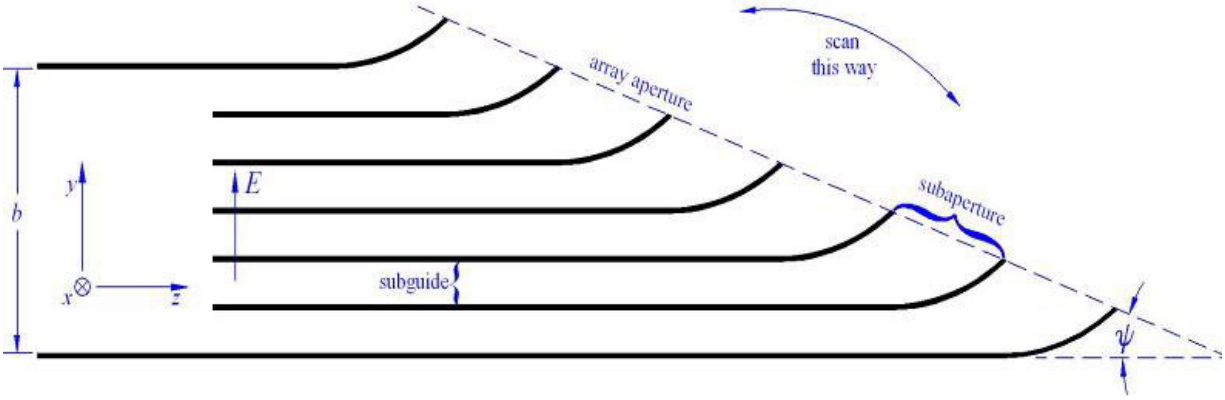

Figure 4b. A high-power split-waveguide antenna [10]: A side view of a split waveguide.

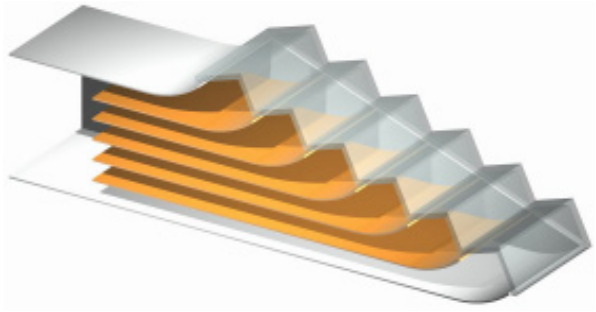

Figure 4c. A high-power split-waveguide antenna [10]: A three-dimensional view of a split waveguide.

the antenna system. Examples are (a) a low-impedance quarter-wave transmission-line oscillator feeding a high-impedance antenna, and (b) a low-impedance half-wave transmission-line oscillator feeding a high-impedance antenna. The transmission-line oscillator would consist of a quarter- or half-wave section of a transmission line (in oil medium for voltage standoff) that is charged by a high-voltage source. This is shown schematically in Figure 5, where the antenna is a TEM-fed half reflector.

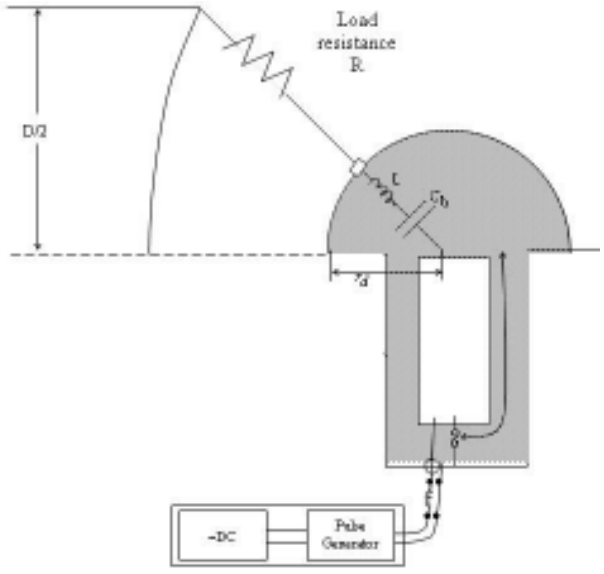

Figure 5. An oscillator that switches into an antenna.

The switched oscillator concept shown in Figure 5 has been realized in hardware, and has been termed the MATRIX [13, 14]. The oscillator is charged up to 150 KV to 300 kV, and the frequency is adjustable in the range of 180 MHz to 600 MHz. This system radiates a damped sinusoidal waveform with a percentage bandwidth of about 10%. An advantage in energizing a high-impedance antenna (100 Ω in the case of the half-reflector shown in Figure 5) from a low-impedance source (~5 Ω) is that the voltage into the antenna nearly doubles, leading to higher radiated fields.

4. Ultra-Moderate-Band Systems (100% < *pbw* < 163.64%) or (3 < *br* < 10)

Some of the H-series systems (for example, H-2), built at the Air Force Research Laboratory, Kirtland AFB, New Mexico, USA, have bandwidths that qualify them as ultra-moderate systems. Specifically, the H-2 generates a 300 kV/250 ps/~2 ns pulse, feeding a TEM horn, which radiates a pulse of 43 kV/m at a distance of 10 m (rE_{peak} ~ 430 kV). A second example is the THOR system [15], with a 1 MV pulse producing a peak electric field of 68 kV/m at 10 m (rE_{peak} = 680 kV) with a FWHM of 400 ps. The bandwidth is from 200 MHz to 1 GHz, or a $br \sim 5$ and a $pbr \sim 133\%$.

5. Hyperband Systems (163.64% < *pbw* < 200%) or (*br* > 10)

Since they were first proposed in 1989 [16], paraboloidal reflectors fed by TEM transmission lines have received significant attention, owing to their main attractive property of extremely wide bandwidth without the adverse effects of dispersion. They have been called impulse-radiating antenna (IRA) systems, A photograph of an example, the prototype IRA, is in Figure 6.

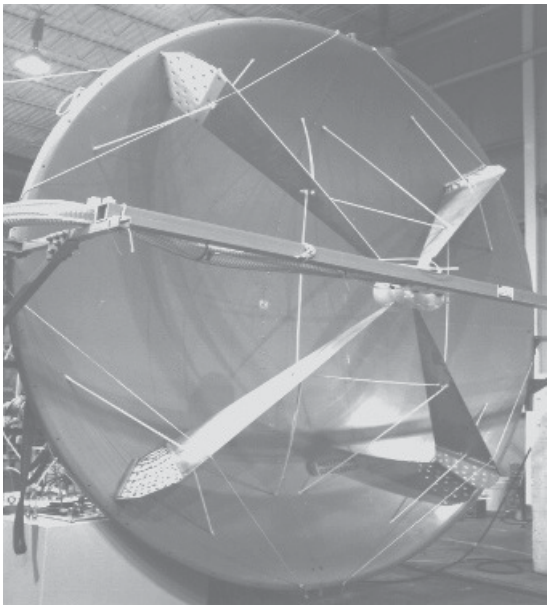

Figure 6. A photograph of the 3.67 m prototype IRA system.

The bandwidth associated with time-domain antennas is to be distinguished from the approximately 10-to-1 bandwidth of the so-called frequency-independent antennas, such as log-periodic antennas, which are highly dispersive, since the phase center of the antenna is not fixed. Different CW frequencies applied to a log-periodic antenna are radiated from different portions of the antenna, which makes it dispersive if all of the frequencies are applied at the same time, as in a pulsed application. Reflector IRAs overcome this problem, and even have equivalent electric and magnetic dipole moments characterizing the low-frequency performance. Even the dipolar radiation at low frequencies is along the optical axis of the reflector. Many optimal reflector IRAs have been designed, fabricated, and tested. Additional details may be found in [17-19].

JOLT (Hyperband Radiator)

The JOLT is a half-IRA system [20, 21], with a 3.05-m diameter, paraboloidal, commercial microwave reflector that has been cut in half, and flanged for attachment to the ground plane. The transient energy source, located at the focal point of this reflector, launches a near-ideal TEM spherical wave onto the reflector, through a polypropylene lens, to be reflected as a collimated beam. A photograph of the JOLT system and a sample boresight measurement are shown in Figures 7 and 8.

The JOLT is a high-voltage transient system built at the Air Force Research Laboratory, Kirtland AFB, New Mexico, USA, during 1997-1999. The pulsed power system centers on a very compact resonant transformer, capable of generating over 1 MV at a pulse repetition frequency of 600 Hz. This is switched via an integrated transfer capacitor and an oil peaking switch onto an 85 Ω half-IRA.

Figure 7. A photograph of the JOLT radiator.

This unique system will deliver a far radiated field with a full-width half-maximum (FWHM) on the order of 100 ps, and a field-range product (rE_{peak}) of ~ 5.3 MV, exceeding all previously reported results. A representative measured far electric field is shown in Figure 8. It is seen that the impulse-like radiated field from the JOLT has an extremely large bandwidth, ranging from about 40 MHz to about 4 GHz, for a band ratio of 100. Such HPEM environments are useful in specialized applications. Hyperband systems can be built in many forms, such as the reflector IRAs described above, or TEM horns [22] and lens IRAs [23]. They have useful applications such as:

- Disrupter (Disrupting Integrated System, Releasing Ultra-Power Transient Electromagnetic Radiation)
- Buried target detection, such as de-mining
- Hostile target detection and identification
- Space debris detection
- Periscope detection
- Source for vulnerability studies via transfer functions
- High-power, hyper-wideband jammers
- Law-enforcement applications such as "seeing through walls"
- Electrical characterization of materials (e.g., wave propagation measurements in materials such as rock, concrete, etc.)

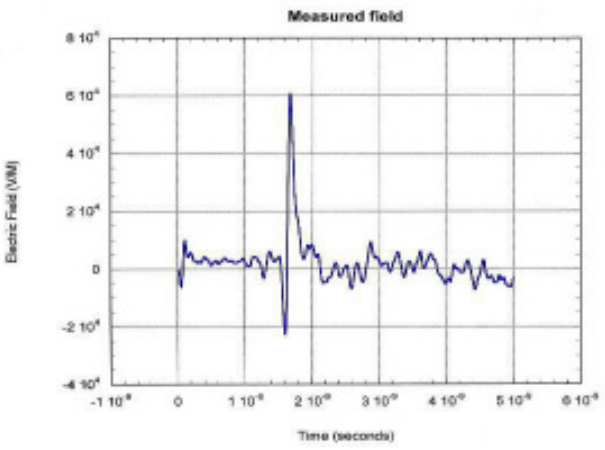

Figure 8. The measured electric field at a boresight distance of $r = 85$ *m.*

Figure 9. A photograph of the demonstration hardware.

- Industrial applications (detection of leaky or defective pipes)
- Detection of human beings in earthquake rubble
- Searching for avalanche victims
- Artillery applications

6. Active Denial Technology

We present this example based on a fact sheet on this system published by the Office of Public Affairs, posted at Air Force Research Laboratory's (AFRL) Web site at http://de.afrl.af.mil. Figure 9 shows the system hardware. This section is treated as a quotation, since this material is extracted from AFRL's Web site.

> This is a breakthrough non-lethal technology that uses millimeter-wave electromagnetic energy to stop, deter and turn back an advancing adversary from relatively long range. It is expected to save countless lives by providing a way to stop individuals without causing injury, before a deadly confrontation develops. The technology was developed by the Air Force Research Laboratory and the Department of Defense's Joint Non-Lethal Weapons Directorate. This non-lethal technology was developed in response to Department of Defense needs for field commanders to have options short of the use of deadly force. Nonlethal technologies can be used for protection of defense resources, peacekeeping, humanitarian missions and other situations in which the use of lethal force is undesirable.
>
> Active Denial Technology uses a transmitter to send a narrow beam of energy towards an identified subject. The electromagnetic radiation reaches the subject and penetrates less than 0.4 mm into the skin, quickly heating up the skin's surface. Within seconds, an individual feels an intense heating sensation that stops when the transmitter is shut off or when the individual moves out of the beam. Despite the sensation, the technology does not cause injury because of the low energy levels used. It exploits a natural defense mechanism that helps to protect the human body from damage. The heat-induced sensation caused by this technology is nearly identical to the sensation experienced by briefly touching an ordinary light bulb that has been left on for a while. Unlike a light bulb, however, active denial technology will not cause rapid burning, because of the shallow penetration of the beam and the low levels of energy used. The transmitter needs only to be on for a few seconds to cause the sensation....

Operational System

Currently, concept demonstration is underway for a vehicle-mounted version. Future versions might also be used onboard planes and ships. The vehicle-mounted version will be designed to be packaged on a vehicle such as a High Mobility Multi-purpose Wheeled Vehicle (HMMWV, more commonly referred to as a Humvee) [see Figure 10]....

7. Summary

We have presented the four-way categorization of HPEM environments based on bandwidth. This categorization is based on emerging technologies, and example systems in each of the four categories were also described. In addition, illustrative examples of hyperband radiators – which are finding many useful applications, both in the military and civilian sectors – were listed. While these anti-material HPEM systems are in the frequency range of ~100 MHz to 5 GHz, there exists an anti-personnel system at ~94 GHz, termed Active Denial Technology, which was also briefly described.

8. Acknowledgment

Figure 10. The vehicle-mounted Active Denial system concept.

This paper is the result of an IR&D project at Pro-Tech. F. M. Tesche was supported by an Air Force Office of Scientific Research (AFOSR) MURI under Grant F49620-01-1-0436. Carl E. Baum was supported partially by AFOSR.

9. References

1. D. V. Giri, "Classification of Intentional Electromagnetic Interference (EMI) Based on Bandwidth," AMEREM 2002, Annapolis, Maryland, 2-7 June 2002.
2. D. V. Giri and F. M. Tesche, "Classification of Intentional Electromagnetic Environments (IEME)," *IEEE Transactions on Electromagnetic Compatibility*, **EMC-46**, 3, August 2004, pp. 322- 328.
3. D. Nitsch, F. Sabath, H.-U. Schmidt, and C. Braun, "Comparison of the HPM and UWB Susceptibility of Modern Microprocessor Boards," *System Design and Assessment Note 36*, July 2002.
4. C. E. Baum and Daniel H. Nitsch, "Band Ratio and Frequency-Domain Norms," *Interaction Note 584*, 1 May 2003.
5. C. E. Baum, "Maximization of Electromagnetic Response at a Distance," *IEEE Transactions on Electromagnetic Compatibility*, **EMC-34**, 3, August 1992, pp.148-153.
6. V. Fortov, F. Loborev, Yu. Parfenov, V. Sizranov, B. Yankovskii, and W. Radasky, "Estimation of Pulse Electromagnetic Disturbances Penetrating into Computers Through Building Power and Earthing Circuits," Metatech Corporation, Meta-R-176, December 2000.
7. V. Fortov, F. Loborev, Yu. Parfenov, V. Sizranov, B. Yankovskii, and W. Radasky, "Estimation of Pulse Electromagnetic Disturbances Penetrating into Computers Through Building Power and Earthing Circuits," Metatech Corporation, Meta-R-176, December 2000.
8. F. Sabath, M. Bäckström, B. Nordstrom, D. Serafin, A. Kaiser, and D. Nitsch," Overview of Four European High-Power Microwave Narrow-Band Test Facilities," *IEEE Transactions on Electromagnetic Compatibility*, **EMC-46**, 3, August 2004, pp. 329- 334.
9. C. E. Baum, "Phaser Utilizing a Half Reflector and a Ground Plane," *Microwave Memo 9*, 15 July 2000.
10. C. E. Baum, "High-Power Scanning Waveguide Array," *Sensor and Simulation Note 459*, September 2001.
11. *C. E. Baum,* "Switched Oscillators," *Circuit and Electromagnetic System Design Note 4*5, 10 September 2000.
12. C. E. Baum, "Antennas for Switched Oscillators," *Sensor and Simulation Note 455*, 28 March 2001.
13. W. D. Prather, C. E. Baum, R. J. Torres, F. Sabath and D. Nitsch, "Survey of Worldwide High-Power Wideband Capabilities," *IEEE Transactions on Electromagnetic Compatibility*, **EMC-46**, 3, August 2004, pp. 335- 344.
14. Burger, C. E. Baum, W. Prather, R. Torres, D. Giri, M.D. Abdalla, M.C. Skipper, B.C. Cockreham, J. Demarest, K. Lee and D. P. McLemore, "Modular Low Frequency High-Power Microwave Generator," Proceedings of AMEREM 2002, Annapolis, MD, June 2002.
15. W. M. Henderson, D. E. Voss and A. L. Lovesee, "The Etcheron Valley Outdoor High-Power Electromagnetic Test Facility and the Transient High Output Radiator," in E. Mokole, M. Kragalott and K. Gerlach (eds.), *Ultra-Wideband Short-Pulse Electromagnetics 6*, New York, Plenum Press, 2003.
16. C. E. Baum, "Radiation of Impulse-Like Transient Fields," *Sensor and Simulation Note 321*, November 25, 1989.
17. D. V. Giri and C. E. Baum, "Temporal and Spectral Radiation on Boresight of a Reflector Type of Impulse Radiating Antenna (IRA)," in C. E. Baum, L. Carin, and A. Stone (eds.), *Ultra-Wideband Short-Pulse Electromagnetics 3*, New York, Plenum Press, 1997.
18. D. V. Giri, H. Lackner, I. D. Smith, D. W. Morton, C. E. Baum, J. R. Marek, W. D. Prather, and D. W. Schofield, "Design, Fabrication and Testing of a Paraboloidal Reflector Antenna and Pulser System for Impulse-Like Waveforms," *IEEE Transactions on Plasma Science*, **25**, 2, April 1997, pp, 318-326.
19. D. V. Giri, J. M. Lehr, W. D. Prather, C. E. Baum, and R. J. Torres, "Intermediate and Far Fields of a Reflector Antenna Energized by a Hydrogen Spark-Gap Switched Pulser," *IEEE Transactions on Plasma Science*, **28**, 5, October 2000, pp.1631-1636.
20. C. E. Baum, W. L. Baker, W. D. Prather, W. A. Walton III, R. Hackett, J. M. Lehr, J. W. Burger, R. J. Torres, J. P. O'Loughlin, H. A. Dogliani, J. S. Tyo, J. S. H. Schoenberg, G. R. Rohwein, D. V. Giri, I. D. Smith, R. Altes, G. Harris, J. Fockler, D. F. Morton, D. P. McLemore, K. S. H. Lee, T. Smith, H. LaValley, M. D. Abdalla, M. C. Skipper , F. Gruner, B. Cockreham and E. G. Farr, "JOLT: A Highly Directive, Very Intensive, Impulse-Like Radiator," *Sensor and Simulation Note 480*, November 10, 2003.
21. C. E. Baum, W. L. Baker, W. D. Prather, J. M. Lehr, J. P. O'Loughlin, D. V. Giri, I. D. Smith, R. Altes, J. Fockler, D. McLemore, M. D. Abdalla, and M. C. Skipper, "JOLT: A Highly Directive, Very Intensive, Impulse-Like Radiator," *Proceedings of the IEEE*, **92**, 7, July 2004, pp. 1096-1109.
22. C. E. Baum, "Low-Frequency Compensated TEM Horn," *Sensor and Simulation Note 377*, 28 January 1995.
23. E. G. Farr, "Boresight Field of a Lens IRA," *Sensor and Simulation Note 370*, October 1994.

Advances in Radio Astrometry

E.B. Fomalont
H. Kobayashi

Abstract

Astrometry is the branch of astrophysics that studies the position and motion of celestial objects. Radio interferometers that span many thousands of kilometers are presently the most accurate astrometric instruments, and have pushed the angular accuracy to 10^{-5}arcsec $= 5\times10^{-11}$rad. After a tutorial on the measurement and use of the visibility phase, we describe the two major aspects of astrometry: absolute astrometry, which defines the quasar reference frame and determines the position of objects within this frame; and relative astrometry, which deals with the differential positions of celestial objects from which stellar motions, evolution, and distances can be determined. Technological advances and more sophisticated observation methods to decrease the astrometric errors are described. Some examples of astrometric results are presented, and a glimpse into the astrometric future over the next 10 years is given.

1. Introduction

Astrometry is the oldest branch of astronomy, and many important advances over the centuries are based on astrometric observations: Kepler's laws concerning the motion of the planets, Copernicus placing the sun at the center of the solar system, Newton's theory of gravity, and Einstein's general relativity prediction of the precise deflection of star light by the solar gravitational field. The innate astrometric accuracy was limited by the resolution of the human eye, one arcmin, about 1/30 the lunar diameter. Early ground optical telescopes increased the resolution to the atmospheric turbulence limit of about one arcsecond, but the use of adoptive optics, and the HIPPARCOS and Hubble telescopes, have decreased this limit by a factor of ten. Over the last 30 years, the use of radio interferometers has significantly increased the astrometric precision of celestial objects, so that accuracies are now routinely made at the milli-arcsecond, level with differential measurements as small as tens of micro-arcseconds. Orbiting optical and radio antennas specifically designed for astrometric observations expect to reach the one micro-arcsecond accuracy by 2020.

Two aspects of astrometry will be covered in this review. First, *absolute astrometry* is concerned with the determination of the precise location of celestial bodies. For this, it is necessary to define a non-rotating and non-accelerating (inertial) reference frame. Since 1998, the distant quasars have been used as the fiducial points to realize this inertial frame, and its development, description, and improvement will be discussed.

Relative astrometry, on the other hand, deals with the relative position and motion of individual celestial objects. For example, the distance to a star can be obtained from the size of its elliptical yearly path in the sky, caused by the Earth orbiting the sun. This motion is called the parallax, and its magnitude varies inversely with the distance to the star. The parallax can be determined accurately when the stellar position is compared with that of other objects that are in nearly the same direction in the sky, but are much more distant.

Figure 1a. One of three major radio arrays: The VLBA, with ten 25-meter telescopes, stretching from Saint Croix, Virgin Islands, to Mauna Kea, Hawaii.

E. B. Fomalont is with the National Radio Astronomy Observatory, Charlottesville, VA 22903, USA; e-mail: efomalon@nrao.edu.
H. Kobayashi is with the Mizusawa VERA Project, National Astronomical Observatory of Japan, Mizusawa, Iwate, 023-0861 Japan; e-mail: hideyuki.kobayashi@nao.ac.jp.

This is one of the invited *Reviews of Radio Science* from Commission J.

Figure 1b. One of three major radio arrays: The EVN, with 17 radio telescopes that devote 25% of the time for VLBI.

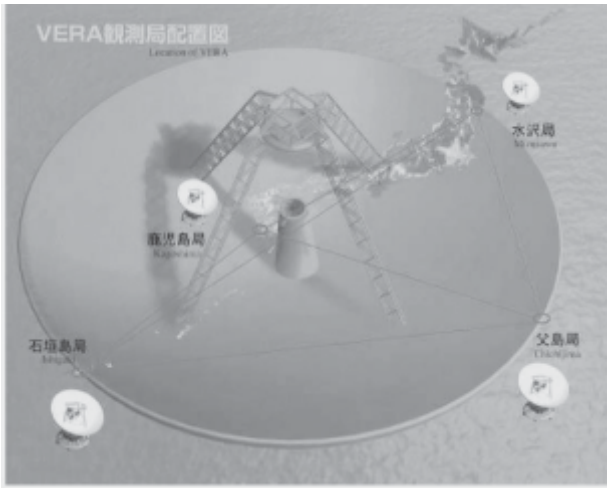

Figure 1c. One of three major radio arrays: The VERA array, consisting of four dual-feed telescopes in Japan.

Very-long-baseline interferometry (VLBI) has been the experimental technique that has led in the development and refinement of both absolute and relative astrometric measurements over the last 20 years. The three major arrays that have led in this development are the Very Long Baseline Array (VLBA) [1], the European VLBI Network (EVN) [2], and the Japanese VLBI Exploration of Radio Astronomy project (VERA) [3], all shown in Figure 1. Hence, it is appropriate that this astrometric review is published in the *Radio Science Bulletin*.

2. Basic Interferometry

The following brief tutorial provides a framework for this review. More detailed discussions of radio interferometers can be found in [4].

2.1 Component of a Two-Element Interferometer

The major components of a two-element interferometer are shown in Figure 2. Two antennas, at locations $\mathbf{R}^i$ and $\mathbf{R}^j$ are pointed toward a quasar (any source of radio emission) with celestial coordinate $\hat{\sigma}$. Since most antennas are large parabolic-shaped reflectors, the angular size of their main response is about that of the moon, so their pointing accuracy must be significantly smaller. The angular discrimination of the interferometer is associated with the *geometric delay*, $\tau_g = \left(\mathbf{R}^i - \mathbf{R}^j\right) \bullet \hat{\sigma}$, which produces a difference in the arrival phase between two antennas of the wavefront from a distant quasar. For

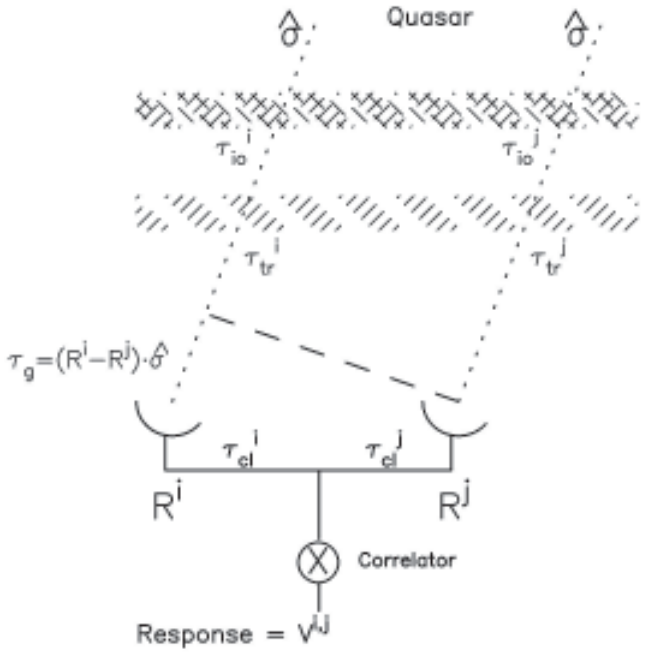

Figure 2. A two-element interferometer: The radio signals from a distant quasar in the direction $\hat{\sigma}$ pass through the Earth's ionosphere and troposphere (with delays τ_{io} and τ_{tr}) before detection at two antennas, located at positions R_i and R_j. The geometric delay, τ_g, is the relevant path-length difference between the two signals, and is the main astrometric observable. The additional delay of the signals from the antennas to the correlator, designed by the X, is τ_{cl}. The response of the correlator, $V^{i,j}$, is described in the text.

example, the geometric delay from a quasar for an antenna separation of 5000 km varies between –17 and 17 msec during the day as the quasar "rotates" in the sky. As the radio waves propagate through the troposphere and ionosphere, anomalous delays, τ_{tr} and τ_{io}, are added to the geometric delay. These delays can be modeled using meteorological information and measurements from the Global Positioning System (GPS) satellites; however, delay uncertainties of many centimeters remain, and these dominate the astrometric errors.

Most radio arrays used for astrometric observations consist of antennas separated by many thousands of kilometers, and operate at frequencies between 0.6 GHz and 86 GHz, with a bandwidth up to 2.0 GHz at the higher frequencies. The weak quasar signals are amplified near the focal point of each antenna, and then converted to a lower frequency by multiplication with a signal from an independent free-running oscillator (usually a hydrogen maser) at each antenna. Because of the high data rate associated with the each antenna – now approaching several gigabits per second – the data are recorded on high-density video tapes or large-capacity disk systems [5-8], and then transported to the central processing unit, called a correlator. Experimental use of e-links have been tested and may be commonly used within the next decade [9, 10]. The instrumental delay at each antenna, associated with the hydrogen-maser oscillator, the accurate clock, and the signal path from the antenna focus to the correlator, is denoted by τ_{cl}.

The correlator is a special-purpose set of hardware, firmware, and software that cross-correlates the signals from each antenna pair to obtain the quasar wavefront-coherence properties. The two major types of digital correlators are the Fourier (FX) correlator, which converts the wideband input signals into many narrowband frequencies before correlation, and the lag (XF) correlator, which cross-correlates the two wideband signals simultaneously with many time lags, from which the narrowband frequency correlation can be determined [11, 12]. These correlator systems are labor-intensive, and require careful maintenance to process the terabytes of data that are the typical throughput. Recent advances in parallel and cluster computing now make software-based correlating systems efficient, and these may supplant the more mechanical systems by 2015 [13, 14].

The correlator response, a complex quantity called the complex visibility function, $V^{i,j}$, for each antenna pair (i, j) at frequency ν, is a quasi-sinusoidal response,

$$V^{i,j}(t) = A^{i,j}\cos\left[2\pi\nu\left(\tau^i - \tau^j\right) + \phi^{i,j} - M^{i,j}\right], \quad (1)$$

where

$$\tau^k = R^k\hat{\sigma} + \tau^k_{tr} + \tau^k_{cl} + \nu^{-2}\tau^k_{io}, \quad k = (i, j)\cdot$$

In order to obtain the complex correlation value, two correlations are made: one with the two signals in phase, and one with $\pi/2$ added to one of the signals. The response has a period up to 10 kHz because of the constantly changing delay between antennas caused by the Earth's rotation. However, this delay variation can be accurately modeled and added to one of the antenna signals before correlation, so that the output response becomes relatively constant over seconds to minutes of time. This added correlator delay term is the called the *model delay*, $M^{i,j}$, and often includes tropospheric and ionospheric delay estimates.

The two quantities in Equation (1) that are properties of the quasar are the visibility amplitude term, $A^{i,j}$, and the visibility phase term, $\phi^{i,j}$. These are essentially the *spatial coherence function* of the quasar emission, sampled at the projected baseline $\mathbf{B} = \left(\mathbf{R}^i - \mathbf{R}^j\right)$ in the source direction [15]. The spatial coherence function is related to the Fourier transform of the quasar's angular power distribution. For a point source, $A^{i,j}$ is proportional to the source flux density, and is independent of the antenna separations. For an extended source, $A^{i,j}$ generally decreases with antenna separation. The visibility phase, $\phi^{i,j}$, contains information about the quasar emission structure and its position in the sky; hence, it is the main parameter associated with astrometric measurements.

The antenna delay term, τ^k, is composed of several parts. The first term, $R^k\hat{\sigma}$, is the geometric delay. The term τ^k_{tr} is associated with the troposphere. The term τ^k_{cl} is produced by the independent clocks and instrumental variations associated with each antenna. The last term, τ^k_{io}, is caused by any plasma refraction in the ionosphere or solar corona, and varies as ν^{-2}.

The correlator response is generally averaged over several seconds to several minutes. This integration time is limited by the temporal variations of the visibility phase, particularly those variations associated with the delay changes in the troposphere, ionosphere, and the oscillators. The maximum integration time before there is a significant loss of signal is called the coherence time, and it varies between 1 min and 10 min. At frequencies above 5 GHz, the tropospheric delay variations limit the coherence time and are weather related. Below 1.4 GHz, the coherence time is limited by ionospheric delay changes and depends on the solar activity.

2.2 The Phase and Its Positional Accuracy

If the quasar emission is point-like, the visibility phase, $\phi^{i,j}$, contains the information about the quasar's position, and the inherent positional accuracy can be estimated as follows. For an operating frequency of $\nu = 8$ GHz, using a sufficiently stable system and strong quasar emission, the relative phase of the two quasar signal paths can be measured to an accuracy of $\sim 1°$, which

corresponds to a delay accuracy of 0.3×10^{-12} sec. The geometric delay that contains the angular-position information of the quasar is of order of 1.0×10^{-2} sec for a 5000-km antenna separation. Thus, the angular discrimination of the location of the quasar in the sky is the ratio of these two numbers, or about 0.03×10^{-9} radian or 6 μarcsec.

The delay stability of 0.3×10^{-12} sec (0.3 psec) is equivalent to a path-length stability of 0.3 mm, which is at least an order of magnitude smaller than the variable environmental terms in Equation (1). For example, a small cloud of water vapor above an antenna can change the path length by a few centimeters in a matter of minutes. However, by making simultaneous observations of two quasars that are in nearly the same direction (or switching quickly between them), only the differential delay terms will affect the measurement of their relative phases, so that relative delay stabilities of 1 psec are possible.

A further problem with the measured visibility phase is that it is only defined over 2π radians. Astrometric analysis using the phase alone can only be obtained if the phase can be converted into the total delay difference of the quasar wavefront impinging between the two antennas. This requires an accurate model delay and a sufficiently stable antenna environment where the phase variation with time or with sky direction can be followed without cycle slips. It is only within the last ten years that sufficiently stable VLBI array systems, with accurate delay models, have led to phase-stable astrometric observations.

The phase-cycle ambiguity problem can be avoided by the measurement of the derivative of the phase with frequency, called the *group delay* [16]. This quantity can be determined by simultaneously or nearly simultaneously observing at many frequency channels, and determining the slope of phase over the spanned frequency. As long as the selected observing frequencies are not spaced too widely apart, there is no ambiguity in deriving the phase slope. The instrumental phase differences among the channels are generally very stable and need be calibrated infrequently. Because most of the astrometric, instrumental, and tropospheric phase errors are associated with nondispersive delay (frequency-independent) effects, the group delay and the phase are nearly equivalent quantities in determining astrometric parameters.

3. Absolute Astrometry

In order to determine the position of celestial objects, an acceptable reference frame is crucial. The frame must be inertial: the origin cannot be accelerating, and the direction of the coordinate axes must be fixed in space. The platforms associated with most astronomical observations (from the Earth's surface or from an Earth-orbiting antenna) are, however, far from inertial; hence, nineteenth-century astronomers adopted the barycenter of the solar system (the center of mass of the solar system that is well within the surface of the sun) as the celestial reference-frame origin. The two axes of this frame were defined by the orientation of the spin-axis of the Earth and a fixed point in the sky, the vernal equinox, at a specific time, called the equinox. This reference frame is quasi-inertial, because of the slight acceleration of the sun in its path around the Milky Way galaxy, and from deeper considerations about truly inertial frames in the universe that deal with absolute space, Mach's principle, and the role of general relativity in the distortion of space. However, these fascinating topics are beyond the scope of this article [17].

The "fixed" stars in the sky provide a set of fiducial objects that should be, on the average, non-rotating in space, and could be used to define the coordinate axes. This frame, called the FK5, was developed in the 20th century, and was based on the positions and motions of thousands of stars [18, 19]. Since most bright stars have a linear motion (in addition to the cyclical parallax motion) in the sky of ~ 0.01 arcsec/yr (which is far from random over the sky, because of the net rotation of all objects around the Milky Way's center), precise observations and many subtle corrections were needed to define an accurate FK5 frame. Other observations, such as the passage of asteroids near the Earth, the transits of Venus across the face of the sun, and observations of planets and spacecraft [20], were used to determine the accurate location of the barycenter of the solar system. By 1990, the accuracy of the FK5 reference frame reached about 0.02 arcsec accuracy.

3.1 The Development of the International Celestial Reference Frame

In the 1970s, VLBI observations demonstrated that many radio sources contain a small radio component, of size < 0.001 arcsec, and were associated with the central region of very distant galaxies, on the order of 1 Gparsecs $= 3\times10^{22}$ km. Hence, these radio components should be stationary in the sky at the level of < 1 μarcsec yr^{-1}, and could define the axes of a (nearly) perfect inertial frame. Over the next 20 years, improvements in the stability and observing procedures of VLBI, with more precise modeling of the Earth's rotation, nutation, orientation, and planetary motions, led to a quasar positional accuracy of < 1 marcsec over the sky.

In the early 1990s, the astronomical community formed working groups in order to define an International Celestial Reference System (ICRS) [21, 22], based on a suitable number of distant quasars. This required the incorporation of astrometric theory and observations, and improvements in the observational techniques. For reasons of continuity with the FK5 system, the directions of the ICRS-defined axes were set to the FK5 frame directions on January 1, 2000, called equinox J2000.0. The resulting catalog of the positions of the quasars that are used to realize

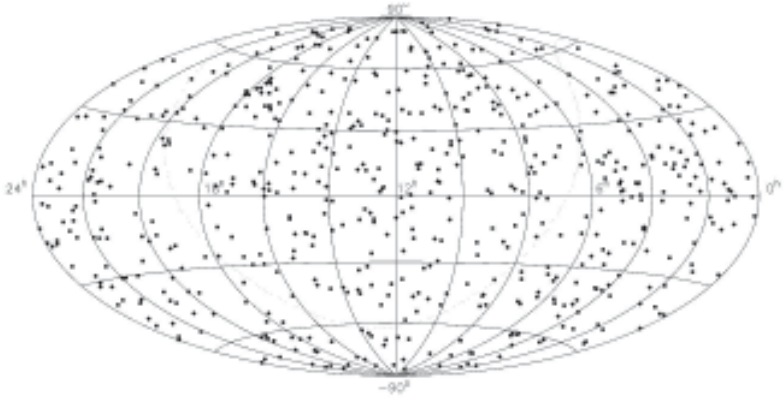

Figure 3. The distribution of the 608 sources in the ICRF-ext1 list. An Aitoff equal-area projection of the celestial sphere has be taken from Figure 13 of [23].

the ICRS is called the International Celestial Reference Frame (ICRF) [23].

The majority of the VLBI observations used for the ICRF determination comes from observations by the NASA Crustal Dynamics Project (CDP), the United States Naval Observatory (USNO), the Jet Propulsion Laboratory (JPL), the VLBA, the EVN, and other groups. Each observing session is 24 hr in length in order to determine the large diurnal phase variations, and the observations are made simultaneously at 2.3 GHz and 8.4 GHz, with a spanned bandwidth of 0.1 GHz and 0.4 GHz, respectively. Each observation scan lasts about 6 min, and each session includes about three observations each of about 80 sources. These data provide accurate values of the group delay for each observation: the phase data is often affected by ambiguities of 2π and cannot be used directly. With a suitable combination of the two-frequency data, the ionospheric refraction, τ_{io}, which produces a dispersive delay proportional to the inverse frequency squared, can be removed.

The data are analyzed by several available software packages [24, 25] in order to obtain the hundreds of parameters that accurately model the experimental conditions. Some parameters are unchanged over many months or years (source positions, antenna properties); some parameters are slowly variable but considered to be constant over each 24-hour session (precession, nutation, Earth's rotation offset and rate, antenna locations); and some parameters are extremely variable, with determinations made every hour (tropospheric zenith path delays and gradients, maser oscillator phase changes). The typical residual delay error for each 24-hour session, after obtaining the best solution, is about 25 psec (1 cm delay), and is dominated by un-modeled tropospheric delay variations.

Since many antennas around the globe participate in VLBI observations, a well-defined terrestrial reference frame is needed. Thus, the International Terrestrial Reference System (ITRS) was formulated to describe the rules for

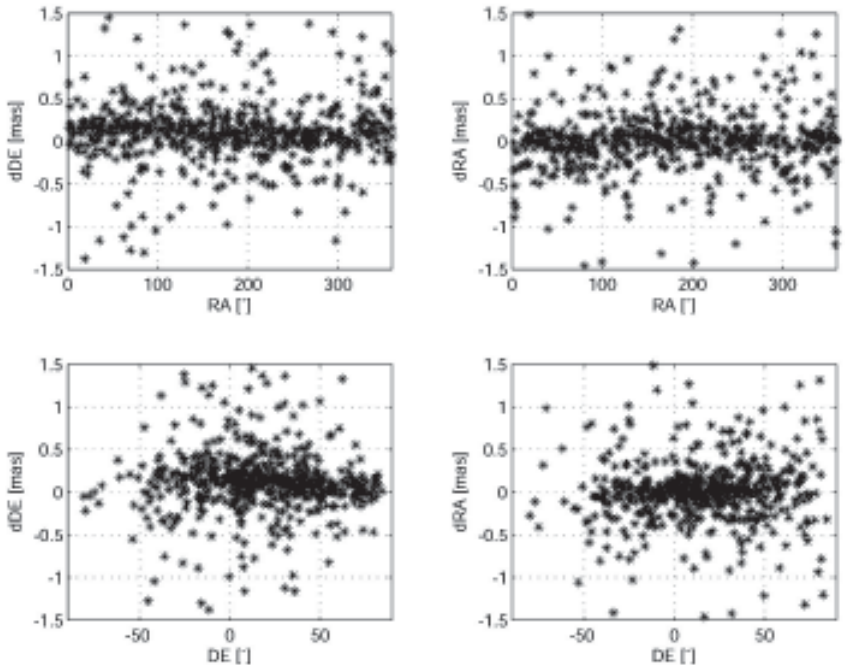

Figure 4. The residual position errors of the ICRF-ext1 list. The distributions of the declination error, dDE, and right-ascension error, dRA, are plotted as functions of the values of the right ascension (RA) and declination (DE) for 549 sources in the ICRF-ext1 list. The errors are the differences between the ICRF-ext1 positions and those from a new solution of 2211 observing sessions between 1984 and 2001.

determining specific locations on the Earth, and plate-tectonic effects are significant [26]. Such geodetic information can also be obtained from space-geodetic techniques (now more accurately than by VLBI techniques), such as the Global Positioning System (GPS), lunar-laser ranging, satellite-laser ranging, and Doppler orbitography and radio-positioning integration by satellite (DORIS): see [27] for a more detailed discussion about the overlapping technology. However, the link between the terrestrial reference frame and the celestial reference frame can only be obtained from VLBI observations.

The ICRF now in use was determined from a solution of 1.6 million data points, taken between 1979 and 1995.5 [23]. The solution provided the accurate position for about 600 quasars, along with hundreds of other observational parameters needed to model each 24-hour session accurately. The 212 quasars with the most stable position over the period and with little extended radio emission were chosen for the defining set for the ICRF. The typical position error for a defining source is 0.2 marcsec, and the ensemble defines the orientation of this quasar-reference to 0.02 marcsec, more than a factor 100 better than the FK5 frame. The additional 400 quasars were included in an extended list of candidate sources, but these were not used in the defining set. The sky distribution of the sources is given in Figure 3.

The positional accuracy of the ICRF-ext1 list is illustrated in Figure 4 [28]. There is little systematic position offset over the sky, and the rms error per source is 0.2 marcsec. The outliers are mainly associated with quasars with variable structures, or those with a small number of observations in the original 1.6 million sample. Improved positions that include data up to 2002.4 are now available in the ICRF-ext2 list [29]. The positions of the 212 defining sources have not changed to avoid a discontinuity in the ICRF reference frame, but improved positions were made for the 396 candidate ICRF sources.

3.2 Current Status and Improvement of the ICRF

Specialized observing strategies to strengthen the ICRF are used in order to understand the dynamics of the Earth and its internal structure. This leads to better modeling parameters in the global solutions that improve the quasar position determination by reducing the residual errors in the solution. The VLBA [2], normally dedicated to the imaging of complex quasars and stars, has been used since 1995 in a 24-hr session every two months to obtain highly accurate, long-term geodetic/astrometric parameters, and an example of the improvement is given in Figure 5 [30]. More dense observations are obtained every few years, when a two-week campaign of continuous global VLBI observations is made. Since 2000, an intensive program of observing sessions is made on an almost daily basis, each session lasting at least 1.5 hours [31]. Figure 6 shows the non-uniformity of the Earth's rotation at the level of 20 μsec, and occasional anomalies of ~ 50 μsec, persisting over a month period, are clearly detected.

In order to obtain robust solutions of astrometric and geodetic parameters, observations of sources over the entire sky in one hour are needed to determine the variable tropospheric refraction component that is mostly source-elevation dependent. These observations require a large

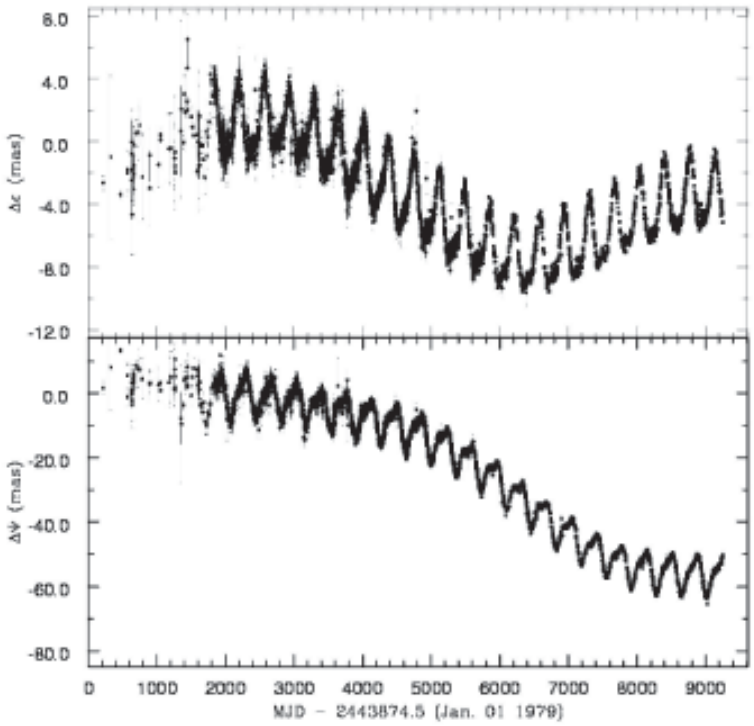

Figure 5. The distribution of the nutation of the pole of the Earth with respect to the nominal 1980 IAU model associated with the FK5 system. The latitude change is $\Delta\varepsilon$ (obliquity) and the longitude change is $\Delta\psi$. Each point and error bar were determined from one 24-hr session from a global solution of all data. The time axis runs from 1979.0 to 2004.0 (day 9130). The improvement in accuracy after 1994 was mainly associated with the inclusion of the VLBA. The data show the 18-yr, 9-yr, 1-yr, 0.5-yr, 121-day, and 14-day nutation periods (from http://rorf.usno.navy.mil/ solutions/i2004a).

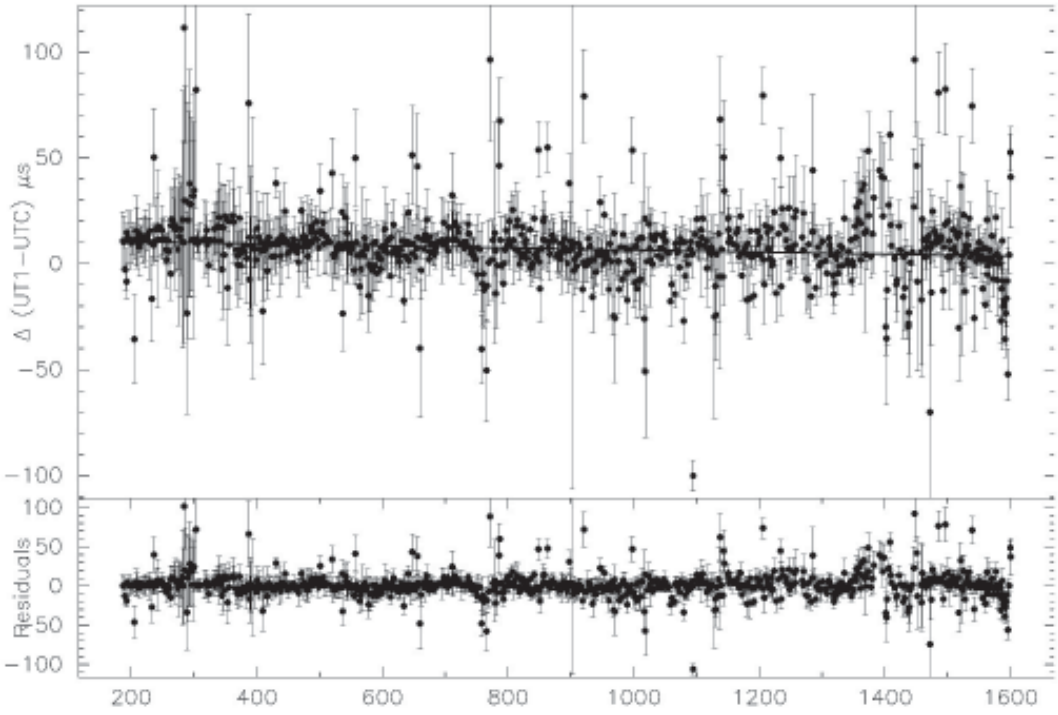

Figure 6. The short term fluctuations in the rotation of the Earth. The upper plot shows the derived time from the VLBI intensive observations of UT1 (essentially, the rotation angle of the Earth with respect to the ICRF) minus the UTC (the universally adopted terrestrial time that has a constant rate, apart from occasional leap seconds to keep it within one second of UT1). The sloping line is the smoothed UT1-UTC correction determined by the International Earth Rotation Service. The bottom plot shows the residual UT1-UTC from the IERS value. Short-term fluctuations of time scales up to one month are seen, and are probably related to the variable momentum transfer between the Earth and the troposphere (from http://rorf.usno.navy.mil/solutions/ i2004a).

number of calibrators from which to choose. The number of good-quality ICRF sources south of declination $-40°$ has recently increased with VLBI observations in Australia [32, 33], and the recent VLBA and VERA observations have increased the number of potential ICRF candidates [34-37] to nearly 3000 sources. Less than 10% of the sky north of $\delta > -40°$ does not have a calibrator within a radius of 4° of a random position. These sources, while not in the formal ICRF system, are tied to the same grid, and have positional accuracies of about 0.5 marcsec.

The optical inertial frame and the solar system dynamic inertial frame have been incorporated within the ICRF. The HIPPARCOS orbiting telescopes cataloged the positions and proper motions of over 100,000 stars brighter than 12 magnitude between 1989 and 1993 [38, 39]. The comparison of positions between the stars that could be observed via both radio and optical means [40, 41] were used to link the two frames. The frame-tie between the ICRF and the planetary ephemeris was obtained in several ways: comparison of the pulsar positions tied to the ICRF frame from interferometric observations, with pulsar positions tied to the solar system frame using pulse-arrival-time data [42]; occultation of radio sources by planetary objects; VLBI observations of spacecraft-orbiting planets; and comparison of lunar ranging and VLBI Earth-orientation parameters [43].

The structure of quasar emission at the milli-arcsecond level is somewhat variable and can produce astrometric uncertainties. Such changes are studied intensely by astrophysicists, in order to understand the relationship between the radio-emitting plasma and the black holes in the center of the host galaxy that ultimately produce the kinetic and radiative energies. The radio emission is generally linear in shape, with the galaxy center associated with a compact radio component (radio core) at one end of the emission structure. Occasionally, a bright plasma component is ejected from the core, and moves at near the speed of light down the spine of the extended region [44]. (The ejection occurs in opposite directions, but the intensity of the component moving toward the observer is greatly enhanced by the Doppler effect.) Since this ejected component can often outshine the radio core, the centroid of the radio emission can change by several marcsec over periods of a month to a year.

An example of this type of evolution is shown in Figure 7, for the ICRF source 2200+420 (not in the 212 defining ICRF set). Two ejections are seen over a 19-month period, and the centroid of the source emission moves north to south by over 1 marcsec over this period [45]. However, we know from theories of radio-source evolution that the

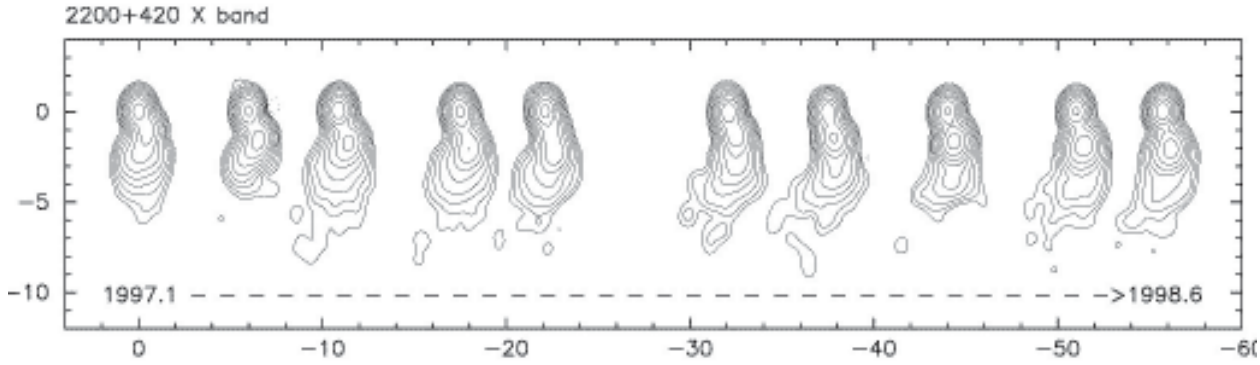

Figure 7. The effect of source structure on astrometry. The contour plots are shown for 10 successive observations, spanning the period 1997.1 to 1998.9. The images have been aligned vertically according to the peak of the northern component (see the text for the reason), and spaced horizontally according to the observing epoch. The scales are in marcsec, and the contour levels increase in powers of two. For the last five epochs, the secondary components moving toward the south are brighter than the core, and the centroid of the emission varies by over 1 marcsec during this period.

compact component at one extreme end of the emission is usually near the black hole within the nucleus of the galaxy, and should be located at a fixed direction in the sky. However, for a source with similar behavior but a factor of 10 smaller in angular size, it would be difficult to determine which end of the structure has the more compact emission. With a typical resolution of 1 marcsec for VLBI, we estimate an positional uncertainty of about 0.05 to 0.1 marcsec for the location of the stationary point in many ICRF sources. A more general analysis of effects of source structure is discussed in [46].

The uncertain tropospheric refraction, τ_{tr}, over each antenna is the largest error component for most astrometric observations. Initial estimates of the refraction from the dry and wet components can be made from ground meteorological data [47, 48]. Additional correction can be modeled directly from the residual delay observations, if the quasars are observed over a wide range of elevation within a 30- to 60-min period. However, the correlation of the tropospheric refraction model and the derived quasar positions – especially the declinations – is illustrated in Figure 8.

The delay in the path between the antenna and the correlators, τ_{cl}, is dominated by the accuracy of the local clock at each antenna. Hydrogen-maser clock-oscillators are commonly used, and they have a stability of about 1×10^{-15} [4]. Less expensive oscillators, such as the laser-pumped Cs gas cell, are under investigation [49]. The delay instabilities of these oscillators are generally smaller than those caused by the troposphere. The use of a central frequency standard, which is then sent to other antennas using a radio or optical-fiber link, cause delay variations along the signal path. Delay changes that are internal within the antennas' propagation paths can be monitored by transmitting faint round-trip test radio tones through the electronics, and the phase difference between the outgoing and incoming test signal is an accurate monitor of the system delay changes [50]. This scheme was successfully used for the VSOP mission, where the oscillator signal at a tracking station was linked to an orbiting spacecraft with a 25000 km apogee [51].

In the next five years, astronomers will provide a better realization of the ICRF, consisting of a revised set of sources with more accurate positions and more uniform all-sky coverage [52, 53]. The accumulated advances in observational techniques, analysis methods, and instrumental and tropospheric calibrations outlined in the previous section will increase the stability of the ICRF

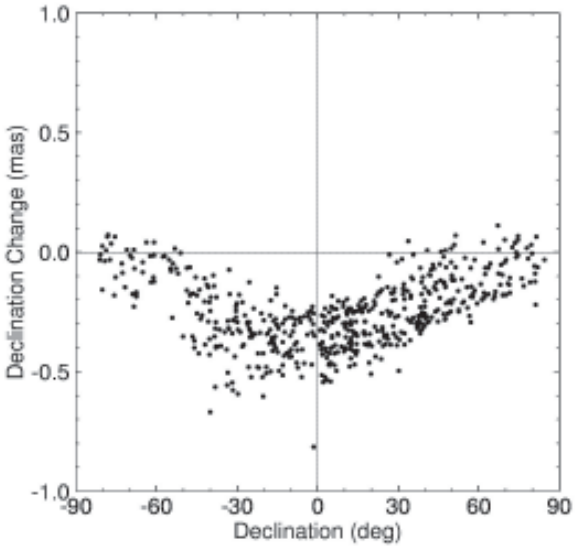

Figure 8. The effect of the tropospheric model on source declinations. Two global solutions of the ICRF database were made: one using a tropospheric all-sky model over each antenna that was azimuthally symmetric, and one using a model that also included a north-south gradient term. The difference in the derived source declinations for the two solutions is plotted as a function of the source declination. This demonstrates the correlation of the tropospheric model and a systematic declination offset for the ICRF of 0.4 marcsec for this model difference. Additional systematic errors are believed to be less than 0.15 marcsec.

frame orientation by at least a factor of two. The transition between the present ICRF and a new ICRF must be made smoothly, so that discontinuities in the associated astrometry parameters are not introduced.

Nearly all astrometric observations for the ICRF have been made at 2.3/8.4 GHz, where the 2.3 GHz observations are mainly used to remove the ionospheric delay: the catalog positions are defined at 8.4 GHz. Because of the NASA decision to move from 8.4 GHz to 32 GHz for spacecraft tracking using wider bandwidths for telemetry, preliminary VLBA observations are now made at 24 GHz and 43 GHz. This is done in order to define the ICRF at higher frequencies [54], where the ionospheric contamination is reduced, and most radio sources are more dominated by a radio core, with little extended structure [55].

4. Relative Astrometry

Many astrophysical phenomena are associated with the position and space motion of celestial objects. For example, a direct measurement of the distance to an object is to measure its parallax: its apparent change in position as seen from the Earth when it is on opposite sides of the sun. For objects in our galaxy, the parallax ranges from about 1 arcsec for the nearest stars to 0.0001 arcsec for stars on the other side of the galaxy. The more linear motion of stars is associated with their rotation around the galaxy's center, their expulsion from cataclysmic events, or minute periodic wiggles from the gravitational effect of orbiting stars or planets. Nearer to the Earth, radio interferometric observations of spacecraft determine the spacecraft's position in the plane of the sky, and complement spacecraft ranging from conventional Doppler tracking. These data have successfully improved the location of spacecraft as they rendezvous with distant planets, moons, or comets [56]. Finally, the effect of the gravitational field in the solar system, or near massive objects such as black holes or pulsars, can be measured and compared with the predictions of general relativity (GR) or other theories of gravity.

4.1 Phase Referencing

Since the ICRF grid provides a background of thousands of calibrator radio sources with positional accuracies of less than 0.5 marcsec, the motion and position of any target source in the sky can be determined by comparing its position with that of a suitable calibrator within a few degrees in the sky. The precise position of the calibrator is only a secondary consideration, *as long as the calibrator is stationary with time*. Over the last ten years, the relative positional precision between close astronomical objects in the sky has decreased by over a factor of 10, and now approaches the 10 μarcsec level.

The usual observation scheme is to quickly alternate between the calibrator and the target, a procedure called *phase referencing* [57]. The switching time between the two sources depends on the phase-variation time scale (coherence time), and is described in more detail below. The highest frequency for which phase referencing is reasonably successful is at 86 GHz [58], where coherence times are less than 1 min and the switching between calibrator and target strains the mechanical ability of large antennas.

The fundamental astrometric quantity for each antenna pair is the residual target phase, the difference between the target phase and the calibrator phase. Assuming that the calibrator is a point source with known position and is located in nearly the same direction as the target, then it is essentially a perfect test signal that contains the same un-modeled delay terms as that in the target. The Fourier transforms of the residual target phase and amplitude then produce an image that displays the quasar structure and position.

A discussion of the errors associated with phase referencing are given in [59, 60], and this is summarized here. First, if the calibrator is not a point source, then its internal structure can be determined using self-calibration techniques and its structure phase removed [61]. Second, if the calibrator position is not accurately known, then to first order its position offset is transmitted to the derived target position, i.e., the calibrator-target separation is actually determined. Next, the calibrator and target are usually sufficiently far apart in the sky so that they cannot be observed simultaneously within the reception area covered by the array antenna. However, the VERA project has developed a dual-directional feed configuration at 23 and 43 GHz that can simultaneously observe a calibrator and target with a maximum separation is about 2.2° [3]. Also, at frequencies below 1.6 GHz, it is often possible to find a calibrator within about one degree of the target, so that both sources are within the reception area of the antennas [62, 63].

If the calibrator and target are not simultaneously observed, there is an error associated with the interpolation of the phase between two successive calibrator scans, and this will decrease the positional accuracy and coherence of the target image. This error is weather dependent, but can be minimized by frequent switching between calibrator and target. As Figure 9 illustrates, the calibrator phase behavior changes appreciably with antenna baseline and time. For these 8 GHz observations, the coherence time (roughly the time for which the phase changes by less than about 60°) varied between one minute and one hour! Tropospheric refraction dominates at frequencies above 5 GHz and is extremely variable. Below 2 GHz, the ionospheric refraction begins to dominate, and at 0.3 GHz, the coherence time may be as short as 1 min near sunrise and sunset, when the ionosphere is most active. With a separation of less than 1°, the relative phase error between a calibrator and target is about 5 psec, about 15° of phase at 8 GHz. This is the main reason why lengthy observations to find thousands of potential calibrators are compiled: to provide a reasonable

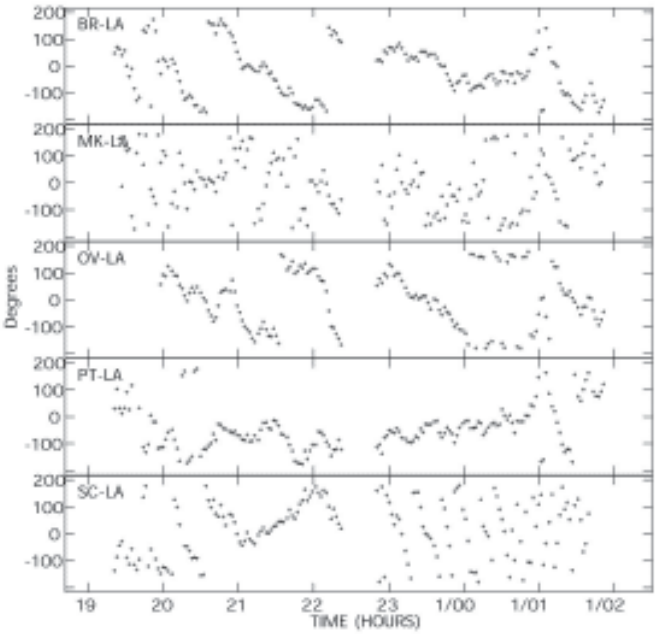

Figure 9. The calibrator phase at 8 GHz. The observed calibrator phases are shown for a VLBA experiment for five baselines to Los Alamos, NM (LA): Brewster, WA (BR); Mauna Kea, HI (MK); Owens Valley, CA (OV); Pie Town, NM (PT); and Saint Croix, VI (SC). The x axis shows the time range, and the y axis is the measured phase. Each point represents the calibrator phase response averaged over a one-minute scan, with each scan separated by three minutes. The short-term variations were produced by tropospheric path-length changes ($100° = 1$ cm delay) over each telescope. The phase between calibrator observations could be interpolated for the BR-LA, OV-LA and PT-LA baselines. The MK-LA phases were noisy because of poor weather conditions, but could be followed with no phase ambiguity but large phase errors. The SC-LA phase changes became large after 23 hr because of the low elevation of the quasar as viewed from Saint Croix. After 1/00 hr, the phase connection between successive points was impossible to follow, so this data was not suitable for phase referencing.

chance of finding a calibrator that is less than a few degrees from the target. However, very fast phase fluctuations, associated with wind speeds of 10 m/s and turbulent cells of 30 m, cause semi-random phase changes with time scales of a few seconds, and make phase referencing difficult or not possible.

Finally, there is a phase-error term that varies approximately linearly with the angular separation of the calibrator and target. The slowly varying part (tens of minutes to many hours) is associated with errors in the a priori model such as the antennas' locations, Earth-orientation parameters, and large-scale tropospheric refraction errors. To first order, these produce a relatively stable delay gradient over each antenna in the calibrator and target region. The gradient can be determined and removed by observing, at relatively frequent intervals, several calibrators that surround the target [64]. See Section 4.3 for more discussion.

4.2 Analysis Techniques

There are two methods of analyzing the residual target phase to obtain astrometric information. If the residual target phase error is less than about 30°, then the Fourier transform of the residual target amplitude and phase will produce a good-quality image of the target. (The amplitude stability of arrays is generally accurate to about 5% over time scales of hours, except for atmosphere absorption at frequencies about 30 GHz. The constant of proportionality of A, between the correlated amplitude and the true sky-flux density scale, in Equation (1) can be obtained by observations of calibrators with known strengths, and these are included in phase-referencing experiments). The peak location of the target image will be at its true sky position with respect to that assumed for the calibrator. Deconvolution techniques may be useful in order to remove the point-spread function associated with the observation coverage to determine a more precise shape of the target [65]. However, if the phase-error terms are generally larger than 60°, the target image will become distorted and scattered, and several relatively large sub-peaks may be present, even for a point source.

Hence, methods for analyzing the target residual phase directly in order to determine its position are also useful. First, if several calibrators are used, then techniques have been developed for removing the apparent phase gradient near the target [60, 66]. If the residual phase error is dominated by an error in the elevation-dependent tropospheric delay term, iterative techniques can be used to improve the target position and structure [67]. However, the main advantage to Fourier imaging is its linearity and coherence. Even for weak sources, in which the measured residual target phase is completely noise dominated, Fourier imaging will produce a target image with the signal-to-noise associated with the entire integration period, which can be last as long as 48 hours. For example, virtually all stars in the HIPPARCOS catalog that are associated with radio sources are faint and their radio positions can only be detected using Fourier techniques, with many hours of integration with good phase-referencing stability.

4.3 Improvements in Phase Referencing

4.3.1 Antenna Positions

The frequent ICRF-type observations provide Earth rotation, orientation, and nutation parameters that are available from the International Earth Rotation and Reference System Service (IERS) [68]. The distribution of time information is organized by the United States Naval

Observatory [69]. These data provide effective antenna-location accuracies of about 3 cm (based on predictions of past observations), and about 2 cm approximately two weeks after an experiment.

The terrestrial location of an antenna can be obtained from surveying techniques and the use of GPS to within 10 cm accuracy. Further improvement can be obtained using VLBI and GPS observations to tie the location of an antenna to those antennas with already known accurate locations. Antenna velocities can be measured over several-year spans, and are consistent with plate tectonic motions. Furthermore, the location of the antenna's focal point with respect to the structure depends on the drive system and, particularly, on the offset between the two orthogonal axes. Second-order effects associated with deformation of the antenna can amount to a 0.5 cm delay difference. Recent improvements of the European VLBI Network (EVN) station locations illustrate the corrections [70].

4.3.2 Reducing Troposphere and Ionosphere Refraction Effects

The temporal variations of the phase response are one of the limitations of astrometric VLBI. The calibrator residual phase between successive observations, typically 1 min to 8 min apart, must be accurately connected, in order to apply to the intermediate target observation. Thus, reducing the phase changes by any techniques will increase the astrometric accuracy.

The most accurate hydrogen-maser oscillators have a stability of 3×10^{-15} in 100 sec, which leads to a phase fluctuation at 8.4 GHz of only 1° of phase, and is insignificant [4]. Hence, the antennas' independent oscillators do not produce significant phase changes, and the changes they do produce can be followed by nominal phase-referencing techniques.

However, the un-modeled delays in the troposphere are of most concern at frequencies above 5 GHz, and these cause delay changes of 3 cm in a period of one minute or less, as shown for some baselines and periods in Figure 9. The wet part of the tropospheric refraction is the most variable at high frequencies [71], and is strongly correlated with the weather. Fortunately, there is good correlation between the variation of the delay due to the wet troposphere and the atmospheric emission from water vapor near 22.6 GHz. In order to remove these fluctuations at a level of path delay to a few millimeters, small, stable water-vapor radiometers (WVR), mounted on or near each antenna, pointed in the same direction as that of the target and calibrator, monitor the emission at several frequencies near the 22.6 GHz-line emission. By appropriately analyzing the emission profile across the water-vapor spectrum, it is possible to deduce the density and approximate temperature of the water vapor, and to determine the expected phase variation from the interferometer response. The results of such an experiment between two antennas operated by the Jet Propulsion Laboratory (JPL), near Goldstone, CA, are

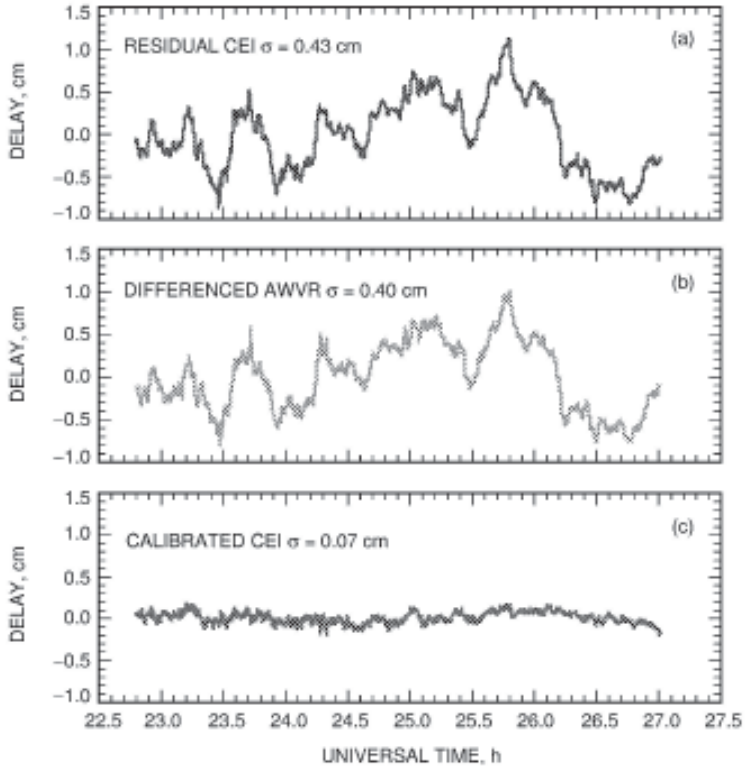

Figure 10. The use of WVR to remove phase fluctuations. (a) The observed delay fluctuations between two telescopes separated by 21 km at the NASA Goldstone site in the California desert. The experimental frequency was 8 GHz, where 1 cm delay equals 100° of phase. (b) The inferred path-length changes in the direction to the sources as determined from WVR measurements. (c). The calibrated delay (observed - WVR measurement). The rms phase fluctuations decreased by a factor of six. The sky was cloudless during this period of time; hence, most of the tropospheric delay was caused by water vapor.

shown in Figure 10 [72]. More-sophisticated monitoring of the water-vapor emission at a higher frequency is being investigated for the Atacama Large Millimeter Array (ALMA) [73]. The WVR emission is not effected by refraction from by liquid water, ice crystals, and the dry-air turbulent component, which can be estimated from ground and meteorological measurements.

The Crustal Dynamics Data Information System (CDDIS) provides a series of maps of the zenith total electron content of the ionosphere as a function of geographical latitude and longitude taken every two hours, and these can be used to determine the approximate ionospheric refraction at each antenna. Even with these approximate models, about 75% of the ionospheric refraction can be modeled [74] and removed from the residual target phase. However, at frequencies below 2.0 GHz, the ionospheric turbulence and waves occasionally produce large phase changes in less than one minute [75]. These changes tend to be largest near sunrise and sunset, when plasma waves in the ionosphere are likely to occur, and the phase referencing often fails during these periods.

4.3.3 Calibrator Structure Changes

One of the major uncertainties in the determination of the long-term (longer than one month) motion of a radio source is the stability of the apparent position of the calibrator. This problem has already been discussed in Section 3.2, and illustrated in Figure 7 [45]. If the calibrator source is very compact, then its position in the sky should not vary by more than about 25% of its angular size or angular size limit, which can be as small as 0.05 marcsec. Otherwise, changes of 0.1 to 0.2 marcsec are more typical, although it is possible to determine the "stationary" part of an extended calibrator by identifying its radio core.

4.3.4 Multi-Calibrator Observations

Observations of several calibrators surrounding the target source are now being used to determine the delay gradient in the sky in the vicinity of the target. With this technique, the astrometric precision in the determination of a target's position with respect to two or more calibrators can be reduced to about 20 μarcsec from the 50 μarcsec generally obtained by using one calibrator [64, 66, 76]. This improvement of the target phase by using two calibrations is illustrate by Figure 11. For this case, the source configuration was almost collinear, and only two calibrators were necessary. The use of three or more calibrators that surround the target can remove any changing phase gradient above the antennas, although short-term and very small angular-scale changes will add noise to this calibration. The image-quality improvement from using more than one calibrator is shown in Figure 12; the error associated with the location of the peak of the target decreased significantly.

4.3.5 Multi-Frequency Observations

Even with good a priori ionospheric modeling and phase referencing there is often a significant residual ionospheric delay, which is the main limitation for astrometric results at frequencies less than 2 GHz. As discussed in Section 3.1, dual-frequency observations can separate the plasma-induced delay (caused by the ionosphere or the solar corona) from the frequency-independent delays. If the observations span a sufficiently large frequency band, then the ionospheric delay can be determined by fitting the

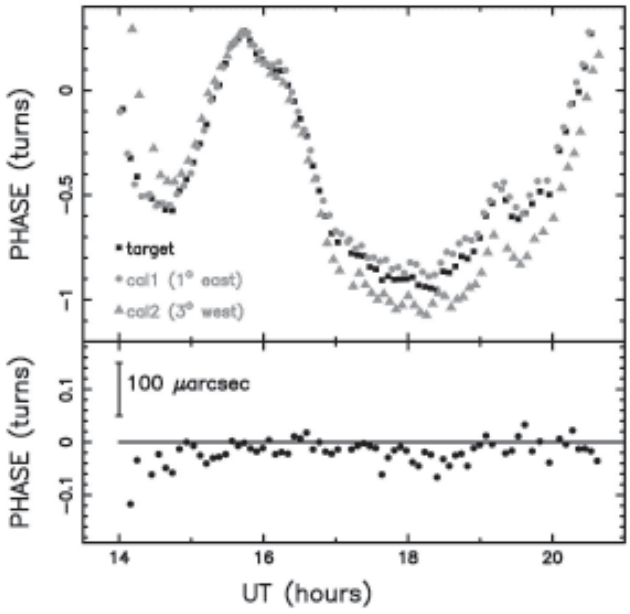

Figure 11. The use of two calibrators to improve astrometric accuracy. (Top) The phases at 8 GHz measured over six hours on a 500-km baseline are plotted from alternating observations among two calibrators and a target. The overall temporal variations of one revolution (4 cm of delay) for all three sources were caused by hour-long tropospheric and ionospheric refraction changes over each antenna. The phase separation among the sources was caused by a changing delay gradient in the vicinity of the sources. (Bottom) The residual phase of the target after removing the average phase (weighted by distance from the target) of the two calibrators. The corrected target phase is now relatively flat, with an rms phase scatter of 0.02 revolution (0.8 mm of delay). The slight offset from zero phase was a measure of the position offset of the target with respect to the a priori positions assumed for all of the sources used in the correlator source models.

phase, ϕ, as a function of the frequency, ν, in the form $\phi(\nu) = A\nu + B\nu^{-1} + 2\pi N$, where N is an arbitrary, small integer. A is the value of the delay term relevant in the astrometric analysis, and B is proportional to the ionospheric refraction. This method is now used by the VLBA in order to measure the motion of pulsars, which are strong at low frequencies [77].

4.4 Examples of Astrometric Results

There are many examples of exciting astrometric results, and only a few can be illustrated in this article. The motions and distances to many pulsars and stars have been determined using the VLBA, EVN, and VERA [78]. One of the fastest-moving pulsars is B1508+55, and its proper motion and parallax observational results are shown in Figure 13 [79]. Extrapolation the motion of the pulsar back for 2.3×10^6 yr suggests that this pulsar was kicked out of a cluster of bright stars, called the Cygnus OB association, by a supernova event. With the parallax precision of < 0.04 marcsec yr^{-1} now being obtained, it is possible to determine the distance of any detectable radio source within the Milky Way galaxy.

A method to determine the distance to nearby galaxies is shown in Figure 14 [67]. The radio-astrometric observations have determined the relative motion of two objects rotating around the center of M33 to be 30.8 ± 4.0 μarcsec yr^{-1}. From many types of optical and radio observations of material and stars that are rotating in the galaxy, an accurate rotational model (from the Doppler effect associated with quantized emission from simple molecules) can be determined, and this gives an expected linear motion of 106 ± 20 km s^{-1} between the two objects. Hence, the distance estimate of 730 ± 160 kpc is simply obtained by taking the ratio of the linear motion to the angular motion.

Multi-epoch phase-referenced observations of the evolution of complex sources have been made into movies, which cover periods of days to years. Examples of three online "movies" are the X-ray source SS433, which shows a precessing jet emitting blobs of plasma from a black hole/normal star binary [80]; the ejection of radio lobes and energy bursts from the neutron star Sco X-1 [81]; and the evolution of the radio galaxy 3C120 [82]. The expansion of a supernova in M81, which occurred in 1993, is shown in Figure 15 [83].

5. The Future

Recent advances in optical and infrared interferometry provide accuracies that are approaching that of radio arrays. The United States Naval Observatory is beginning operation of the six-element Navy Prototype Optical Interferometer (NPOI) at the Lowell Observatory in Arizona [84]. It is primarily an optical imager, although accurate astrometry is done. A European group is developing an infrared interferometer in conjunction with the Very Large Telescope (VLT) interferometers near Cerro Paranal, Chile. This European Southern Observatory project, Phase-Referenced

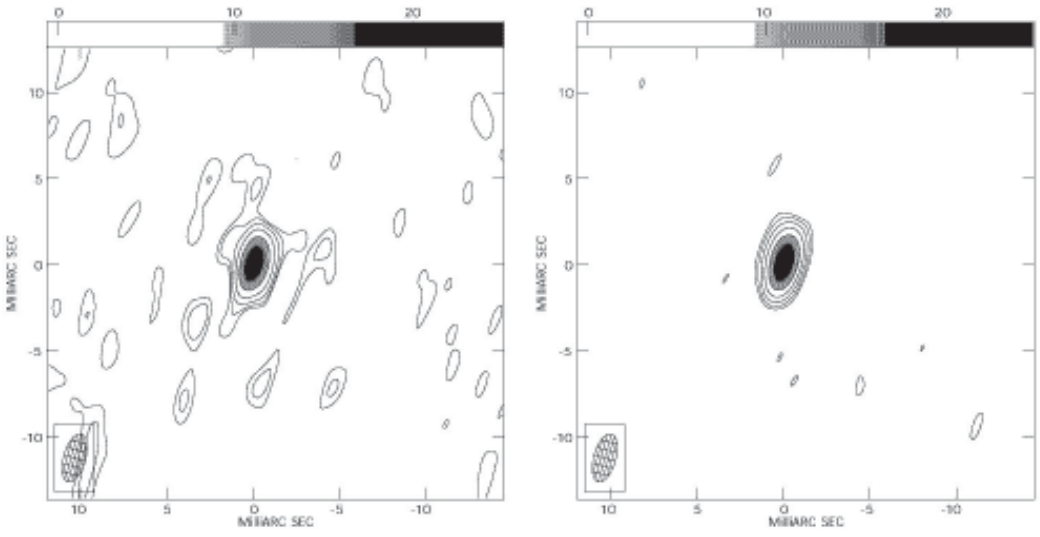

Figure 12. The use of two calibrators to improve image quality. The contour levels are at 0.6, 1.2, 2.4, 4.8, and 9.6 mJy/beam, and the gray-scale range is shown above each plot. The ellipse in the lower left shows the full-width at half-power resolution, and a deconvolution method was used to remove the effects of the point-spread function. (left) The image of the target after using one calibrator as reference. The peak flux density was 25.9 mJy, and the maximum sidelobe level was 1.7 mJy. (right) The image of the target after using two calibrators. The peak flux density was 27.5 mJy, and the maximum sidelobe level was 0.7 mJy. The radio source had a slight asymmetry to the north-east (upper left). The rms error in the source location decreased from 55 to 15 μarcsec.

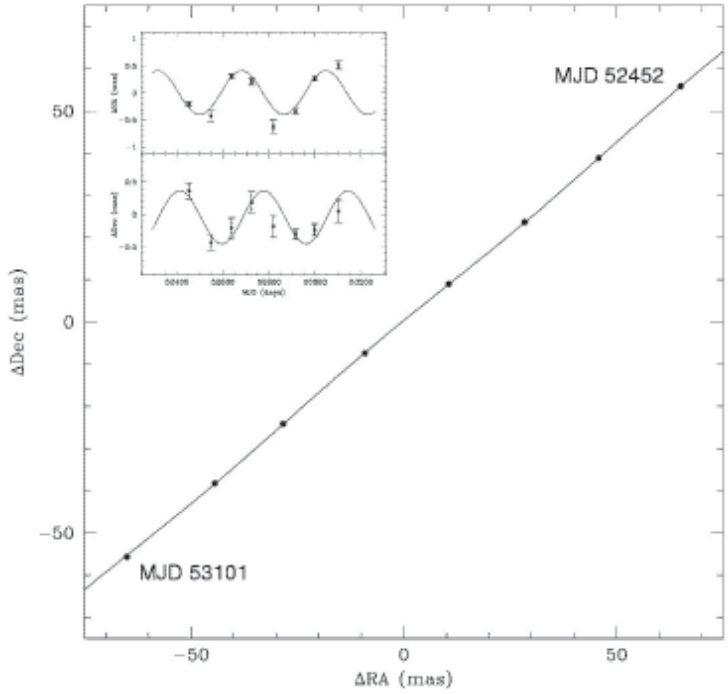

Figure 13. the parallax and proper motion of the pulsar B1508+55. The main plot shows the best-fit of the proper motion and parallax to eight observations over two years. The error estimates for each point were smaller than the size of the plots. The inlay shows the parallax part of the motion, with the best-fit proper motion subtracted. The proper motion was 73.61 ± 0.04 *marcsec* yr^{-1} *west,* 62.62 ± 0.09 *marcsec* yr^{-1} *south. The parallax was* 0.42 ± 0.04 *marcsec , giving a distance of* 2.4 ± 0.2 *kpc or* 7100 ± 700 *light years. This gave a linear proper motion of 1100 km* s^{-1}*, fast enough to be kicked out of the Milky Way galaxy.*

Imaging and Microarcsecond Astrometry (PRIMA) [85], is now under development. Because the optical and infrared refraction fluctuations between objects separated by less than about 10 arcsec in the sky are somewhat correlated over a few seconds of time, it is possible to measure the separation of two stars (one a bright calibrator, the other a weaker target) to an accuracy of 10 μarcsec between wavelengths of 1.2 to 20 μm. The Keck Interferometer is also being used to determine both images and accurate astrometry of stars [86].

Two space-based optical interferometers are proposed in the coming decades. The NASA Space Interferometry Mission (SIM) will be able to determine the relative positions of about 2000 bright stars with an accuracy of about 10 μarcsec [87, 88]. By bootstrapping the relative positions into a global grid and including the brightest 100 quasars, they hope to define an inertial frame with an accuracy of 4 μarcsec. The earliest launch date is 2012. The European Space Agency's Global Astrometric Interferometer for Astrophysics (GAIA) mission is a survey instrument that will measure 10^9 objects down to the 20th magnitude. Although not much more accurate than the present ICRF radio observations, the immense number of stars and quasars that it can observe will provide a more-accurate global radio/optical reference frame [89].

Significantly improved radio accuracy could be

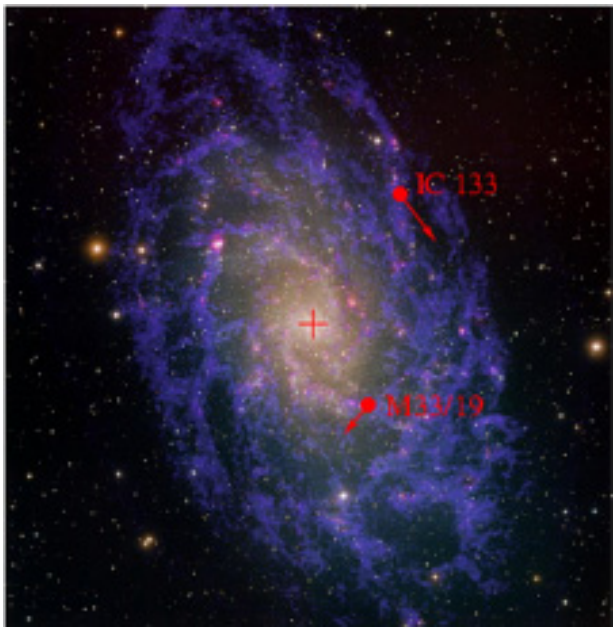

Figure 14. The relative motion of two maser sources in M33. The arrows show the expected motion, derived from the known rotation model of the galaxy, of the stimulated maser emission at 23.6 GHz in the atmosphere for two stars rotating around the center of M33. The radio observations of the relative angular motion of the two maser sources were made over a 2.5-year period. The ratio of the relative angular motion to the relative rotation velocity for these two objects gave the distance to M33 with an uncertainty of 15%.

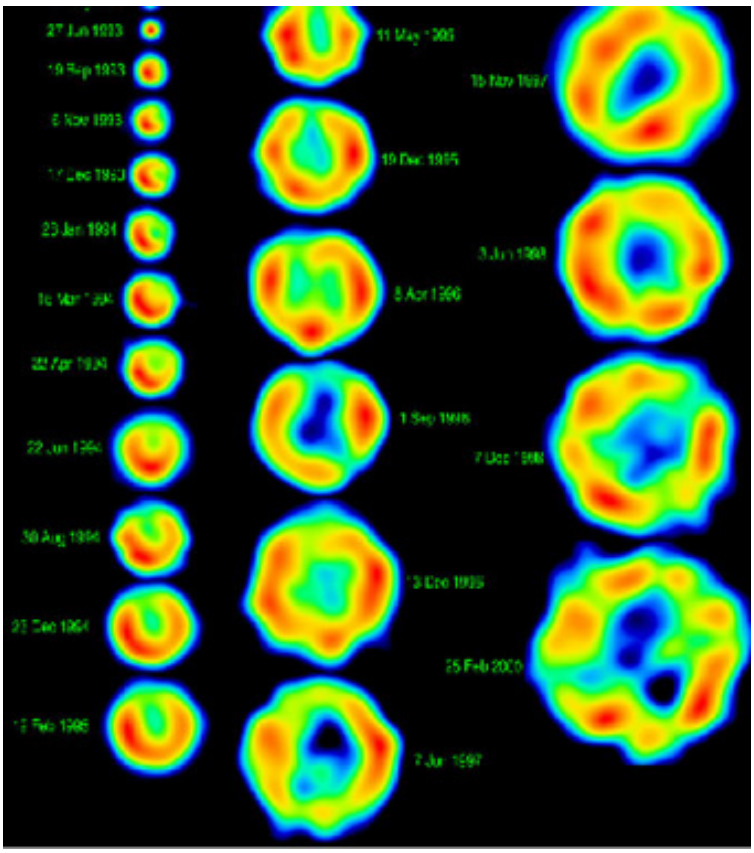

Figure 15. The evolution of the supernova 1993J in the galaxy M81. The observations were made using the VLBA + EVN arrays.

obtained with space-based telescopes, because of their higher resolution and lack of tropospheric and ionospheric delay contamination. However, many space antennas are needed, since correlation of any space antenna with a ground antenna would still be subject to tropospheric and ionospheric delay variations [90]. At present, there are two missions to place a small radio antenna in Earth orbit. Radioastron is a Russian-led program, with a possible launch in the next few years [91]. A Japanese program, VSOP-2, may be launched in 2012 [92].

The Square Kilometer Array (SKA) is being planned by an international consortium [91]. It will be over 100 times more sensitive than existing arrays, and will operate between 0.14 and 20 GHz, or higher. The astrometric capabilities, if sufficiently long baselines are part of the SKA design, will enable micro-arcsecond astrometric measurements to be made [92], both for relative and absolute astronomical measurements. The array is anticipated to be operating before 2020.

6. References

1. http://www.vlba.nrao.html.
2. http://www.evlbi.org.
3. http://veraserver.mtk.nao.ac.jp.
4. A. R. Thompson, J. M. Moran, and G. W. Swenson, *Interferometry and Synthesis in Radio Astronomy, Second Edition*, New York, John Wiley & Sons, 2001, pp. 342-352.
5. A. R. Thompson, J. M. Moran, and G. W. Swenson, *Interferometry and Synthesis in Radio Astronomy, Second Edition*, New York, John Wiley & Sons, 2001, pp. 353-356.
6. A. R. Whitney, "The Mark IV Data-Acquisition and Correlation System," in I. I. Mueller and B. Kolaczek (eds.), *Developments in Astrometry and Their Impact on Astrophysics and Geodynamics*, IAU Symp. 156, Dordrecht, Kluwer, 1993, pp. 515, 157.
7. J. D. Romney, "The VLBA GigaBit-Per-Second Data Recording System," *New Astronomy Reviews*, **43**, November 1999, pp. 523-526.
8. A. R. Whitney, "The Mark 5B VLBI Data System," *IVS 2004 General Meeting Proceedings*, 2004, pp. 177-181; (http://ivscc.gsfc.nasa.gov/publications/gm2004/whitney1/).
9. A. R. Whitney, H. F. Hinteregger, T. Kondo, and Y. Koyama, "Data Acquisition and Transport – Looking 2010 and Beyond," *IVS 2004 General Meeting Proceedings*, 2004, pp. 85-89; (http://ivscc.gsfc.nasa.gov/publications/gm2004/whitney2/).
10. S. Parsley, "eVLBI Research in the European VLBI Network," *IVS 2004 General Meeting Proceedings*, 2004, pp. 205-209; (http://ivscc.gsfc.nasa.gov/publications/gm2004/parsley/).
11. Y. Chikada, M. Ishiguro, H. Hirabayashi, M. Morimoto, K. I. Morita, T. Kanzawa, H. Iwashta, K. Nakazimi, S. I. Ishiwaka, T. Takashi, K. Handa, T. Kasuga, S. Okumura, T. Miyazawa, T. Nakazuru, K. Miura, and S. Nagasawa, "A 6 × 320 MHz 1024-Channel FFT Cross Spectrum Analyzer for Radio Astronomy, *Proc. IEEE*, **75**, 1987, pp. 1203-1287.
12. J. A. Benson, "The VLBA Correlator" in J. A. Zensus, P. J. Diamond, and P. J. Napier (eds.), *Very Long Baseline Interferometry and the VLA*, Astron. Soc. Pacific Conf. Ser., **82**, pp. 117-131.
13. H. Takeuchi, T. Kondo, Y. Koyama, and J. Nakajima, "VLBI@home – VLBI Correlator by GRID Computing System," *IVS 2004 General Meeting Proceedings*, 2004, pp. 200-204; (http://ivscc.gsfc.nasa.gov/publications/gm2004/

takeuchi/).
14. http://www.atnf.csiro.au/vlbi/evlbi2005/ presentations/evlbi_Workshop2/tingay_4th-eVLBI-workshop.ppt.
15. B. Clark, "Coherence in Radio Astronomy," *Synthesis Imaging in Radio Astronomy*, ASP Conf Series, **180**, 1999, pp. 1-10.
16. A. E. E. Rogers, "Very-Long-Baseline Interferometry with Large Bandwidth for Phase-Delay Measurements," *Radio Science*, **5**, 1970, pp 1239-1248.
17. http://www.bun.kyoto-u.ac.jp/ sim suchii/ mach.pr.html
18. W. M. Fricke, H. Schwan, and T. Lederle, "Fifth Fundamental Catalog, Part I," *Veroff. Astron. rechen Inst.*, 32, Heidelberg.
19. N. Capitaine, "The Essential Contribution of VLBI to Fundamental Astrometry," *IVS 2002 General Meeting Proceedings*, 2002, pp. 14-23; (http://ivscc.gsfc.nasa.gov/publications/gm2002/capitaine/).
20. E. M. Standish, "The Observational Basis for JPL's DE200, the Planetary Ephemerides of the Astronomical Almanac," *Astronomy and Astrophysics*, **233**, 1990, pp. 252-271.
21. S. Ferraz-Mello, B. Morando, J.-E. Arlot, *Dynamics, Ephemerides and Astrometry of the Solar System*, (IAU Symposium No. 172), Dordrecht, Kluwer, 1996.
22. N. Feissel and F. Mignard, "The Adoption of ICRS on 1 January 1998: Meaning and Consequences," *Astronomy and Astrophysics*, **331**, 1998, pp. L33-L36.
23. C. Ma, E. F. Arias, T. M. Eubanks, A. L. Fey, A.-M. Gontier, C. S. Jacobs, O. J. Sovers, B. A. Archinall, and P. Charlot, "The International Celestial Reference Frame as Realized by Very Long Baseline Interferometry," *Astronomical Journal*, **116**, 1998, pp. 516-546.
24. O. J. Sovers, J. L. Fanslow, and C. S. Jacobs, "Astrometry and Geodesy with Radio Interferometry: Experiments, Models, Results," *Reviews of Modern Physics*, **70**, 1998, pp. 1393-1454.
25. J. W. Ryan, T. A. Clark, C. Ma, D. Gordon, D. Capretee, and W. E. Himwhich, in D. E. Smith and D. L. Turcotte (eds.), *Contributions of Space Geodesy to Geodynamics, Earth Dynamics*, Washington, American Geophysical Union, 1993, pp. 37ff.
26. http://www.iers.org/iers/products/itrf.
27. M. Rothacher, "Combination of Space_Geodetic Techniques" *IVS 2002 General Meeting Proceedings*, 2002, pp. 33-41; (http://ivscc.gsfc.nasa.gov/publications/gm2002/rothacher).
28. V. Tesmer, H. Kutterer, and H. Drewes, "Simultaneous Estimation of a TRF, the CRP and a CRF," *IVS 2004 General Meeting Proceedings*, 2004, pp. 311-314; (http://ivscc.gsfc.nasa.gov/publications/gm2004/tesmer2/).
29. A. L. Fey, C. Ma, E. F. Arias, P. Charlot, M. Feissel-Vernier, A.-M. Gontier, C. S. Jacobs, J. Li and D. S. MacMillan, "The Second Extension of the International celestial Reference Frame: ICRF-EXT.2," *Astronomical Journal*, 2004, pp. 3587-3608.
30. D. Gordon, "VLBA Impact on Geodesy and Astrometry" *IVS 2004 General Meeting Proceedings*, 2004, pp. 351-355; (http://ivscc.gsfc.nasa.gov/publications/gm2004/gordon1/).
31. K. Baver, D. MacMillan, L. Petrov, and D. Gordon, "Analysis of the VLBI Intensive Sessions," *IVS 2004 General Meeting Proceedings*, 2004, pp. 394-398; (http://ivscc.gsfc.nasa.gov/publications/gm2004/baver/).
32. A. L. Fey, R. Ojha, J. E. Reynolds, S. P. Ellingsen, P. M. McCulloch, D. L. Jauncey and K. J. Johnston, "Astrometry of 25 Southern Hemisphere Radio Sources from a VLBI Short Baseline Survey," *Astronomical Journal*, **128**, 2004, pp. 2593-2598.
33. A. L. Fey, R. Ojha, D. L. Jauncey, K. K. Johnston, J. E. Reynolds, J. E. J. Lovell, A. E. Tzioumis, J. E. Quick, G. D. Nicolson, S. P. Ellingsen, P. M. McCulloch, and K. Yasuhiro, "Accurate Astrometry of 22 Southern Hemisphere Radio Sources," *Astronomical Journal*, **127**, 2004, pp. 1791-1795.
34. A. J. Beasley, D. Gordon, A. B. Peck, L. Petrov, D. S. MacMillan, E. B. Fomalont, and C. Ma, "The VLBA Calibrator Survey-VCS1," *Astrophysical Journal Supplement*, **141**, 2002, pp. 13-21.
35. E. B. Fomalont, L. Petrov, D. S. MacMillan, G. Gordon, and C. Ma, "The Second VLBA Calibrator Survey: VCS2," *Astronomical Journal*, **126**, 2003, pp. 2562-2566.
36. L. Petrov, Y. Y. Kovalev, E. B. Fomalont, and D. Gordon, "The Third VLBA Calibrator Survey – VCS3," *Astronomical Journal*, **129**, 2005, pp. 1163-1170.
37. M. Honma, O. Tomoaki, et al., "J-Net Galactic-Plane Survey of VLBI Radio Sources for VLBI Exploration of Radio Astronomy (VERA)," *Publications of the Astronomical Society of Japan*, **52**, 2000, pp 631-643.
38. M. A. C. Perryman, L. Lindegren, J. Kovalevsky, E. Hoeg, U. Bastian, P. L. Bernacca, and M. Crévé "The HIPPARCOS Catalog," *Astronomy and Astrophysics*, **323**, 1997, pp. L49-L52.
39. J. Kovalevsky, L. Lindegren, M. A. C. Perryman, P. D. Hemenway, K. J. Johnston, V. S. Kislyuk, J. F. Lestrade, L. V. Morrison, and I. Platais, Röser, "The HIPPARCOS Catalog as a Realisation of the Extragalactic Reference System," *Astronomy and Astrophysics*, **323**, 1997, pp. 620-633.
40. J. F. Lestrade, R. B. Phillips, D. L. Jones, and R. A. Preston, "VLBI Astrometry for Detection of Planets Orbiting Radio-Emitting Stars," *Astronomy and Space Science*, **212**, 1994, pp 251-260.
41. D. A. Boboltz, A. J. Fey, K. J. Johnston, M. J. Claussen, C. deVegt, N. Zacharias, and R. A. Gaume, "Astrometric Positions and Proper Motions of 19 Radio Stars," *Astronomical Journal*, **126**, 2003, pp. 484-493.
42. R. Dewey, M. R. Ojeda, C. R. Gwinn, D. L. Jones, and M. M. Davis, "VLBI Astrometry of the Millisecond Pulsar B1937+21," *Astronomical Journal*, **111**, 1996, pp. 315-319.
43. W. M. Folkner, P. Charlot, M. H. Finger, J. G. Williams, O. J. Sovers, X. Newhall, and E. M. Standish, "Determination of the Extragalactic-Planetary Frame Tie from Joint Analysis of Radio Interferometric and Lunar Laser Ranging Measurements," *Astronomy and Astrophysics*, **287**, 1994, pp, 279-289.
44. http://www.cv.nrao.edu/abridle/images.htm.
45. P. Charlot, "Modeling Radio Source Structure for Improved VLBI Data Analysis," *IVS 2002 General Meeting Proceedings*, 2002, pp. 233-242; (http://ivscc.gsfc.nasa.gov/publications/gm2002/charlot/).
46. O. J. Sovers, P. Charlot, A. L. Fey, D. Gordon, "Structure Corrections in Modeling VLBI Delays for RDV Data" *IVS 2002 General Meeting Proceedings*, 2002, pp. 243-247; (http://ivscc.gsfc.nasa.gov/publications/gm2002/sovers/)
47. J. Boehm and H. Schuh, "Vienna Mapping Function in VLBI Analyses," *IVS 2004 General Meeting Proceedings*, 2004, pp. 277-281; (http://ivscc.gsfc.nasa.gov/publications/gm2004/boehm1/).
48. A. E. Niell, "Preliminary Evaluation of Atmospheric Mapping Functions Based on Numerical Weather Models," *Phys. Chem. Earth*, **26**, 2001, pp. 475-480.
49. K. Takahei, H. Suga, Y. Ohuchi, H. Sutoh, M. Uchino, S. Mattori, M. Tsuda, Y. Saburi, Y. Koga, K. Hagimoto, T. Ikegami, "Laser-Pumped Cs Gas-Cell Type Atomic Clock for VLBI," *IVS 2002 General Meeting Proceedings*, 2002, pp. 189-194; (http://ivscc.gsfc.nasa.gov/publications/gm2002/takahei/).
50. A. R. Thompson, J. M. Moran, and G. W. Swenson, *Interferometry and Synthesis in Radio Astronomy, Second Edition*, New York, John Wiley & Sons, 2001, pp. 223-228.
51. H. Hirabayashi, H. Hirosawa, H. Kobayashi, Y. Murata, et al., "Overview and Initial Results of the Very Long Baseline Interferometry Space Observatory Programme," *Science*, **281**, 1998, pp. 1825-1829.
52. C. Ma, "Refinement of the ICRF," *IVS 2004 General Meeting Proceedings*, 2004, pp. 337-350; (http://ivscc.gsfc.nasa.gov/publications/gm2004/ma1/).
53. P. Charlot, "The ICRF: 2010 and Beyond," *IVS 2004 General Meeting Proceedings*, 2004, pp. 12-21; (http://ivscc.gsfc.nasa.gov/publications/gm2004/charlot/).
54. C. S. Jacobs, P. Charlot, E. B. Fomalont, D. Gordon, G. E. Lanyi, C. Ma, C. J. Naudet, O. J. Sovers, and L. D. Zhang,

"Extending the ICRF to Higher Radio Frequencies: 24 and 43 GHz Astrometry" *IVS 2004 General Meeting Proceedings*, 2004, pp. 75-79; (http://ivscc.gsfc.nasa.gov/publications/gm2004/jacobs1/).
55. D. A. Boboltz, A. L. Fey, P. Charlot, E .B. Fomalont, G. E. Lanyi, and L. D. Zhang, "Extending the ICRF to Higher Radio Frequencies – Imaging and Source Structure," *IVS 2004 General Meeting Proceedings*, 2004, pp. 361-365; (http://ivscc.gsfc.nasa.gov/publications/gm2004/boboltz/).
56. Chris Jacobs, "JPL VLBI Analysis Center IVS Annual Report for 2002," http://ivs.nict.go.jp/mirror/publications/ar2002/acjpl/.
57. A. J. Beasley and J. E. Conway, in J. A. Zensus, P. J. Diamond, and P. J. Napier (eds.), *Very Long Baseline Interferometry and the VLBA*, ASP Conf. Ser. 82, San Francisco, ASP, 1995, pp. 328-343.
58. R. W. Porcas and M. J. Rioja, "VLBI Phase-Referencing Investigations at 86 GHz," in E. Ros, Porcas, Lobanov, and J. A. Zensus (eds.), *Proceedings of the 6th VLBI Network Symposium*, http://www.mpifr-bonn.mpg.de/div/vlbi/evn2002/book/ RPorcas1.ps.gz.
59. N. Pradel, P. Charlot, and J.-F. Lestrade, "Astrometric Accuracy of Phase-Referenced Observations with the VLBA and EVN," *Astronomy and Astrophysics*, **452**, 2006, pp. 1099-1106.
60. Akihiro Doi, "Bigradient Phase Referencing," *Publications of the Astronomical Society of Japan*, **58**, 2006 (http://arxiv.org/abs/astro-ph/0604596).
61. T. Cornwell, and E. Fomalont, "Self-Calibration," in *Synthesis Imaging in Radio Astronomy*, ASP Conf Series, **180**, 1999, pp 187-199.
62. M. A. Garrett, J. M. Wrobel, and R. Rafaella, "The Deepest and Widest VLBI Survey Jet: VLBA+GBT 1.4 GHz Observations in Bootes, *New Astronomy Reviews*, **47**, September 2003, pp. 385-389.
63. C. J. Bradshaw, E. B. Fomalont, and B. J. Geldzahler, "High-Resolution Parallax Measurements of Scorpius X-1," *Astrophysical Journal*, **512**, 1999, pp. L121-L124.
64. E. B. Fomalont and L. Kogan, "Phase Referencing Using More than One Calibrator," AIPS Memo 111, 2004, pp. 1-11; (ftp://ftp.aoc.nrao.edu/pub/software/ aips/TEXT/PUBL/AIPSMEM111.PS).
65. J. A. Högbom, "Aperture Synthesis with a Non-Regular Distribution of Interferometric Baselines," *Astronomy and Astrophysics Supplement*, **15**, 1974, pp. 417-426.
66. E. B. Fomalont and S. M. Kopeikin, "The Measurement of the Light Deflection from Jupiter: Experimental Results," *Astrophysical Journal*, **598**, 2003, pp. 704-711.
67. A. Brunthaler, M. Reid, H. Flacke, L, J. Greenhill, and C. Henkel, "The Geometric Distance and Proper Motion of the Triangulum Galaxy (M33)," *Science*, **307**, 2005, pp. 1440-1443.
68. http://hpiers.obspm.fr/.
69. http://tycho.usno.navy.mil/time.html.
70. P. Charlot, R. M. Campbell, et al., "Improved Positions on Non-Geodetic EVN Telescopes," in E. Ros, Porcas, Lobanov, and J. A. Zensus (eds.), *Proceedings of the 6th VLBI Network Symposium*, http://http://www.mpifr-bonn.mpg.de/div/vlbi/evn2002/ book/PCharlot.ps.gz.
71. R. N. Treuhaft and G. E. Lanyi, "The Effect of the Dynamic Wet Troposphere on Radio Interferometric Measurements," *Radio Science*, **22**, 1987, pp. 251-165.
72. G. M. Resch, S. J. Keihm, G. E. Lanyi, R. P. Linfield, C. J. Naudet, A. L. Riley, H. W. Rosenberger, and A. B. Tanner, "The Media Calibration System for Cassini Radio Science: Part III," *IPN Progress Report*, **42-148**, February 15, 2002, pp. 1-12.
73. C. L. Carilli and M. A. Holdaway, "Tropospheric Phase Calibration in Millimeter Interferometry," *Radio Science*, **34**, 1999, pp. 817-826.
74. ftp://cddisa.gsfc.nasa.gov.pub/gps/products/ionex/.
75. A. R. Thompson, J. M. Moran, and G. W. Swenson, *Interferometry and Synthesis in Radio Astronomy, Second Edition*, New York, John Wiley & Sons, 2001, pp. 554-564.
76. N. Pradel, P. Charlot, and J.-F. Lestrade, "Astrometric Accuracy of Phase-referenced Observations with the VLBA and EVN," *Astronomy and Astrophysics*, 2006 (in press).
77. W. F. Brisken, J. M. Benson, A. J. Beasley, E. B. Fomalont, W. M. Goss, and S. E. Thorsett, "Measurement of the Parallax of PSR B0905+08 Using the VLBA," *Astrophysical Journal*, **541**, 2000, pp. 959-962.
78. M. Honma et al. "Multi-Epoch VERA Observations of OH34.8-01," *Publications of the Astronomical Society of Japan*, **57**, 2005, pp. 595-603.
79. W. H. Chatterjee et al., "Getting Its Kicks: A VLBA Parallax for the Hyperfast Pulsar, B1508+55," *Astrophysical Journal*, **630**, 2005, pp. 61-64
80. A. Mioduszewski, M. Rupen, C. Walker and M. Rupen, http://www.nrao.edu/pr/2004/ss433.
81. E. B. Fomalont, B. J. Geldzahler and C. J. Bradshaw, http://www.nrao.edu/pr/2001/scox1.
82. J. L. Gómez, A. P. Marscher, A. Alberdi, S. M. Jorstad and C. Garcia-Miró, http:// www.astro.brandeis.edu/movies/3C120.html.
83. M. F. Bietenholz, N. Bartel and M. Rupen, "SN 1993J VLBI. III. The Evolution of the Radio Shell," *Astrophysical Journal*, **597**, 2003, pp. 374-398.
84. J. T. Armstrong, D. Mozurkewich, L. J. Rickard, D. J. Hutter, J. A. Benson, P. F. Bowers, N. M. Elias II, C. A. Hummel, K. J. Johnston, D. F. Clark, J. H. Clark III, L. Ha, L.-C. Ling, N. M. White, and R. S. Simon, "The Navy Prototype Optical Interferometer," *Astrophysical Journal*, **496**, 1993, pp. 550-571; (http://arxiv.org/ pdf/astro-ph/0409611).
85. A. Quirrenbach, V. Coudedu Foresto, G. Daigne, K.-H. Hoffman, R. Hoffmann, M. Lattanzi, R. Osterbart, R. LePoole, D. Queloz, and F. Vakili, "PRIMA – Study for a Dual Beam Instrument for the VLT Interferometer," (http://www.eso.org/projects/vlti/ instru/prima/publink/prima_quirrenbachspie1998.ps).
86. G. T. vanBelle, A. F. Boden, M. M. Colavita, M. Shao, G. Vasisht, and J. K. Wallace, "Astrometry with the Keck Interferometer," in R. D. Reasonberg (ed.), *Astronomical Interferometry*, 1998, pp. 362-372.
87. M. Shao, S. Unwin, A. Boden, D. van Buren, and S. Kulkarni, "Space Interferometry Mission," in C. Eiroa et al. (eds.), *Infrared Space Interferometry: Astrophysics and the Study of Earth-Like Planets*, Dordrecht, Kluwer Academic, 1997, pp. 267ff.
88. http://planetquest.jpl.nasa.gov/SIM/Demo/.
89. http://www.astro.estec.esa.nl/GAIA/ Info_sheets.html.
90. J. C. Guirado, E. Ros, D. L. Jones, J. F. Lestrade, J. M. Marcaide, M. A. Perez-Torres, and R. A. Preston, "Space-VLBI Phase-Referencing Mapping and Astrometry," *Astronomy and Astrophysics*, **371**, 2000, pp. 766-770.
91. http://www.asc.rssi.ru/radioastron.
92. http://vsop.mtk.nao.ac.jp/vsop2/.
93. http://astrosun2.astro.cornell.edu/research/projects/ ska/main.shtml.
94. E. Fomalont and M. Reid, "Microarcsecond Astrometry Using the SKA," *New Astronomy Reviews*, **48**, 2004, pp 1473-1482.

Assessment of Health Effects Associated with Electromagnetic Fields by WHO, IARC, and ICNIRP

P. Vecchia

1. Introduction

Intensive research has been performed over the last decades on the biological and health effects of electromagnetic fields. The studies have covered different areas due to the complexity of the issue, including analysis of sources, exposure assessment, dosimetry, in vitro and in vivo biological research, and epidemiological surveys. An evaluation of possible risks of EMF exposure therefore requires a multidisciplinary approach, with expertise in the areas of biology, medicine, epidemiology, physics, and engineering. To this purpose, expert groups in several countries have been set up by national governments or health authorities.

At the international level, assessment of health effects associated with exposure to electric, magnetic, and electromagnetic fields had been performed in the past by the World Health Organization (WHO), jointly with the International Committee on Non-Ionizing Radiation of the International Radiation Protection Association (IRPA/INIRC) and the United Nations Environmental Program (UNEP). The outcome of such analyses consisted of comprehensive reports, published by WHO in the series of Environmental Health Criteria (EHC) Documents.

Following the wide research carried out in the last decades, and the substantial improvement of knowledge, an extensive revision of these documents was deemed necessary. However, some changes in the organization of work, with the participation of different partners and a better assignment of tasks, were introduced.

WHO still plays a central role. However, in 1996, an International EMF Project was launched to deal specifically with health issues related to EMF exposure [1], and the development of EHC Documents became one of the main goals of the project. The IRPA/INIRC was replaced in 1992 by the International Commission on Non-Ionizing Radiation Protection (ICNIRP), an independent non-governmental organization formally recognized by WHO and the International Labour Organization (ILO). The aim of ICNIRP is to provide guidance and advice on the health hazards of non-ionizing radiation exposure, including EMF.

Finally, the International Agency for Research on Cancer (IARC) has been formally involved in the process of health-risk assessment. In fact, while the possibility of long-term effects had received limited attention in previous reviews, the findings of epidemiological research and the concerns that these findings have raised with the public have made the risk of cancer a central issue.

The three organizations have established tight links, to avoid redundant activities and to create the most effective synergies. In particular, a specific sequence of actions has been established in order to provide to authorities, workers, and the public the best possible advice on all health issues related to EMF.

On commitment by WHO, ICNIRP carries out a comprehensive review of the scientific literature concerning exposure assessment and dosimetry, biological effects, and epidemiology. On its side, IARC evaluates the available data specific to a possible role of EMF in the development of cancer, with the final aim of classifying electric, magnetic, and electromagnetic fields based on their carcinogenic power. With these inputs, WHO performs a global evaluation of all possible health risks of EMF exposure. Finally, ICNIRP uses the conclusions of all of the above steps to revise and update its guidelines, as appropriate. The actions are therefore complementary. However, each organization has its own criteria, depending also on its mission. A clarification of the different methodologies is therefore useful for a better understanding of the whole process.

Paolo Vecchia is with the National Institute of Health, Viale Regina Elena, 299 – 00141 Rome, Italy; e-mail: paolo.vecchia@iss.infn.it.

This paper is based on the invited Commission K Tutorial Lecture given at the XXVIIIth General Assembly of URSI, October 25, 2005, New Delhi, India.

2. The IARC Criteria of Risk Assessment

IARC scientifically evaluates carcinogenic risks to humans through a program the objective of which is to prepare, with the help of international working groups of experts, critical reviews of the scientific literature relative to carcinogenicity of a wide range of human exposures. The reviews are published in the form of monographs [2]. The evidence for carcinogenicity is separately evaluated for studies on humans and experimental animals, using standard terms that include *sufficient evidence*, *limited evidence*, *inadequate evidence*, and *evidence suggesting lack of carcinogenicity*. Other data relevant to the carcinogenic action are also considered; these include, e.g., the results of in vitro studies or of studies on the interaction mechanisms of the agent with biological systems. As the final step, based on the overall strength of evidence the agent is classified as either *carcinogenic to humans* (group 1); *probably carcinogenic to humans* (group 2A); *possibly carcinogenic to humans* (group 2B); *not classifiable as to its carcinogenicity to humans* (group 3); or *probably not carcinogenic to humans* (group 4).

It is important to note that the evaluation of IARC represents only the first step in the assessment of carcinogenic risks, consisting of the qualitative judgment of the strength of the available evidence that certain exposures could alter the incidence of cancer in humans. The second step – that is, the quantitative estimation of risk – is not part of the IARC monographs. In other words, IARC assesses the credibility that a given agent in particular electromagnetic fields may be a cause of cancer, but does not estimate the dimension of the possible health impact.

IARC explicitly notes that its mandate is purely scientific, and recognizes that its evaluations represent only part of the information on which regulatory measures may be based. Other components of regulatory decisions may vary from one situation to another and from country to country, responding to different socioeconomic and national priorities. Therefore, no recommendation is given by IARC with regard to regulation or legislation. Such recommendations are the responsibility of individual governments and other international organizations.

3. The ICNIRP Criteria of Risk Assessment

ICNIRP carries out independent reviews of the scientific literature on the health effects of electromagnetic fields, and of biological effects that may be relevant for health [3]. Cancer effects are included in the review: the evaluations of IARC, where available, are obviously taken into account, but not uncritically accepted a priori.

These reviews are the first step in a process to finalize the development of protection standards, and it is the opinion of ICNIRP that only established effects may form the basis for science-based standards. According to generally accepted scientific criteria, only those effects that are consistently indicated by different studies meeting adequate criteria of scientific quality are accepted as established. Such effects generally become relevant above given levels of exposure, which may be different for different groups of the population (e.g., children, the elderly, or people with health impairment). Special attention is therefore paid to the so-called *critical effect*, i.e., the effect that becomes relevant at the lowest exposure level. The exposure limits recommended by ICNIRP aim at protecting against the critical effect, and are conservative with respect to any other established hazard.

If available data allow the identification of an adverse effect, but not a detection of a threshold, the scope of ICNIRP is to analyze the risk in terms of consequences that could be quantified. Such risks are therefore evaluated by ICNIRP in terms of both plausibility and health consequences.

ICNIRP also recognizes that science-based risk assessment is only one component of health policies, and that the risk management involves social and economic considerations, which, however, fall outside its scope.

4. The WHO Criteria of Risk Assessment

In the framework of the International EMF Project, and in the first phase of it, a preliminary evaluation of the available literature on biological and health effects of electromagnetic fields has been planned and carried out. The objective was to identify possible gaps in knowledge, or uncertainties and inconsistencies in the data, which required additional research before a reliable risk assessment could be performed. This activity was mainly performed in collaboration with ICNIRP, through the organization of appropriate workshops.

When the recommended research in a given area has been completed, and the body of evidence is considered adequate, WHO commissions an expert group to draft a comprehensive report on all the aspects of electromagnetic field exposures that may be relevant for health. While the documents produced by IARC and ICNIRP are fundamental inputs to this process, further independent judgment is expressed by WHO experts.

The procedure of evaluation of the scientific literature, the selection criteria, and the balance of evidence do not differ from IARC and ICNIRP. However, the scope of WHO is in some respects wider than other organizations, and risks of electromagnetic fields are put into a broader perspective. In particular, WHO acknowledges that concern and worries have been expressed by the public that cannot be simply disregarded as nonscientific. Apart from other

social considerations, anxiety is per se a health detriment, and as such should be prevented or mitigated.

WHO stresses the necessity that protection standards be based on the best available science, and not be undermined by arbitrary measures taken for the sake of precaution. At the same time, it recognizes that under given circumstances, precautionary actions complementary to – but not conflicting with – science-based standards may be justified by uncertainties in knowledge, or by the public concern. This may require a consideration different from IARC and ICNIRP for some pieces of literature, including, for example, medical case reports, or research findings that are only preliminary or not adequately replicated.

5. Present Risk Assessments

The procedure outlined in the introduction has been separately implemented for different types of EMF, namely static magnetic fields, extremely low-frequency (ELF) electric and magnetic fields, and radio-frequency (RF) electromagnetic fields. The present states of advancement are different, depending mainly on the research in progress.

5.1 Static Magnetic Fields

Existing protection standards, including ICNIRP guidelines [4], are largely based on an EHC Document issued by WHO in 1987 [5].

IARC evaluated static magnetic fields in 2001, and published the corresponding monograph in 2002 [6]. The expert group concluded that there was inadequate evidence for carcinogenicity in humans, whereas no data relevant to the carcinogenicity in experimental animals were available. Consequently, static magnetic fields were evaluated as non-classifiable as to their carcinogenicity to humans.

In 2003, ICNIRP issued a comprehensive review of exposure to, and effects of, static and ELF fields [7]. It concluded that the studies on static magnetic fields, although limited in their number, only indicate the possibility of minor biological effects, even at quite high magnetic flux densities, with no plausible implications for human health.

In December, 2004, WHO convened a task group to finalize the updated EHC Document, which is expected to be published in the near future. The conclusions are therefore not yet available. However, the draft report, which was open to comments, presented a picture that is consistent with those of ICNIRP and IARC: several biological effects have been identified, such as orientation of magnetically polarized biological structures, but the studies of effects on humans are mostly negative.

No health risks are therefore envisaged at present exposure levels. Nevertheless, it was noted that the development of new technologies using very intense magnetic fields, especially for medical diagnosis, requires special attention, precaution, and focused research.

5.2 ELF Electric and Magnetic Fields

The EHC Document relative to ELF electric and magnetic fields dates back to 1984 [8], and does not include most relevant studies that have been carried out after that date. This is especially true for the epidemiological research, the impetus for which started in the mid-1980s.

The IARC monograph [6] deals mainly with ELF magnetic fields. The effects of electric fields are, in fact, expected to be low based on theoretical grounds, and have actually not been indicated by experimental research. Although limited, the available data allowed an evaluation of the electric fields, which have been considered as non-classifiable as to their carcinogenicity to humans.

On the contrary, magnetic fields have been classified as possibly carcinogenic (group 2B), based on a limited evidence of carcinogenicity in relation to childhood leukemia. In the opinion of the expert group, the studies on experimental animals have provided only inadequate evidence of carcinogenicity.

The extensive review of ICNIRP [7] reported a variety of biological effects. However, those findings that have been consistently replicated by different studies do not suggest adverse consequences to human health at exposures below the limits recommended by present guidelines. This is consistent with the conclusion of IARC, according to which the results of laboratory studies do not give biological plausibility to the hypothesis of a causal relationship between exposure and cancer. Also, the judgment on the weight of epidemiological evidence is in full agreement with IARC.

Of special interest is the evaluation of subjective symptoms, i.e., disturbances that are reported by individuals with alleged hypersensitivity to EMF. ICNIRP concluded that these studies do not indicate any general ability of the subjects to react differently to the presence or absence of the field in controlled experiments. On the contrary, more recent studies have confirmed the existence of acute effects – related to the induction of internal electric voltages and currents –following exposure to electric and magnetic fields of intensity above the reference levels of the ICNIRP guidelines.

The EHC Document will be finalized by an ad hoc task group in October, 2005, and is expected to be published in the spring of 2006.

5.3 Radio-Frequency Fields

The very rapid development of mobile telephony and other communication technologies has triggered a great deal of research activity, and the scientific data base has increased enormously in the last few years. A revision of the EHC Document, issued in 1993 [9], is therefore urgently needed. However, some important studies are still in progress, the findings of which will have a major impact on the final evaluation of health risks. These include the EC-sponsored Interphone, a case-control study on the development of head and neck cancer in relation to the use of mobile phones, which is being carried out in parallel, and with a common protocol, by 14 teams in 13 countries.

The evaluation of cancer effects by IARC is tentatively scheduled in 2006, following the conclusion of the Interphone study. In the meantime, ICNIRP has appointed a task group to produce a comprehensive report on exposure to, and biological and health effects of, RF fields, which is expected to be completed by the end of 2006.

An updated EHC Document can be reasonably expected to be issued by WHO in 2007.

While the review process is ongoing, both WHO and ICNIRP maintain their judgment [10, 11] that the only established health effects of RF fields are acute in nature, and related to an increase of the general or local body temperature following absorption of electromagnetic energy by tissues (thermal effects).

6. Impact on Protection Policies

The global process of risk assessment requires a long time. Several years have passed since the publication of the last Environmental Health Criteria Documents, and of the ICNIRP guidelines [4, 11]. However, that does not mean that the status of knowledge is analyzed by international organizations only at large intervals. On the contrary, both WHO and ICNIRP continuously monitor the advancement of research, and suggest priorities for future studies. The evaluations of IARC are also never definitive, and the classification of an agent can be upgraded or downgraded if new evidence emerges that justifies doing so.

The common objective of the international organizations is to provide advice based on the most comprehensive and updated scientific knowledge. The critical reviews that have been completed or are in progress will provide a solid rationale for advice to authorities and the public, including revised versions of the guidelines.

However, in the opinion of ICNIRP the most recent data do not substantially change the general picture on which the present standards were based. While some refinement or clarification statements may be appropriate, there is no justification for major changes, and no need for urgent revisions of the ICNIRP guidelines.

7. References

1. WHO, "Electromagnetic Fields and Public Health: The International EMF Project" (Fact Sheet 181), http://www.who.int/docstore/peh-emf/publications/ facts_press/efact/efs181.html.
2. IARC, "Preamble to IARC Monographs," http://www-cie.iarc.fr/monoeval/preamble.html.
3. ICNIRP, "General Approach to Protection Against Non-Ionizing Radiation," *Health Phys.*, **82**, April, 2002, pp. 540-548; available at: http://www.icnirp.org/ documents/philosophy.pdf.
4. ICNIRP, "Guidelines on Limits of Exposure to Static Magnetic Fields," *Health Phys.*, **66**, 1994, pp. 100-106; available at: http://www.icnirp.org/documents/static.pdf.
5. WHO, *Magnetic Fields*, Environmental Health Criteria Document 69, Geneva, World Health Organization, 1987.
6. IARC, "Non-Ionising Radiation Part 1: Static and Extremely Low Frequency (ELF) Electric and Magnetic Fields," *Monographs on the Evaluation of Carcinogenic Risk to Humans*, **80**, 2002, Lyon, International Agency for Research on Cancer.
7. R. Matthes, A. F. McKinlay, J. H. Bernhardt, P. Vecchia, and B. Veyret (eds.), *Exposure to Static and Low frequency Electromagnetic Fields, Biological Effects and Health Consequences (0-100 kHz)*, Munich, International Commission on Non Ionizing Radiation Protection, 2003.
8. WHO, *Extremely Low Frequency (ELF) Fields*, Environmental Health Criteria Document 35, Geneva, World Health Organization, 1984.
9. WHO, *Electromagnetic Fields (300 Hz to 300 GHz)*, Environmental Health Criteria Document 137, Geneva, World Health Organization, 1993.
10. WHO, "Electromagnetic Fields and Public Health: Health Effects of Radiofrequency Fields" (Fact Sheet 183), http://www.who.int/docstore/peh-emf/ publications/facts_press/efact/efs183.html.
11. ICNIRP, "Guidelines for Limiting Exposure to Time-Varying Electric, Magnetic, and Electromagnetic Fields (up to 300 GHz)," *Health Phys.*, **74**, 1998, pp. 494-522; available at http://www.icnirp.org/documents/ emfgdl.pdf.

Kilometric Continuum Radiation

J.L. Green
S. Boardsen

Abstract

The kilometric continuum (KC) is the high-frequency component (~100 kHz to ~800 kHz) of the non-thermal continuum (NTC). Unlike the lower-frequency portion of the non-thermal continuum (~5 kHz to ~100 kHz), the source of which is around the dawn sector, the source of the kilometric continuum occurs at all magnetic local times. For most events, the latitudinal beaming of the kilometric continuum as observed by GEOTAIL is restricted to $\pm 15°$ magnetic latitude. The kilometric continuum has been observed during periods of both low and strong geomagnetic activity, with no significant correlation of wave intensity with K_p index. However, statistically, the maximum observed frequency of the kilometric continuum emission tends to increase with K_p index; the effect is more pronounced around solar maximum, but is also detected near solar minimum. There is strong evidence that the source region of the kilometric continuum is from the equatorial plasmapause during periods when a portion of the plasmapause moves significantly inwards from its nominal position. Case studies have shown that kilometric-continuum emissions are nearly always associated with plasmaspheric notches, shoulders, and tails. There is a recent focus on trying to understand the banded frequency structure of this emission, and its relationship to plasmaspheric density ducts and irregularities in the source region.

1. Introduction

There are two escaping electromagnetic emissions at radio frequencies that can be measured outside the influence of the Earth's magnetic field, which are generated within the Earth's magnetosphere. They are the auroral kilometric radiation (AKR) and the non-thermal continuum radiation (NTC). Even though they are generated over nearly the same frequency range (~5 kHz to 800 kHz), their sources and generation mechanisms are completely different. As its name implies, auroral kilometric radiation is associated with discrete auroral arcs, and is generated by the Doppler-shifted gyro-emission. On the other hand, the source region of the non-thermal continuum is believed to be embedded in the plasmapause or outer plasmasphere region (see [1] for an explanation of the plasmasphere), and its generation mechanism is not well understood.

The non-thermal continuum is one of the fundamental electromagnetic emissions in planetary magnetospheres (c.f. the review by [2]). It has been observed in every planetary magnetosphere visited by spacecraft with wave instruments, and even found to be generated in the magnetosphere of the Galilean moon Ganymede [3]. Although this emission has been observed and studied for more than 35 years, there are still several unverified theories of how this emission is generated, and much more we don't know about the emission and its relationship to plasmaspheric dynamics.

The non-thermal continuum is observed over a very broad frequency range, from as low as 5 kHz [4, 5] to as high as 800 kHz [6], and is observed to propagate largely in the free-space L-O mode. Even though its name, non-thermal continuum, refers to an emission with a continuous spectrum, this is only the case for the lowest-frequency portion of the emission. In fact, the non-thermal continuum is typically made up of discrete narrow-frequency emission bands, and in some cases is found to be associated with strong narrowband electrostatic emissions at the plasmapause at low latitudes [7]. The non-thermal-continuum emission spectrum has been delineated as either "trapped" within the Earth's magnetosphere or "escaping" from the magnetosphere. However, it is now clear that from recent observations a new component of the non-thermal continuum has now been determined, called the kilometric continuum (KC). For the kilometric continuum, the emission is generated only at the high-frequency portion of the spectrum (above 100 kHz) by the same mechanism as the

James Green is with the NASA/Goddard Space Flight Center, Greenbelt, MD 20771 USA; e-mail: James.Green@nasa.gov.
Scott Boardsen was with L3 Communications GSI, NASA Goddard Space Flight Center, Greenbelt, MD 20771 USA. He is now with UMBC/GEST, NASA Goddard Space Flight Center, Greenbelt, MD 20771 USA.

This is one of the invited *Reviews of Radio Science* from Commission H.

lower-frequency non-thermal continuum emission. It is important to note that another low-frequency continuous electromagnetic emission in the 1 to 4 kHz frequency range, believed to be generated in the plasma-sheet boundary layer of the distant magnetotail, named the lobe-trapped-continuum radiation or LTCR (see, for example, [8, 9]), has been observed to be trapped in the tail lobes. But it is uncertain if the lobe-trapped continuum and the non-thermal continuum are generated by the same mechanism, and therefore the lobe-trapped continuum will not be discussed further in this review.

The purpose of this paper is to provide a review of the current state of knowledge about the kilometric continuum, and to suggest future research directions that would yield a better understanding of the non-thermal-continuum emission mechanism.

2. Overview of Non-Thermal Continuum

Recent non-thermal continuum research has focused on improving our understanding of the source location, emission-cone characteristics, and detailed spectral measurements, primarily in the kilometric frequency range. Much of what has emerged from these studies in terms of source location is summarized in Figure 1 (adapted from [10]). The lower-frequency trapped and escaping continuum is typically generated in the pre-noon local time sector [4, 11], and has been called the "normal continuum" by a number of authors (e.g., [12, 6]). The continuum enhancement is generated in the morning sector [12-14], and the kilometric continuum is generated in deep plasmaspheric notch structures that co-rotate with the plasmasphere [15]. Figure 1 shows that the non-thermal continuum is made up of narrow emission bands, except for the trapped continuum (lower-left panel) observed by the wideband instrument on IMP-6, which has a much more continuous frequency-emission structure. It was from observations of the trapped component of the continuum that the name of this emission originates.

2.1 Trapped and Escaping Non-Thermal Continuum

From its unique polar-orbiting vantage point, the IMAGE/RPI instrument has observed the non-thermal continuum over a large frequency range at many local times. Figure 2 shows a frequency-time spectrogram from the RPI instrument during a pass of IMAGE through the magnetic equator. The non-thermal continuum extends from about 30 kHz to about 500 kHz, forming a Christmas-tree pattern in the spectrogram, nearly symmetric about the magnetic equator, which is clearly delineated by the

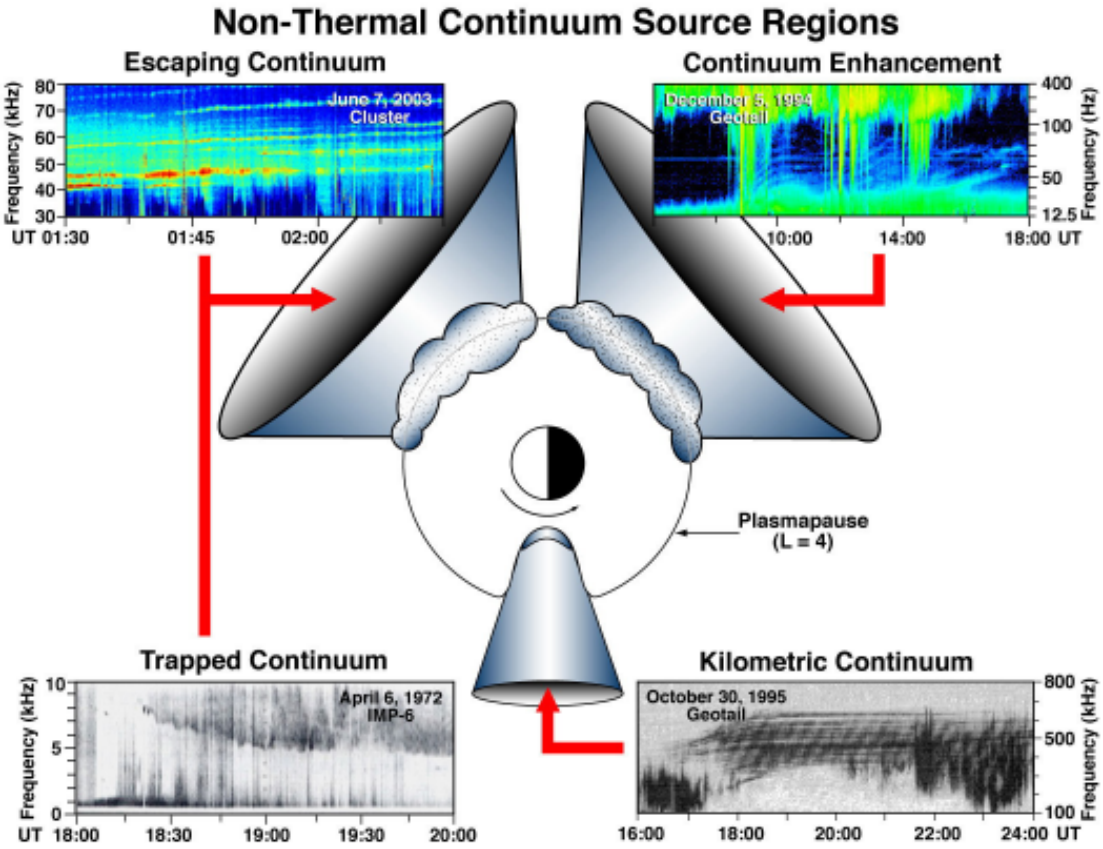

Figure 1. The observed source locations of the escaping (after [22]), trapped (after [39]), kilometric (after [6]), and continuum-enhancement (after [12]) emissions.

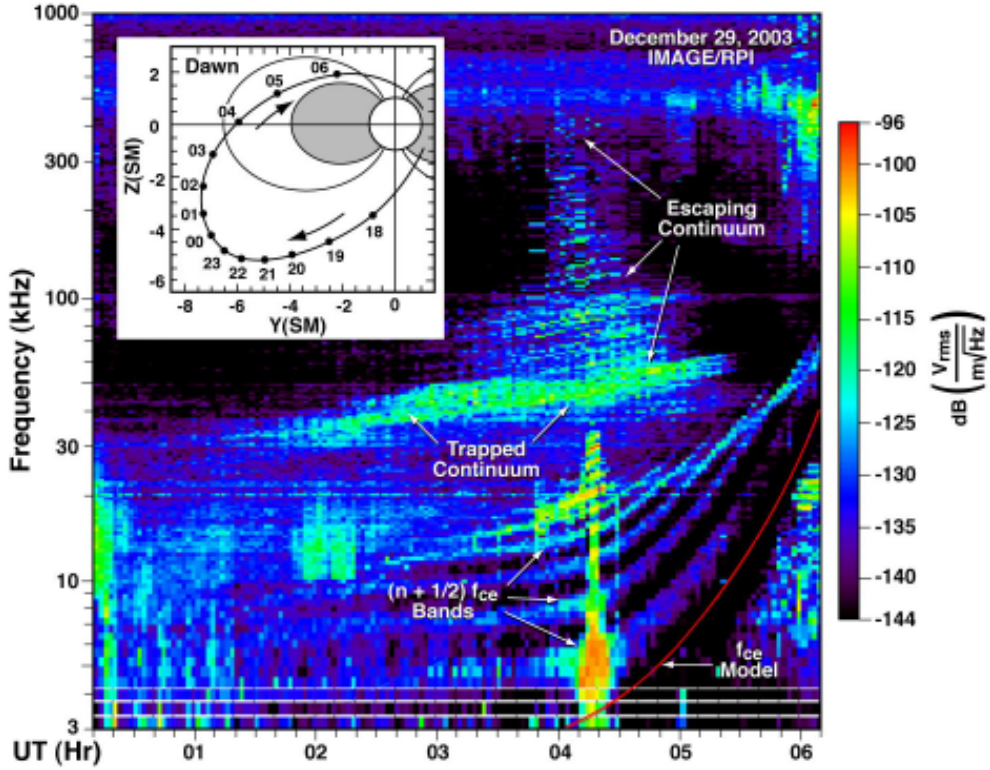

Figure 2. An RPI frequency-time spectrogram taken during a passage through the magnetic equator on the dawn side (see orbit insert). The Christmas-tree pattern of the non-thermal continuum is clearly shown nearly centered about the magnetic equator, delineated by the intense electrostatic emissions. These "normal continuum" emissions contain both magnetospherically trapped and escaping emissions.

increased intensity of the $(n+1/2)f_{ce}$ (cyclotron frequency) electrostatic-emission bands. The orbital position of the IMAGE during these observations is shown in the upper-left panel of the spectrogram in Figure 2. Due to the relative weak nature of the emission, the non-thermal continuum observations in Figure 2 were made during quiet geomagnetic times on the dawn side of the magnetosphere. At frequencies less than the magnetopause plasma frequency (~40 kHz in this example), the continuum radiation has been referred to as the "trapped" component [16], since it is observed primarily in the magnetospheric density cavity between the plasmapause and magnetopause. The trapped continuum spectrum is observed as a broadband emission, with very little frequency structure. The broadband structure of the trapped continuum spectrum is believed to be produced from a series of narrowband emissions at slightly different frequencies. It is produced from an extended source region at the plasmapause, the emission of which then mixes, due to multiple reflections (with some Doppler broadening) in the magnetospheric density cavity. As shown in Figure 2, the trapped continuum is observed first (the widest part of the Christmas-tree pattern), since multiple reflections from the magnetopause broadens its angular distribution [17].

The non-thermal continuum at frequencies above the magnetopause plasma frequency has been referred to as the "escaping" component [18], since it propagates from the Earth's plasmapause to well outside the magnetosphere. From Figure 2, the escaping component extends from above ~40 kHz. A common characteristic of all the escaping continuum radiation is that it has narrow frequency bands of emissions, showing that the name continuum is not entirely descriptive of the radiation in this frequency range. Although there are few published examples of normal continuum radiation extending above 100 kHz, Figure 2 shows that the high-frequency portion of the non-thermal continuum is beamed within a few degrees around the magnetic equator, and is the weakest portion of the emission, in this example.

2.2 Enhanced Continuum

Another type of continuum that is also observed is called the enhanced continuum (see the upper-right panel of Figure 1). The enhanced continuum is characterized by a strong variation in intensity and frequency, and has been observed to last for several hours [12-14]. The spectrum of the enhanced continuum is distinct, with discrete emissions at almost uniform spacing. The spacing of the discrete enhanced continuum is believed to be at the electron cyclotron frequency, with the source embedded in the plasmapause. This has allowed one to predict the radial location of the source, and if the wave direction can be determined, the location of the source in magnetic local time (MLT) can also be inferred. Direction-finding indicates that these emissions originate at midnight and propagate

dawn-ward. Gough [13] interpreted this to be due to the inward motion of the plasmapause due to enhanced convection, while Filbert and Kellogg [14] associated it with the dusk-to-dawn motions of injected electrons.

2.3 Kilometric Continuum

The kilometric continuum (KC) is observed in the 100-800 kHz frequency range and, as such, once generated, it escapes the magnetosphere. It is important to note that the kilometric continuum is always observed without an accompanying lower-frequency trapped component. Hashimoto et al. [6] discovered this type of emission, and sparked considerable interest in the further understanding of various aspects of this radiation that make it different from its lower-frequency trapped and escaping counterpart, generated in the pre-noon sector and shown in Figure 1. The lower-right-hand panel of Figure 1 clearly shows the discrete emission bands of the kilometric continuum extending from 17-24 UT. The frequency range for the kilometric continuum is approximately the frequency range of auroral kilometric radiation (AKR), but as shown in the lower-right-hand panel of Figure 1, there are significant differences that can be used to easily distinguish between these two emissions. The kilometric continuum has a narrowband structure over a number of discrete frequencies, while auroral kilometric radiation is observed to be a broadband and sporadic emission, and can be seen from 16-17:00 and from 21:30 to 24:00 UT in that spectrogram.

The kilometric continuum has been observed at all local times, although it has been difficult to make a positive identification of the emission during the times when GEOTAIL (see [19] for an overview of wave observations by GEOTAIL) was in the late evening or early morning local-time sector when auroral kilometric radiation was active [6]. From GEOTAIL and IMAGE observations, Hashimoto et al. [6] and Green et al. [20] found that the kilometric continuum is confined to a narrow latitude range of approximately 15° about the magnetic equator. Although these characteristics make it different from the normal continuum discussed in the previous section, the similar spectral characteristics of the emission and its relationship to the plasmapause supports the conclusion by Menietti et al. [21] from Polar observations that the radiation is generated by the same mechanism.

Recent observations from the Whisper instrument on Cluster by Décréau et al. [22] and Darrouzet et al. [23] point out the importance of small-scale density structures in locally amplifying the low-frequency component of the non-thermal continuum. For the kilometric continuum, Green et al. [15] showed that in one example, the field lines threading the kilometric-continuum source region supported high-frequency RPI sounder echoes. The conditions in the plasma that support field-aligned high-frequency sounder echoes were shown by Fung and Green [24] to be field-aligned density ducts, with density variations from 2% to 10% perpendicular to the local magnetic field. The density ducts associated with the kilometric-continuum sources appear to be completely consistent with the Cluster observations of density variations in the low-frequency non-thermal-continuum source regions, since field-aligned density ducts would have the appearance of small-scale density structures by the in situ Cluster observations. The similarities in these observations also lend support to the conclusion that the kilometric continuum is generated by the same mechanism as the lower frequency non-thermal continuum.

At lower frequencies, beaming of continuum radiation around the magnetic equator to latitudes as high as 50° has also been observed by Jones et al. [25] (from 80 to 100 kHz), by Morgan and Gurnett [26] (from 45 to 154 kHz), and by Green and Boardsen [17] (from 24 to 56 kHz). The narrow beaming of the kilometric continuum in magnetic latitude has made this emission difficult to routinely observe, or observable only for short periods of time, except for equatorial-orbiting spacecraft with the proper instrumentation, such as GEOTAIL.

Kuril'chik et al. [27] presented observations of kilometric continuum at 252 kHz and 500 kHz from the AKR-X experiment on the Interball-1 Tail Probe. They found that the latitudinal extent of the emission cone varied from 1° to 6° during solar minimum, and from 10° to 20° during solar maximum. Using PWI data onboard the GEOTAIL spacecraft, Hashimoto et al. [28] could not confirm this latitudinal difference with solar cycle. In addition, Kuril'chik et al. [27] also noted that the kilometric continuum was observed more often during solar minimum than solar maximum. Once again, in contrast, Hashimoto et al. [28] found only a slight difference in occurrence with solar cycle, and had more observations of the kilometric continuum during solar maximum than in solar minimum. However, both papers confirmed a high probability of occurrence of observing the kilometric continuum about the magnetic equator. The difference between these studies may be the result of viewing perspective, with GEOTAIL largely orbiting in the equatorial region and Interball-1 in a more-polar (65° inclination) orbit, with significantly fewer chances overall to observe kilometric continuum emissions.

Due to the high emission frequency of the kilometric continuum and its lack of correlation with geomagnetic activity, the source of the kilometric continuum was originally believed to lie deep within the plasmasphere [6]. Although there are still some instances of kilometric continuum observed deep within the plasmasphere (see [28]), it is now generally believed that the majority of kilometric-continuum emissions originate from the equatorial plasmapause under conditions where a small part of the plasmapause has moved inwards from its nominal position. This is indirectly supported by Figure 3, which is a scatter plot of the maximum frequency of the kilometric continuum observed by GEOTAIL as a function of K_p index, using observations from the study by Green et al.

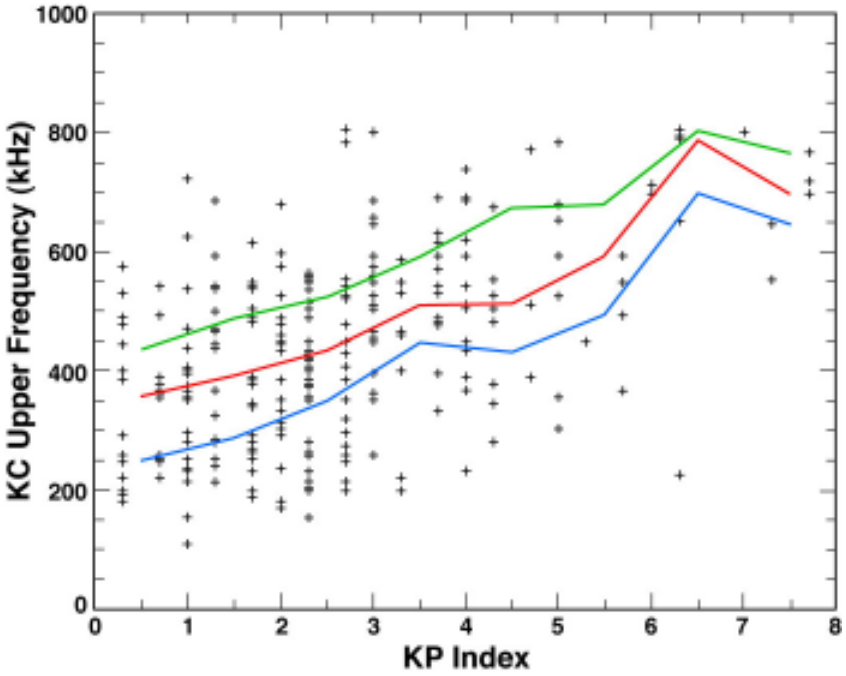

Figure 3. A scatter plot of the maximum frequency of kilometric continuum as observed by GEOTAIL around solar max as a function of the K_p index.

[20]. The centerline is the median, the bottom line is the 25th percentile, and the top line is the 75th percentile, computed by binning the upper frequency data in bins of K_p in ranges of 1. Figure 3 shows that even though the kilometric continuum occurs at all ranges of K_p, its maximum frequency tends to increase as the K_p index increases. A similar but weaker trend was observed by Hashimoto et al. [6] using GEOTAIL observations nearer to solar minimum. Since statistically the plasmapause moves inwards as K_p increases, resulting in a greater plasma-density drop across the plasmapause, one would expect the non-thermal continuum to be generated at higher frequencies in the kilometric-continuum range if these emissions originated from the plasmapause.

The source region for the kilometric continuum was originally suggested by Carpenter et al. [29] as coming from plasmaspheric cavities. However, more recently Green et al. [15] and Green et al. [20] clearly identified the kilometric continuum as being generated at the plasmapause, deep within notch structures that approximately co-rotate with the Earth. Figure 4 has been adapted from Figure 8 of Green et al. [15] and Figure 1 of Green et al. [20]. Figure 4 illustrates that the location of the kilometric-continuum source region within a plasmaspheric notch, and the resulting emission-cone pattern of the radiation as shown from ray-tracing calculations, are consistent with the observations. The top panel of Figure 4 is a frequency-time spectrogram from the PWI instrument on GEOTAIL, showing the banded structure of the kilometric continuum. The slanted vertical emissions were all Type III solar radio bursts. The center panel of Figure 4 shows the magnetic longitude as a function of the equatorial radial distance of the plasmapause (derived from the inserted extreme ultraviolet – EUV – image of the plasmasphere from the IMAGE spacecraft) and the position of GEOTAIL during the kilometric-continuum observations of the top panel. The bottom pane is a ray-tracing analysis, showing that the structure of the plasmaspheric notch has a significant effect on the shape of the resulting emission cone through refraction.

The correspondence of kilometric-continuum observations with plasmaspheric notches as shown in Figure 4 is not an isolated instance. Green et al. [20] found that from a year's worth of observations of GEOTAIL kilometric-continuum observations and IMAGE EUV images of plasmaspheric notches, the vast majority (94%) of the 87 cases studied showed this correspondence. Their results also showed that a density depletion or notch structure in the plasmasphere is typically a critical condition for the generation of kilometric continuum, but that the notch structures do not always provide the conditions necessary for the generation of the emission.

3. Generation Theories

There are three types of theoretical models (see [30, 31] for reviews) that try to explain the generation of continuum radiation. These are: 1) synchrotron radiation [32, 33], 2) linear mode-conversion models [34-36], and 3) nonlinear mode-conversion models [37, 38].

The synchrotron radiation model is believed to be a factor of 10 too weak for non-thermal continuum generation, and is generally disregarded. The linear and nonlinear theories both assume that strong-trapped waves at the plasmapause in the magnetic equator are converted into

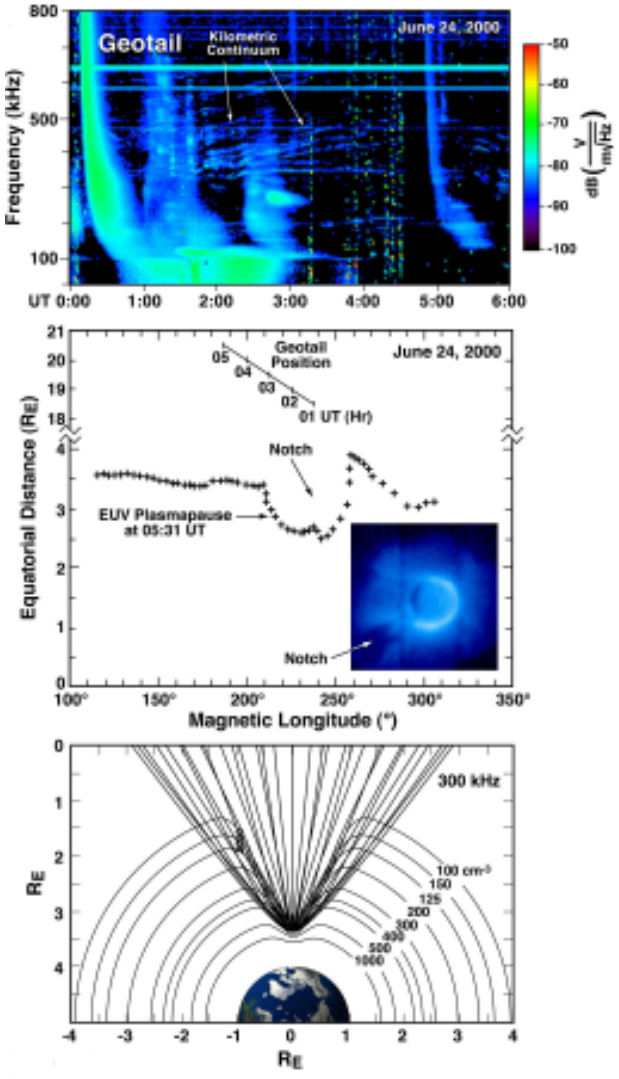

Figure 4. Kilometric-continuum wave observations from GEOTAIL/PWI (top panel) map to a plasmaspheric notch structure, as observed by IMAGE/EUV (middle panel), where the resulting emission-cone pattern (bottom panel) is modeled with ray-tracing calculations (after [15, 20]).

electromagnetic O-mode waves as non-thermal continuum. The free energy source, generating the trapped waves, are most likely energetic electrons in the 10s of keV energy range with highly anisotropic phase-space density distributions [39], which become unstable when the resonant wave-particle interaction conditions are satisfied. Sharp boundaries such as the plasmapause are good regions for instabilities to occur, because the resonance conditions vary greatly as the particles are moving across that boundary.

Figure 5 illustrates how the banded structure of the non-thermal continuum is generated in the linear mode-conversion theory (LMCT). Figure 5 shows profiles of plasmaspheric plasma frequency (f_p) from the empirical model of Gallagher et al. [40] for different K_p. The $(n+1/2)$ harmonics of the equatorial cyclotron frequencies (f_{ce}) are plotted, and the Z-mode cutoff ($L=0$) frequency is plotted in the inset. As the K_p index increases, the plasmapause is observed to occur at lower L values. The key feature of the linear mode-conversion theory is that trapped Z-mode waves are converted into free escaping L-O mode electromagnetic waves [34-36, 41, 42] at selected wave normal angles (angles with respect to the geomagnetic field). For example, for a K_p of 5 (see inset in Figure 5), one emission band is predicted at ~150 kHz, where the $(n+1/2)f_{ce}$ line crosses the f_{uhr} line (dashed line). The quasi-electrostatic emissions at this point propagate inwards as Z-mode waves, where they refracted outwards by the Z-mode cutoff, finally reaching the radio window where their frequency equals f_p. The Z-to-L-O-mode radio window occurs where the wave frequency is equal to f_p and the wave vector is either parallel or anti-parallel to the ambient magnetic field: At this point, the indices of refraction for these two modes are equal. Efficient conversion requires that the local plasma-density gradient be strong and nearly perpendicular to the ambient magnetic field. Under these conditions, after leaving the radio window the wave vector of the L-O mode will rapidly rotate to the angle α given by the formula shown in the inset in Figure 5. This formula is an approximation that strictly holds only for a constant magnetic field and a planar density gradient perpendicular to the ambient magnetic field. Horne [43] performed detailed ray-tracing calculations of this propagation process, showing that wave energy can be efficiently transported into the radio window using the linear theory.

If the linear mode-conversion theory is generating a non-thermal continuum, then Figure 5 illustrates the number of expected non-thermal-continuum emission bands and their location as a function of K_p. Since kilometric continuum is generated at the plasmapause, in the magnetic equator, the maximum observed non-thermal continuum frequency should increase with increasing K_p, as illustrated in Figure 5. Although this figure suggests qualitative trends, it is not quantitatively correct. Figure 3 shows that for $K_p < 2$, the maximum observed frequency for a number the events was greater than 200 kHz. However, Figure 5 would predict no emissions above ~150 kHz, using the Gallagher et al. [40] model. This is true regardless of the magnetic local time. The current empirical plasmasphere models do not reflect the dynamical nature of the plasmasphere, failing to model such observed plasmaspheric structures as shoulders, notches, or plumes.

Over the frequency range from about 350 kHz to 600 kHz, there are eight kilometric-continuum emission bands in Figure 1, and 10 bands in Figure 4. Assuming that a plasmapause density profile for a kilometric continuum source region in a notch structure can be represented – regardless of K_p – by the f_p curve at $L=2.5$, then only two, or at most, three, emission bands would be predicted, with deeper notch structures producing even fewer bands. Based on these results, the linear mode-conversion theory does not appear to adequately account for the large number of observed bands of the higher-frequency kilometric continuum emissions that are generated in deep plasmaspheric notch structures.

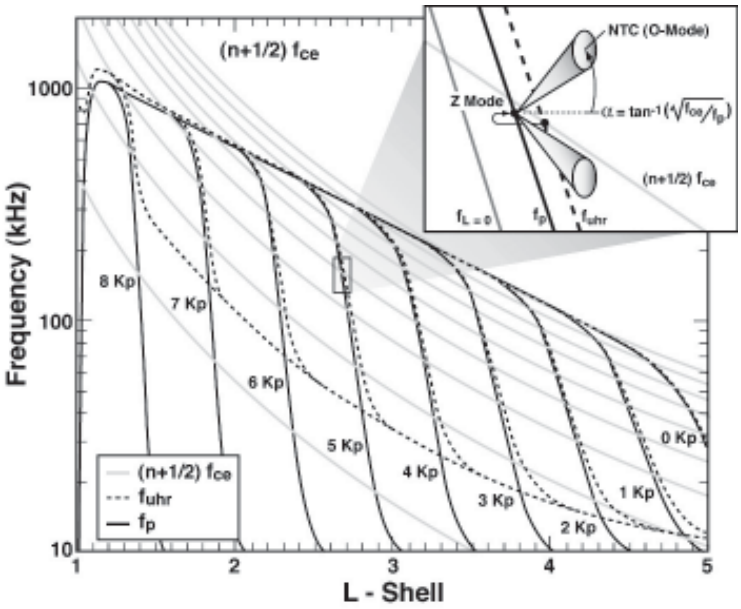

Figure 5. Plasmaspheric f_p curves for different K_p indices are plotted as a function of the L shell at the magnetic equator. Also shown are curves for $(n+1/2)f_{ce}$, $f_{L=0}$ (inset only), and f_{uhr}. In the linear-mode Z-to-O-mode conversion theory, regions of sharp plasma gradient at the plasmapause are potential source regions of non-thermal continuum, as shown in the inset.

In the nonlinear model of Melrose [37], density irregularities formed by low-frequency waves coalesce with upper-hybrid waves, generating this radiation. In the nonlinear model of Fung and Papadopoulos [38], an electrostatic wave propagating into a density gradient can nonlinearly interact with its reflected wave to generate an electromagnetic wave at twice the electrostatic-wave frequency. Both linear and nonlinear theories predict that the electromagnetic waves will be beamed in magnetic latitude, with the beaming becoming more perpendicular to the magnetic field as the ratio of the electron plasma to cyclotron frequency increases. At a sharp plasmapause, since the cyclotron frequency is almost constant, this means that the higher the wave frequency, the closer it is beamed to the magnetic equator.

Recently, research has focused on plasmaspheric density irregularities in the emission spectra of electrostatic waves that then mode-convert to a non-thermal continuum or kilometric continuum. A theory by Yoon and Menietti [44] used eigenvalue analysis of upper-hybrid/Langmuir waves in cavities and found that emission spectra with spacing less than f_{ce} can be generated. Menietti et al. [45], using wideband data from Polar and Cluster, found non-thermal continuum near the source, with banded spectral-line spacing much less than f_{ce}. More theoretical work needs to be done in order to encompass all the characteristics of non-thermal continuum that are observed.

4. Concluding Remarks

Many of the characteristics of the lower-frequency portion of the non-thermal continuum (trapped component) have been difficult to determine, due to the multiple reflections of the emission from the magnetopause and plasmapause. Recently, there is a renewed interest in studying the high-frequency extension of this emission (the escaping component), especially in the kilometric frequency range (see, for example [6, 15, 20]). Several new features of the high-frequency escaping kilometric continuum, such as the narrow latitudinal beam structure and the relationship to plasmaspheric notch structures, provide a new opportunity to observe the triggering of this emission and its relationship to plasmaspheric dynamics. The insight gained in performing multi-spacecraft correlative measurements should provide key measurements on separating spatial from temporal effects, which are essential in verifying existing theories. Observing the radiation while the instability has been initiated and grows, and examining the dynamics of the large-scale plasmasphere, should lead to significant advances in delineating the best theory for the generation of this emission.

There are a number of outstanding questions that need to be addressed concerning the generation and propagation of the kilometric continuum:

1. Is the movement of the plasmapause inwards coupled with a sufficiently large density gradient necessary and sufficient for the generation of kilometric continuum? Is the free-energy source necessary for the creation of electrostatic waves that are precursors to the kilometric continuum always present, or is the free-energy source dependent on the state of the magnetosphere?
2. The kilometric continuum has been detected over a wide range of geophysical conditions. What is the statistical dependence on geomagnetic activity of plasmaspheric structures, such as shoulders and notches, that are good locations for kilometric-continuum generation? Since the kilometric continuum is also detected during low geophysical activity, something must happen to move part of the plasmapause inwards. Can the observation of kilometric continuum during quiet times only be accounted for by the presence of shoulders or notches?

3. The kilometric continuum often exhibits a banded frequency structure, consistent with an $(n+1/2)f_{ce}$ source, but frequently the structure appears more complex. Can density ducts near the plasmapause explain the more-complex structure, or do other mechanisms need to be investigated, such as dynamic motion of the plasmapause boundary layer? Sounding of the plasmapause by IMAGE RPI indicates that the plasmapause surface is far from smooth [1]. What effect does this non-smoothness have on the emission of kilometric continuum, and non-thermal continuum in general?
4. Do the kilometric-continuum emission "Christmas tree" patterns detected by IMAGE exhibit the same frequency dependence with K_p as observed by GEOTAIL near solar minimum and near solar maximum?
5. For highly disturbed times, Tsyganenko and Sitnov [46] found that large changes occurred in the inner-magnetosphere magnetic-field intensity. Can this change be detected remotely in the spectral-band spacing of escaping non-thermal continuum and kilometric continuum? Can the analysis of the frequency structure of escaping non-thermal continuum and kilometric continuum indicate the state of the plasmasphere and the inner-magnetosphere magnetic field?

5. References

1. D L. Carpenter, "Remote Sensing the Earth's Plasmasphere," *Radio Science Bulletin*, 308, 2004, pp. 19-30.
2. M. L. Kaiser, "Observations of Nonthermal Radiation from Planets," in B. T. Tsurutani and H. Oya (eds.), *Plasma Waves and Instabilities at Comets and in Magnetospheres*, Washington, American Geophysical Union, 1989, pp. 221-237.
3. W. S. Kurth, D. A. Gurnett, A. Roux, and S. J. Bolton, "Ganymede: A new radio source," *Geophys. Res. Lett.*, **24**, 1997, pp. 2167-2170.
4. D . A. Gurnett, "The Earth as a Radio Source: The Nonthermal Continuum," *J. Geophys. Res*., **80**, 1975, pp. 2751-2763.
5. L. W. Brown, "The Galactic Radio Spectrum Between 130 kHz and 2600 kHz," *Astrophys. J*., **180**, 1973, pp. 359-370.
6. K. Hashimoto, K. W. Calvert, and H. Matsumoto, "Kilometric Continuum Detected by GEOTAIL," *J. Geophys. Res.*, **104**, 1999, pp. 28645-28656.
7. W. S. Kurth, "Detailed Observations of the Source of Terrestrial Narrowband Electromagnetic Radiation," *Geophys. Res. Lett.*, **9**, 1982, pp. 1341-1344.
8. F. V. Coroniti, F. L. Scarf, C. F. Kennel, and D. A. Gurnett, "Continuum Radiation and Electron Plasma Oscillations in the Distant Geomagnetic Tail, *Geophys. Res. Lett.*, **11**, 1984, pp. 661-664.
9. H. Takano, I. Nagano, S. Yagitani, and H. Matsumoto, "Lobe Trapped Continuum Radiation Generated in the Distant Magnetotail," in M. Hoshino, Y. Omura, and L. J. Lanzerotti (eds.), *Frontiers of Magnetospheric Plasma Physics: Celebrating 10 Years of GEOTAIL Operation*, Elsevier, 2005, pp. 224-227.
10. J. L. Green and S. F. Fung, "Advances in Inner Magnetospheric Passive and Active Wave Research," *Physics and Modeling of the Inner Magnetosphere*, (AGU Monograph **155**), Washington, DC, American Geophysical Union, 2005, pp. 181-202.
11. W. S. Kurth, M. M. Baumback, and D. A. Gurnett, "Direction-Finding Measurements of Auroral Kilometric Radiation, *J. Geophys. Res*., **80**, 1975, pp. 2764-2770.
12. Y. Kasaba, H. Matsumoto, K. Hashimoto, R. R. Anderson, J.-l. Bougeret, M. L. Kaiser, X. Y. Wu, and I. Nagano, "Remote Sensing of the Plasmapause During Substorms: GEOTAIL Observation of Nonthermal Continuum Enhancement," *J. Geophys. Res.*, **103**, 1998, pp. 20389-20405.
13. M. P. Gough, "Nonthermal Continuum Emissions Associated with Electron Injections: Remote Plasmapause Sounding," *Planet. Sp. Sci.*, **30**, 1982, pp. 657.
14. P. C. Filbert and P. J. Kellogg, "Observations of Low-Frequency Radio Emissions in the Earth's Magnetosphere," *J. Geophys. Res.*, **94**, 1989, pp. 8867-8885.
15. J. L. Green, B. R. Sandel, S. F. Fung, D. L. Gallagher, and B. W. Reinisch, "On the Origin of Kilometric Continuum," *J. Geophys. Res.*, **107** (A7), 2002, p. 1105, doi:10. 1029/2001JA000193.
16. D. A. Gurnett and R. R. Shaw, Electromagnetic Radiation Trapped in the Magnetosphere Above the Plasma Frequency, *J. Geophys. Res.*, **78**, 1973, pp. 8136-8149.
17. J. L. Green and S. A. Boardsen, "Confinement of Nonthermal Continuum Radiation to Low Latitudes," *J. Geophys. Res.*, **104**, 1999, pp. 10307-10316.
18. W. S. Kurth, D. A. Gurnett, and R. R. Anderson, "Escaping Nonthermal Continuum Radiation," *J. Geophys. Res.*, **86**, 1981, pp. 5519-5531.
19. H. Matsumoto, I. Nagano, R. R. Anderson, H. Kojima, K. Hashimoto, M. Tsutsui, T. Okada, I. Kimura, Y. Omura and M. Okada, "Plasma Wave Observations with GEOTAIL Spacecraft," *J. Geomag. Geoelectr.*, **46**, 1994, pp. 59-95.
20. J. L. Green, S. Boardsen, S. F. Fung, H. Matsumoto, K. Hashimoto, R. R. Anderson, B. R. Sandel, and B. W. Reinisch, "Association of Kilometric Continuum Radiation with Plasmaspheric Structures," *J. Geophys. Res.*, **109**, 2004, A03203, doi:10. 1029/2003JA010093.
21. J. D. Menietti, R. R. Anderson, J. S. Pickett, and D. A. Gurnett, "Near-Source and Remote Observations of Kilometric Continuum Radiation from Multi-Spacecraft Observations," *J. Geophys. Res.*, **108**, 11, 2003, 1393, doi:10. 1029/2003JA009826.
22. P. M. E. Décréau, C. Ducoin, G. Le Rouzic, O. Randriamboarison, J.-L. Rauch, J.-G. Trotignon, X. Vallieres, P. Canu, f. Darrouzet, M. P. Gough, A. M. Buckley, and T. D. Carozzi, "Observation of Continuum Radiations from the Cluster Fleet: First Results from Direction Finding," *Ann. Geophys*, **22**, 2004, pp. 2607-2624.
23. F. Darrouzet, P. M. E. Décréau, J. De Keyser, A. Masson, D. L. Gallagher, O. Santolik, B. R. Sandel, J. G. Trotignon, J. L. Rauch, E. Le Guirriec, P. Canu, F. Sedgemore, M. André, and J. F. Lemaire, "Density Structures Inside the Plasmasphere: Cluster Observations," *Ann. Gephys.*, **22**, 2004, pp. 2577-2585.
24. S. F. Fung and J. L. Green, "Modeling of Field-Aligned Radio Echoes in the Plasmasphere," *J. Geophys. Res*., **110**, 2005, A01210, doi:10. 1029/2004JA010658.
25. D. Jones, "Planetary Radio Emissions from Low Magnetic Latitudes – Observations and Theories," in H. O. Rucker, S. J. Bauer, and B. -M. Pedersen (eds.), *Planetary Radio Emissions II*, Vienna, Austria, Austrian Academy of Science, 1988, pp. 255-293.
26. D. D. Morgan and D. A. Gurnett, "The Source Location and Beaming of Terrestrial Continuum Radiation, *J. Geophys. Res*., **96**, 1991, pp. 9595-9613.
27. V. N. Kuril'chik, I. F. Kopaeva, and S. V. Mironov, "INTERBALL-1 Observations of the Kilometric 'Continuum' of the Earth's Magnetosphere," *Cosmic Research*, **42**, 2004, pp. 1-7.
28. K. Hashimoto, R. R. Anderson, J. L. Green, and H. Matsumoto, "Source and Propagation Characteristics of Kilometric Continuum Observed with Multiple Satellites," *J. Geophys. Res.*, **110**, A09229, doi:10. 1029/2004JA010729, 2005.
29. D. L. Carpenter, R. R. Anderson, W. Calvert, and M. B. Moldwin, "CRRES Observations of Density Cavities Inside

the Plasmasphere," *J. Geophys. Res.*, **105**, 2000, pp. 23323-23338.
30. D. D. Barbosa, "Low-Level VLF and LF Radio Emissions Observed and Earth and Jupiter," *Rev. of Geophys. and Space Phys.*, **20**, 2, 1982, pp. 316-334.
31. L. C. Lee, "Theories of Nonthermal Radiations from Planets," in B. T. Tsurutani and H. Oya (eds.), *Plasma Waves and Instabilities at Comets and in Magnetospheres*, Washington, American Geophysical Union, 1989, pp. 239-249.
32. M. S. Frankel, "LF Radio Noise from the Earth's Magnetosphere," *Radio Sci.*, **8**, 1973, pp. 991-1005.
33. J. F. Vesecky and M. S. Frankel, "Observations of a Low-Frequency Cutoff in Magnetospheric Radio Noise Received on IMP 6," *J. Geophys. Res.*, **80**, 1975, pp. 2771-2774.
34. D. Jones, "Source of Terrestrial Nonthermal Radiation," *Nature*, **260**, 1976, pp. 686-689.
35. D. Jones, "Latitudinal Beaming of Planetary Radio Emissions," *Nature*, **288**, 1980, pp. 225-229.
36. D. Jones, "Beaming of Terrestrial Myriametric Radiation," *Adv. Space Res.*, **1**, 1981, pp. 373-376.
37. D. B. Melrose, "A Theory for the Nonthermal Radio Continuum in the Terrestrial and Jovian Magnetospheres, *J. Geophys. Res.*, **86**, 1981, pp. 30-36.
38. S. F. Fung and K. Papadopoulos, "The Emission of Narrow-Band Jovian Kilometric Radiation," *J. Geophys. Res.*, **92**, 1987, pp. 8579-8593.
39. D. A. Gurnett and L. A. Frank, "Continuum Radiation Associated with Low-Energy Electrons in the Outer Radiation Zone," *J. Geophys. Res.*, **81**, 1976, pp. 3875-3885.
40. D. L. Gallagher, P. D. Craven, and R. H. Comfort, "An Empirical Model of the Earth's Plasmasphere," *Adv. Space Res.*, 1988, pp. 8(8), (8)15-(8)24.
41. K. G. Budden, "The theory of Radio Windows in the Ionosphere and Magnetosphere," *J. Atmos. Terr. Phys.*, **42**, 1980, pp. 287-298.
42. K. G. Budden, "The theory of Radio Windows in the Ionosphere and Magnetosphere II," *J. Atmos. Terr. Phys.*, **48**, 1986, pp. 663-641.
43. R. B. Horne, "Path-Integrated Growth of Electrostatic Waves: The Generation of Terrestrial Myriametric Radiation," *J. Geophys. Res.*, **94**, 1989, pp. 8895-8909.
44. P. H. Yoon and J. D. Menietti, "On Fine Structure Emission Associated with Plasmaspheric Density Irregularities," *Geophys. Res. Lett.*, **32**, 2005, L23103, doi:10.1029/2005GL023795.
45. J. D. Menietti, O. Santolik, J. S. Pickett, and D. A. Gurnett, "High Resolution Observations of Continuum Radiation," *Planetary and Space Sci.*, **53**, 2005, pp. 283-290.
46. N. A. Tsyganenko and M. I. Sitnov, "Modeling the Dynamics of the Inner Magnetosphere During Strong Geomagnetic Storms," *J. Geophys. Res.*, **110**, A03208, doi:10. 1029/2004JA010798, 2005.

Radio-Frequency Radiation Safety and Health

James C. Lin

Heart Surgery with Microwaves

Putting a microwave oven inside the heart: you must be kidding! Not exactly! However, in recent years, a revolution has taken place in cardiology to bring forth a new, minimally invasive interventional procedure: microwave transcatheter ablation for cardiac arrhythmias.

According to the American Heart Association, in the United States more than two million persons suffer from tachyarrhythmias – irregularly high heartbeat rates – and another two million suffer from atrial fibrillation and flutter. The prevalence worldwide is about the same. Until recently, the treatment of patients with cardiac arrhythmias was mostly palliative, involving lifelong dependence on medication. Moreover, in a significant portion (10% to 15%) of these patients, available drug therapy has been found unsatisfactory, because of a lack of meaningful response or unacceptable side effects. Surgical intervention has been the principal method of treatment in these cases. However, alternatives to surgery have been sought, in an effort to reduce the cost and morbidity of surgical treatment.

During the past decade, minimally invasive microwave and radio-frequency (RF) cardiac ablation – in particular, RF cardiac ablation – has become a widely used procedure for the treatment of cardiac arrhythmias. Minimally invasive intervention offers many benefits: long incisions are replaced with a puncture wound; major cardiac and pulmonary complications are sidestepped; the need for postoperative intensive care is significantly reduced; and, in many cases, minimally invasive intervention offers a "cure" without major surgery. Furthermore, it has important advantages over drugs that are merely palliative, and only alleviate symptoms: namely, it avoids the side effects and inconvenience of chronic drug therapy

An arrhythmia is any kind of abnormal heart rate or rhythm. There are several causes of arrhythmia. However, they all have one thing in common: preventing the heart from pumping enough blood to meet the body's needs. The heart's natural pacemaker – a small cluster of specialized cells, called the sinus-atrial node (SA node) – is located in the right atrium, the upper-right chamber of the heart. It sends out an electrical impulse that signals muscles in the heart's four chambers (two upper atria and two lower ventricles) to contract, each at the proper time. The SA node can malfunction and develop an abnormal impulse rate. The normal electrical conduction pathways from the SA node through the atrioventricular node (AV node) – a second cluster of cells located near the center of the heart – can be interrupted. Because all heart muscle tissues are capable of starting a beat, any part of the heart muscle also can interrupt the electrical rhythm, or even take over as the heart's pacemaker, setting off an abnormal heartbeat. When one of these events interrupts the heart's normal rhythm, arrhythmias can occur [1].

Atrial fibrillation is found most often in people over 60 years of age. It develops when a disturbance in the electrical signals causes the two upper atrial chambers of the heart to quiver, rather than pump efficiently. The rate of atrial impulses can range from 300-600 beats per minute (bpm), in contrast to a normal 60-80 bpm. When the faster-than-normal impulse-caused quivering occurs, not all the blood is forced out of the atria. The blood can pool inside the atrium, and sometimes clots. Blood clots can cause a stroke if they detach, travel through the vascular system, and block an artery in the brain. Symptoms of atrial fibrillation vary with individuals. Some people with atrial fibrillation experience fluttering (skipping beats), pounding in the chest, or palpitations (sensation of one's heartbeat). Sometimes, because the heart is not pumping efficiently during atrial fibrillation, a person may feel short of breath, dizzy, lightheaded, or may faint.

Supraventricular tachyarrhythmias are caused by abnormal electrical pathways inside the heart. The SA node's impulse normally travels from the SA node through the AV node. The AV node then sends the signals out to the ventricles. The AV node conducts impulses very slowly, requiring 60-120 ms to traverse about 1 cm of node. The

James C. Lin is with the University of Illinois, Chicago, IL, USA; E-mail: lin@uic.edu.

AV node's slowing of the impulse protects the ventricles from speeding in response to atrial tachyarrhythmias (such as atrial fibrillation) by not allowing all impulses through. Supraventricular tachyarrhythmia is often associated with the Wolff-Parkinson-White syndrome, where there is an accessory (extra) AV conduction pathway. The extra pathway allows the electrical signal to bypass the normal conduction delay of the AV node, and causes supraventricular tachyarrhythmia. Symptoms of supraventricular tachyarrhythmia are similar to atrial fibrillation, and may include chest pain.

Ventricular tachycardia is caused by a rapid heartbeat, arising in the ventricles. It is the most severe and life-threatening of arrhythmias. It affects the contraction of the ventricles, the main pumping chambers of the heart. During ventricular tachycardia, the heart's electrical-pacemaker signals may come from the ventricular muscles instead of the SA node. Ventricular tachycardia can make the heart beat extremely fast. The heart rate may be as rapid as 200 bpm or higher. There is not enough time for the ventricles to fill with blood between beats, and the heart becomes incapable of pumping adequate blood through the body. If this fast heart rate continues, the brain and body may receive insufficient blood and oxygen. As a result, one may experience dizziness, fainting spells, blackouts, or temporary blind spots. The person may become unconscious, and might collapse from cardiac arrest (the heart completely stops).

Cardiac ablation is a procedure in which electromagnetic energy is delivered to the myocardium (heart muscle) via a catheter to create thermal lesions. The frequencies typically used for RF ablation are between 500 and 750 kHz, while microwave catheter ablation uses 2.45 GHz. The thermal lesions are relied upon to disrupt, eliminate, or isolate conduction pathways supporting the arrhythmia, instead of using a surgical blade. Cardiac ablation has advanced to the point where RF cardiac ablation is now offered as a standard therapy for most supraventricular arrhythmias involving the AV node between the upper and lower heart chambers, and, likewise, microwave ablation has become a preferred treatment for atrial fibrillation involving the upper chamber [2-4].

The procedure involves introducing a small catheter into the vein of an anesthetized patient, and placing the catheter at the responsible heart-muscle substrate, with the aid of radiographic and electrophysiologic monitoring. A pulse of RF or microwave energy is then delivered through the same catheter electrode or antenna until an irreversible conduction block is achieved. This commonly would require an average power of 30 to 50 W, applied for 30 to 60 s, for the tissue temperature to reach 60 to 70° C. The temperature is kept well below 100° C to prevent induction of coagulation, especially on the tip of the RF electrode.

When an RF voltage is applied, a 500 or 750 kHz current is induced to flow between a pair of electrodes. In ablation therapy, the current flows between a small electrode inside the heart to a large, grounded electrode on the body's surface. The current rapidly diverges from the small electrode, so that the current density is the highest at the electrode-tissue interface. The tissue's resistance to current flow results in thermal lesions: desiccation and coagulation of tissue in direct contact with the electrode. The desiccated and coagulated tissue raise the resistance to current flow, which impedes effective tissue heating, and limits the size of RF-induced lesions. Thus, lesions beyond the immediate vicinity of the electrode-tissue interface occur as a result of passive heat transfer from the thin, high-temperature region. Studies have shown that RF-induced lesions increase rapidly in size during the initial period of power application, and that then the rate of the increase diminishes rapidly as the resistance rises at the electrode-tissue interface and the current flow falls.

Changes in electrode impedance provide a convenient way to monitor ablation effectiveness, and to ascertain proper current flow during ablation procedures. In particular, a rise in electrode impedance during ablation would indicate coagulative adhesion of tissue components at the electrode-tissue interface. For example, impedance is stable up to a maximum temperature of 90° C. However, blood clots as the temperature rises to above 90° C. The desiccated and coagulated tissue and blood increase the resistance to the current flow across the electrode-tissue interface. The impedance rises sharply (the voltage jumps and the current drops, due to poor coupling between the electrode and adjacent tissue). The reduction in RF current flow is followed by a decrease in temperature. This thwarts effective tissue heating and limits the size of RF-induced lesions.

It is noteworthy that RF ablation has emerged as an effective therapy and, indeed, it has become accepted as the treatment of choice for many cardiac arrhythmias, including those mentioned above. As noted, the lesions induced by RF current are quite small and shallow. Moreover, increasing the output power to heat tissue at depth often results in excessive temperatures at the electrode-tissue interface, without the desired enlargement of lesion size.

As expected, the coupling of RF energy to the endocardium (inner heart tissue) is facilitated by maintaining a slight pressure from the electrode. In addition, the efficacy of RF catheter ablation depends on catheter-tissue orientation and the angle of electrode contact. With ablation catheters positioned parallel, perpendicular, or oblique to the myocardium, it has been found that tissue temperature differed significantly with perpendicular or oblique placement, when compared to the parallel electrode-tissue orientation. The lesions are larger and deeper for an oblique electrode angle.

The use of temperature sensing and control also can increase lesion size and the safety of cardiac ablation, since they can be used to prevent the tip temperature from overheating. Some recent innovations with RF ablation

designs have included catheters with a cooled electrode. A catheter with cooling makes it possible to produce larger lesions, which somewhat mitigates the problem of insufficient lesion size in certain applications. Nevertheless, studies comparing the power-deposition patterns of RF and microwave catheters have shown that the absorbed microwave energy could be 10 times higher than the RF energy at the same tissue depth.

The development of cardiac ablation using microwave energy was reported in 1987, the same year when the initial clinical use of RF energy for the ablation of cardiac arrhythmias appeared. However, clinical trials of microwave cardiac ablation did not take place until recently. Thus, microwave cardiac ablation is a relatively new concept for clinical treatment of cardiac arrhythmias.

The propagation and radiation of microwaves in biological tissue are governed by frequency, power, and the antenna radiation pattern, as well as by tissue composition and dielectric permittivity. In thermal therapeutic applications, the final temperature may be affected by tissue blood flow and thermal conduction. However, for applications of short duration, the time rate of heating and the spatial distribution of radiated microwave energy are functions of power deposition (the rate of energy absorption) and the antenna radiation patterns, respectively.

The biological tissues of interest in this case are blood, muscle, and tissues with low water content, such as fat, bone, or desiccated tissue. There is a modest change in dielectric constant and conductivity as a function of frequency for all three types of tissues. However, differences among the three types of tissues are quite large. As microwave fields propagate in the tissue medium, energy is extracted from the field and absorbed by the medium. This absorption results in a progressive reduction of the microwave power intensity as it advances into the tissue. The portion of energy extracted from the propagating microwave field is converted into heat production.

The reduction of the microwave power intensity is quantified by the depth of penetration. At 2.45 GHz, the depths of plane-wave penetration for blood, muscle, and fat are 19, 17, and 79 mm, respectively. For microwave-catheter antennas that do not have plane wavefronts, the penetration depth is reduced according to the specific antenna design. Nevertheless, these values clearly suggest that microwave energy can deposit energy directly into tissue at a distance, through radiative interaction of microwaves with cardiac tissues. Furthermore, the differences in the dielectric permittivity yield a depth of penetration for tissues with low water content that is about four times deeper than for muscle (or higher-water-content tissue) at 2.45 GHz. This means that a microwave field can propagate more readily through (is absorbed less) by low-water-content tissues than in tissues of high water content. It also implies that microwaves can propagate through intervening desiccated tissue to deposit energy directly into more-deeply-lying tissue. At 2.45 GHz, the dielectric constant for muscle is 20% lower than for blood, but it is about 800% higher than for fat. While conductivities for blood and muscle are approximately the same, they are about 300% higher than for tissues with low water content. Indeed, these inherent features have been demonstrated in phantom, animal, and human subjects for microwave energy. Specifically, larger and deeper lesions have been produced by microwave radiation [3]. These results show that microwave catheter ablation is a safe and suitable procedure for the treatment of cardiac arrhythmias, including arrhythmias due to conduction pathways located deep in the myocardium.

A recent review [4] evaluated the clinical efficacy of microwave ablation and other alternative ablative treatments and the classical "cut and sew" surgical approach, which claims a 97%-99% sinus rhythm success rate. It was found that the clinical outcome of minimally invasive microwave ablation treatment of atrial fibrillation did not show any significant difference in the postoperative sinus rhythm conversion rates from the classical "cut and sew" treatment procedure. The review included data on the number and percentage of treated patients, age and gender distributions, postoperative morbidity, and survival rate. The study thus affirmed that microwave ablation is as effective as the traditional surgical approach used to treat atrial fibrillation.

References

1. J. W. Heger, J. T. Niemann, R. F. Roth, and J. M. Criley (eds.), *Cardiology, Fourth Edition*, Baltimore, Williams & Wilkins, 1998.
2. S. K. S. Huang and D. J. Wilber (eds.), *Radiofrequency Catheter Ablation of Cardiac Arrhythmias: Basic Concepts and Clinical Applications, Second Edition*, Armonk, New York, Futura, 2000.
3. J. C. Lin, "Studies on Microwaves in Medicine and Biology: From Snails to Humans," *Bioelectromagnetics*, **25**, 2004, pp 146-159.
4. K. Khargi, B. A Hutten, B. Lemke, and T. Deneke, "Surgical Treatment of Atrial Fibrillation: A Systematic Review," *Eur. J. Cardiothorac. Surg.*, **27**, 2005, pp. 258-265.

Conferences

CONFERENCE REPORT

From Sensors to Imagery
ISPRS Commission I Symposium

Marne-la-Vallée, France, 4 - 6 July 2006

The International Society for Photogrammetry and Remote Sensing (ISPRS) is a non-governmental international organisation, devoted to the development of international co-operation for the advancement of knowledge, research, development, education and training in the photogrammetry, remote sensing and spatial information sciences, their integration and applications, to contribute to the well-being of humanity and the sustainability of the environment.

An Ordinary Member of ISPRS shall be the single organisation of a country, or a geographic region thereof having an independent budget, which should represent the whole community of photogrammetry, remote sensing and spatial information specialists in the country or region. In France the ordinary member is the SFPT (Société Française de Photogrammétrie et de Télédétection).

The ISPRS Congress includes all specialists in photogrammetry, remote sensing and space information; it holds its general assembly every four years. The last took place in July 2004 in Istanbul and the next will take place from 3rd to 11 July 2008 in Beijing.

1. International Society for Photogrammetry and Remote Sensing (ISPRS): Technical Commissions

The scientific and technical work of the ISPRS is accomplished by **8** Technical Commissions. Each Commission is entrusted to an Ordinary Member organisation for the four-year term between Congresses.

1) Image Data Acquisition - Sensors and Platforms
2) Theory and Concepts of Spatio-temporal Data Handling and Information
3) Photogrammetric Computer Vision and Image Analysis
4) Geo databases and Digital Mapping
5) Close-Range Sensing: Analysis and Applications
6) Education and Outreach
7) Thematic Processing, Modelling and Analysis of Remotely Sensed Data
8) Remote Sensing Applications and Policies.

France is responsible for Technical Commission I (TC#I) for the period 2004-2008; consequently 200 people attended the symposium "From sensors to imagery" in Marne la Vallée (4-6 July 2006), in the premises of ENSG (Ecole Nationale des Sciences Géographiques) with the help of SFPT, CNES (Centre National d'Etudes Spatiales) et IGN (Institut Géographique National) and thanks to the support of Région Ile-de-France and companies Spot Image, Intergraph et ITT.

2. Opening session

In his opening statement Alain Baudoin, Chairman of the TC #I stressed the need to control the acquisition of useful data, i.e. data that can be used by the largest possible number of applications. Mr. Ian Dowman, Chairman of ISPRS underlined the interest of this symposium namely with respect to ISPRS's international relations with other organisations such as the Global Earth Observation System of Systems (GEOSS), the European Spatial Data Research (EuroSDR) and the Institute of Navigation (ION).

Madame Pascale Utré Guirard, representing the Chairman of CNES, Monsieur Yannick d'Escatha, gave a description of the current spatial programme of CNES, showing their evolution over the last 20 years since the setting up of the SPOT programme in February 1986.

Mr. Bertrand Lévy, Director General of IGN, recalled that IGN had already taken the decision some time ago to put all geographic information at the disposal of the public at large; he also mentioned that airborne instruments remain important for high resolution. He concluded that activities within EU are increasing (INSPIRE project).

Madame Marie-José Lefèvre-Fonollosa, Chairperson of SFPT, recalled that the year 2006 will be remembered as a fruitful one with the launching of the Franco-American satellite Calypso which reached the Aqua train on the 21st of April. She gave a synoptic presentation of the main tendencies in this area which are fourfold :

- diversity of observation instruments (fig. 1)
- complementarity of platforms (rovers, balloons,

airplanes, UAVs, satellites…)
- harmonisation of airborne and space techniques
- towards platform autonomy and smaller and cheaper satellites

3. Plenary session

The introductory plenary session comprised three presentations of the three organisations with which ISPRS co-operates closely.

The role of EuroSDR in the emerging world of integrated spatial information.

After having outlined the evolution of European Spatial Data Research (EuroSDR), Keith Murray explained that its role was to support the lifecycle of geographic information by processing data, checking the quality of data bases and ensuring the dissemination of adequate information.

Among current activities he mentioned the large scope of information for mapping from SAR and optical imagery.

The material from some of the projects and workshops is considered for use in the e-learning programme which is now in its fourth year of existence, known as EduServe.

The Institute of Navigation: advancing modern navigation technologies

The Institute of Navigation (ION) is a non-profit professional society dedicated to the advancement of the art and science of navigation. Although basically a national organisation (USA), its membership is world wide and it is affiliated with the International Association of Institutes of Navigation. Ms. Dorota Grejner-Brzezinska explained the role of ION in advancing the navigation technology, with a special emphasis on GNSS (Global Navigation Satellite Systems) extension and modernisation, space-based and ground-based augmentation and integration with other sensors, such as inertial and imaging technology, in order to improve positioning, navigation and timing.

The GEOSS challenge: what role for the scientific community?

The Group on Earth Observations (GEO) is leading a world wide effort to build a Global Earth Observation System of Systems (GEOSS) over the next ten years. GEO involves 64 countries, the European Commission and 43 international organisations.

In a transverse approach, José Achache made clear that the project required three types of action,
1) build a sustainable , comprehensive and co-ordinated observation system of systems: as a "system of systems" GEOSS will work with and build upon existing national, regional and international systems,
2) provide open and easy access to data anytime and anywhere,
3) increase the use of Earth observations.

It goes without saying that this requires a large co-operation between the various scientific communities as he demonstrated by several examples.

4. Thematic sessions

The various thematic sessions were prepared by the working groups (WG) of the TC#I; out of some hundred communications made either orally or posted we can only report on some of them with the view to giving an idea on the broad scale of subjects.

Airborne photogrammetric sensors (radiometry)

The invited paper by Prof. Gordon Petrie and Stewart Walker ("Airborne digital images: an overview and analysis") sets out the current situation regarding the development of airborne digital images for photogrammatric and remote sensing applications. The authors covered the main aspects of the domain,
- sensor technologies that are used in airborne digital imagers, including both CCD and CMOS detectors,
- airborne digital frame cameras,
- airborne pushbroom line scanners,

as well as a comparison of the relative merits of airborne digital frame cameras and pushbroom imagers.

Development in airborne Lidar systems

Many applications require the creation of DTM (Digital Terrain Model) beneath forest canopy. This is often a difficult or expensive task, particularly if the forest area of interest is extended. InSAR (Inerferometric SAR) has proven itself valuable for acquiring DEMs (Digital Evaluation Models) over large areas relatively inexpensively. However, X-band and C-band InSAR, which are the major sources of DEM data from airborne and satellite platforms respectively, are usually measuring the elevation of the upper part of the canopy but not the ground below. Longer wavelengths InSARs – for example L-band (λ=24 cm) and P-band (λ=75cm) – have demonstrated their ability to penetrate to or close to the ground in several forest cover situations.

In their paper Bryan Mercer et al. summarised the result of two P-band projects in heavily forested areas of Washington State USA, reporting observed ground elevation accuracy in the order of two to four meters depending on terrain configuration.

Multi-platform and intelligent sensing, sensor networks.

Scene interpretation using multi-sensor images becomes an active field of interest in the Earth observation domain. In this context the joint use of radar and optical images remains a hard task. Indeed, major differences exist between images as well on geometric as radiometric features.

The paper "On the use of SAR and optical images combination" by David Petit and al. interestingly presents not only the advantages of this combination, but also an inventory of the difficulties which this implies. In particular the authors underline the difficulty to simultaneously record images and geometric reference points including their accuracy.

DEM Generation

Recalling that Digital Elevation Models (DEM) from satellite data are generated mainly from two types of data sets using completely different methods – photogrammetry for optical stereo images (e.g. SPOT 5, IKONOS), and interferometry from SAR data (InSAR,e.g. ERS-Tandem, SRTM) – Ms. Danielle Hoja et al. ("Comparison of DEM generation and combination methods using high resolution optical stereo imagery and interferometric SAR data") showed the potential for combined usage of several DSM derived from different sensors and methods to improve the overall accuracy. The authors reported that an improvement of the fused SDM and the integrated DSM can be quantitatively measured, the overall accuracy of the combined DSM being higher.

New space borne and airborne SAR techniques

TanDEM-X is a German public/private partnership project between DLR (Deutsches Zentrum für Luft- und Raumfahrt) and EADS Astrium for a novel satellite constellation based on TerraSAR-X with the goal to generate a global digital elevation model (DEM) with 10 metres horizontal spacing and 1-2 metres vertical accuracy. After a system overview of the interferometric SAR and its properties Michael Eineder et al. ("First data acquisition and processing concepts for the TanDEM-X-mission") focus their presentation on the structure of the SAR processing chain to be developed. Indeed, the aim of the project is to launch a second identical satellite in 2009 on the same orbit carrying a special device for accurate measuring of the distance between the two satellites. The processing will require new algorithms [1].

In their paper "Interest of fully polarimetric SAR data for classification and land use cartography", Cedric Lardeux et al. present a monograph of plants on a French Polynesia island based on data coming from airborne SAR in P,L and C band.

5. SFPT-IGN-CNES combined show

In addition to the thematic sessions and an industrial exhibition several shows took place at the combined counter of SFPT-IGN-CNES . We noted an IGN presentation on the performance of new digital cameras on the one hand and on the other an overview of its current research programme on algorithms. We also noted an interesting CNES presentation on the architecture of the future PLEIADES satellite, its acquisition modes and new applications. In addition there was a conference on high resolution SARs (resolution better than 1 meter) their potential and their limits in terms of acquisition.

6. Conclusion

During the symposium an industrial exhibition provided opportunities for fruitful discussions.

There is no doubt that all organisations (SFPT,CNES,IGN,ENSG) co-operating in this symposium put an enormous effort into making it a success and it can be said that they achieved their goal. Warmest thanks to all, namely to Marie-José Lefèvre-Fonollosa and Alain Dupéret from SFPT as well as Alain Baudoin and Nicolas Paparoditis from the Technical Commission I of ISPRS.

Jean Isnard
Comité National Francais de l'URSI (CNFRS)
Chairman Commission F

[1] On the same project see also paper "TerraSAR-X active radar ground calibration system" by Rainer Lenz, Karin Schuler et al. in IEEE A & S Magazine, May 2006, pp.30-33

CONFERENCE ANNOUNCEMENTS

International School on Atmospheric Radar
ISAR-NCU 2006

National Central University, Chung-li, Taiwan, 9 - 27 October 2006

Over the past decades the application of radar techniques to study the structure and dynamics of the mesosphere, stratosphere and the troposphere has continuously grown and quite a few new systems of this kind have been added in the past years. This radar technique has further evolved into applications for operational meteorology, which have become known as wind profiling and Doppler weather radars have become standard instruments for weather nowcasting. The wide-spread applications of these radars for scientific research of the atmosphere and for meteorological operations demand a proper knowledge of such atmospheric radar systems, and of the analysis, validation and interpretation of the acquired data.

The ISAR-NCU directors are: Professors. J. Roettger and C.J. Pan. The International School of Atmospheric Radar - ISAR-NCU - is sponsored by the National Central University through funding by the Ministry of Education and the National Science Council of Taiwan, the Scientific Committee on Solar Terrestrial Physics (SCOSTEP) and the International Union of Radio Science (URSI) et al.

The school ISAR-NCU follows the format of the earlier international schools on atmospheric radar. ISAR-NCU is held for the purpose of training young researchers, students and engineers, who are active in or have a proven relation to this area, or can certify a solid interest and a sound perspective on this research and the technique.

Topics

- Fundamentals of atmospheric radars
- Hardware and basics of signal acquisition
- Data analysis and validation
- Special applications such as interferometry and polarimetry
- Scattering of radar waves
- Atmo-spheric winds
- Precipitation studies
- Waves and turbulence
- Meteorology of the troposphere and strato- sphere
- Mesosphere and the basics of radar observations of the ionosphere

Distinguished lecturers from the atmospheric radar community will be available for teaching and hands-on training.

Contact

C.J. Pan and Jürgen Röttger
Co-Directors of ISAR-NCU
Institute of Space Science
National Central University
Chung-Li, TAIWAN
isar@jupiter.ss.ncu.edu.tw
cjpan@jupiter.ss.ncu.edu.tw
http://www.ss.ncu.edu.tw/~ISAR/

3rd International Conference on Microwaves, Antenna, Propagation and Remote Sensing
ICMARS - 2006

"Om Niwas", Jodhpur, India, 18 - 22 December 2006

The 3rd International Conference on Microwaves, Antenna, Propagation and Remote Sensing, which will be held in "Om Niwas", Jodhpur, India from 18 tot 22 December, is organised by the International Centre for Radio Science (ICRS) and is sponsored by the International Union of Radio Science (URSI) and Departments of the Govt. of India, New Delhi.

ICRS has been organizing annual conference on the related topics. It has already organized five National conferences and two International conferences in December 2003 & November 2004. Now this is 3rd International Conference on "Microwaves, Antenna, Propagation and Remote Sensing"

Topics

- Antenna arrays and Antenna pattern synthesis.
- Dielectric property measurement.
- Expert systems for antenna design and smart antenna.
- Microstrip antenna and wideband antenna

- Microwave and millimeter wave device and circuits.
- Microwave measurements.
- Radar Cross section.
- Microwave remote sensing of land, Ocean and atmosphere.
- Passive and active microwave sensors including radiometer and radar systems.
- Data products generations for different applications.
- Antenna measurement using planar Near Field facility compact antenna test facility.
- Microwave Tubes
- Microwave Systems
- Terahertz Application
- DSP, Signal Processing

Along with these topics we will be covering three special technical sessions given below.

- Microwave Integrated Circuits (MIC) and Monolith Microwave Integrated Circuits (MMIC).
- Microwave solid-state devices
- Microwave Remote Sensing

Contact

Prof. O.P.N. Calla, Chairman, ICRS (Conf)
Mr. Rajesh Vyas, Organizing Secretary
"OM NIWAS", A-23, Shastri Nagar
Jodhpur 342 003, INDIA
Tel: +91-0291-2613123
Fax: +91-0291-2626166
E-Mail: opncalla@yahoo.co.in

VIIth International Symposium on Electromagnetic Compatibility and Electromagnetic Ecology EMC'2007

St. Petersburg, Russia, 26 - 29 June 2007

Objective

The 7th International Symposium on Electromagnetic Compatibility and Electromagnetic Ecology (EMC&EME) will offer a new opportunity for scientists, engineers and students working in the area of EMC to present the progress in their work and to discuss problems of current mutual interest.

The Symposium traditionally takes place at St. Petersburg State Electrotechnical University "LETI", St. Petersburg, Russia. The Symposium EMC'2007 will be held in June in the fine period of White Nights. This is a pleasant time to get acquainted with the architecture and museums of the city (the Hermitage, the Russian museum and others), for walks around the city and for visiting famous palaces (Peterhof, Pavlovsk, Pushkin).

This Symposium is supported by the Federal Agency for Education, the Ministry of Information Technologies and Communications of RF, the Russian Academy of Sciences, the Users Association of National Radio-Frequency Resource – National Radio-Association, the St. Petersburg State Polytechnical University, the St. Petersburg State University of Telecommunications named after M.A. Bonch-Bruevich, the St. Petersburg State Maritime Technical University, the Moscow Technical University of Communication and Information Science, the Radiofrequency Centre of the North-West Federal District, the Research Institute of Radio, The Research Institute of Pulse Engineering, the Research Test Centre for EMC, the Research-and-production Enterprise "Proryv", Kedah Electronics Engineering Ltd, the IEEE Russian (North-West) Section, the Russian Branch of IEEE "Engineering-management" and Elemcom Ltd.

Symposium Organizers

- St. Petersburg State Electrotechnical University "LETI"
- St. Petersburg Scientific and Technical Society of Radio Engineering, Electronics and Communication named after A.S. Popov
- Leningrad Radio Research and Development Institute
- Discone-Nentre Ltd.

Topics

1. Theoretical problems of EMC&EME
2. EMC of radio-electronic equipment
3. Spectrum management and monitoring
4. EMC in electrical engineering and power systems
5. EMC and EME specifically for mobile objects (vessels, airplanes, railway transport and others)
6. Research of natural electromagnetic radiations
7. Equipment design with regard to EMC&EME, technology, materials and components
8. Electromagnetic monitoring, measurement, certification and test equipment
9. EME problems: influence of electromagnetic radiation on biological objects, allowable norms of radiation and ecological protection
10. EMC&EME education

Deadlines

October 15, 2006: Second Call for Papers
January 15, 2007: Deadline for Electronic Submission of the Preliminary Registration Form and the Abstract
January 30, 2007: Notification of Acceptance for Authors and Call for Papers
March 30, 2007: Deadline for Electronic Submission of Papers and for the Registration Fee

Contact

Discone-Centre Ltd.
St. Petersburg State Electrotechnical University "LETI"
Tel: +7 812 234-48-40
Fax: +7 812 234-46-81
E-mail: discone@mail.wplus.net
Website: http://www.eltech.ru/emc

XIXth Asia-Pacific Microwave Conference APMC 2007

Bangkok, Thailand, 11 - 14 December 2007

The Nineteenth Asia-Pacific Microwave Conference (APMC 2007) will be held at Grand Hyatt Erawan Hotel inside Bangkok, Thailand, on December 11-14, 2007.

This conference will be organized by IEEE MTT/AP/ED Thailand Chapter, IEEE CAS Thailand Chapter, IEEE ComSoc Thailand Chapter, IEEE LEOS Thailand Chapter and IEEE Thailand Section. The sponsor is the Electrical Engineering, Electronics, Computer, Telecommunications and Information Technology (ECTI) Association of Thailand. The technical sponsor is IEEE MTT-S.

Topics

- Solid States Devices and Circuits
- Scattering and Propagation
- Low-Noise Devices and Technique
- Microwave Remote Sensing and Sensors
- High-Power Devices and Techniques
- Microwave and Millimeter Wave Systems
- Monolithic Integrated Circuits
- Communication Systems
- Passive Devices and Circuits
- High Speed Digital Circuits and SI
- Packaging, Interconnects, and MCMs
- Biological Effects and Medical Applications
- Ferrite and SAW Components
- Submillimeter Wave Techniques
- Superconducting Components and Technology
- EMI and EMC
- Microwave-Optical Design
- Photonics and Optics
- Computer Aided Design
- Wireless and RF Components and Systems
- Instrumentation and Measurement Techniques
- Wide Band Gap Semiconductor Devices
- Electromagnetic Field Theory
- Radar and Broadband Communication Systems
- Computational Electromagnetics
- MEMS
- Microwave Antennas
- PBG and Metamaterials
- Smart Antennas, Phased and Active Array
- Any other relevant topics

Deadlines

May 15, 2007: Proposal for Tutorial/ Special Session Deadline
June 15, 2007: Paper Submission Deadline
August 15, 2007: Acceptance Notification
September 10, 2007: Final Camera - Ready Papers Due
September 10, 2007: Advance Registration Deadline

Contact

Dr. Chuwong Phongcharoenpanich
General Secretary of APMC 2007
King Mongkut's Institute of Technology Ladkrabang
Bangkok 10520, Thailand
Email: kpchuwon@kmitl.ac.th

CONFERENCE ANNOUNCEMENTS

An up-to-date version of this Conference Calendar, with links to various conference web sites can be found at www.ursi.org/ Calendar of supported meetings

If you wish to announce your meeting in this meeting in this calendar, you will gind more information at www.ursi.org URSI cannot held responsible for any errors contained in this list of meetings

September 2006

ISROSES - International Symposium on Recent Observations and Simulations of the Sun-Earth System
Varna, Bulgaria, 17-22 September 2006
cf. Announcement in the Radio Science Bulletin of March 2006, p. 53-54.
Contact : E-mail : isroses2006@abv.bg, Web : http://www.isroses.org/

Vertical Coupling in the Atmospheric/Ionospheric System
Varna, Bulgaria, 18-22 September 2006
Contact : Dr. Dora Pancheva, Centre for Space, Atmospheric & Oceanic Science, Dept. of Electronic and Electrical Engineering, University of Bath, Bath BA2 7AY, United Kingdom, Fax : +44 1225-386305, E-mail : eesdvp@bath.ac.uk, Web : http://www.iaga.geophys.bas.bg/

IVth International Workshop on Electromagnetic Wave Scattering
Gebze, Kocaeli, Turkey, 18-22 September 2006
Contact : E-mail : ews2006@gyte.edu.tr, Web : http://www.gyte.edu.tr/gytenet/Dosya/102/ews/2006/index.html

International conference on Ultrawideband
Waltham, MA, USA, 24-27 September 2006
Contact : Dr. A. F. Molisch, Mitsubishi Electric Research Labs, 201 Broadway, Cambridge, MA 02139, USA, Fax : +1 617 621 7550, E-mail : Andreas.Molisch@ieee.org , http://www.icuwb2006.org

Second VERSIM workshop 2006, ELF/VLF Radio Phenomena
Sodenkylä, Finland, 26-30 September 2006
Contact : Dr. Jyrki Manninen, Sodankylä Geophysical Observatory, Tähteläntie 62, FIN-99600 Sodankylä, FINLAND, Telephone: +358-16-619824, Fax: +358-16-619875, http://www.sgo.fi/Events/versim-2006/versim-2006.php

October 2006

ISAR – NCU - International School on Atmospheric Radar
Chung-li, Taiwan, 9-27 October 2006
cf. Announcement in the Radio Science Bulletin of September 2006, p. 49
Contact : E-mail : isar@jupiter.ss.ncu.edu.tw, cjpan@jupiter.ss.ncu.edu.tw, Web : http://www.ss.ncu.edu.tw/~ISAR

IRI Workshop 2006 - New Measurements for Improved IRI TEC Representation
Buenos Aires, Argentina, 16-20 October 2006
Contact : Marta Mosert, Av. Espana 1512 (sur), Capital, CP 5400, Ciudad de San Juan, Argentina, Fax +54 2644213653, mmosert@casleo.gov.ar , Web : http://www.casleo.gov.ar/WSIRI2006

November 2006

EuCAP 2006 - European Conference on Antennas and Propagation
Nice, France, 6-10 November 2006
Contact : EuCAP 2006 Secretariat, ESA Conference Bureau, Postbus 299, NL-2200 AG Noordwijk, The Netherlands, Tel. : +31 71 565 5005, Fax : +31 71 565 5658, E-mail : eucap2006@esa.int, Web : www.eucap2006.org and http://www.congrex.nl/06a08/

December 2006

International Workshop on Technical and Scientific Aspects of MST Radar
Gadanki/Tirupati, India, 11-15 December 2006
cf. Announcement in the Radio Science Bulletin of March 2006, p. 54-55.
Contact : Prof. D. Narayana Rao, Director, National Atmospheric Research Laboratory, Post Box 123, Tirupati-517 502, India, Fax : +91 8585 272018/272021, E-mail : mst11@narl.gov.in , Web : http://www.narl.gov.in/mst-11.html

APMC 2006 - 2006 Asia-Pacific Microwave Conference
Yokohama, Japan, 12-15 December 2006
cf. Announcement in the Radio Science Bulletin of September 2005 p. 44
Contact : Dr. Takashi Ohira, 2-2-2 Hikaridai, Keihanna Science City, Kyoto 619-0288, Japan, Fax : +81 774-95 15 08, E-mail : ohira@atr.jp , Web : http://www.apmc2006.org

ICMARS-2006 - 3rd International Conference on Microwaves, Antenna, Propagation and Remote Sensing
Jodhpur, India, 20 -22 December 2006
cf. Announcement in the Radio Science Bulletin of September 2006, p. 49-50.
Contact : Prof O.P.N. Calla, ICRS, "OM NIWAS" A-23 Shatri Nagar, Jodhpur, Rajasthan, 342003, India, Phone : 0291-2613123, Fax : 0291-2626166, E-mail : opncalla@yahoo.co.in, Web : http://www.radioscience.org, http://www.icrsju.org

March 2007

Telecom & JFMMA
Fes, Morocco, 14-16 March 2007
Contact in France : Pr. A. MAMOUNI , IEMN CNRS, Cité scientifique, Av. Poincaré, BP 60069, 59652 Villeneuve d'Ascq Cédex, France , Email: ahmed.mamouni@iemn.univ-lille1.fr , Tél.: +33 (0) 3 20 19 79 39 , Fax.: 33 (0) 3 20 19 78 80 ;

Contact in Morocco : Pr. M. EL BEKKALI et Pr. A. BENBASSOU , Ecole Supérieure de Technologie de Fès , Route D'Immouzer - BP: 2427 – 30000 Fès - MAROC , Tél.: +212 (0) 35 60 05 85/86 , Fax: + 212 (0) 35 60 05 88, E mail: , moulhime.el.bekkali@caramail.com , ali.ben bassou@caramail.com ,moulhime_el_bekkali@hotmail.com, Web : http://www.est-usmba.ac.ma/telecom2007/ .

April 2007

URBAN 2007 - Urban Remote Sensing Joint Event 2007
Paris, France, 11-13 April 2007
cf. Announcement in the Radio Science Bulletin of June 2006, p. 66.
Contact : Paolo Gamba, Dipartimento di Elettronica, Università di Pavia, Via Ferrata 1, 27100 Pavia, Italy, Fax +390 382-422583, e-mail : paolo.gamba@unipv.it , Web : http://tlc.unipv.it/urban-remote-sensing-2007/index.html

May 2007

12th Microcoll - Colloquium on Microwave Communications
Budapest, Hungary, 14-16 May 2007
Contact : Prof. L. Nagy, BUTE, Dept. of Broadband Communications, H-1111 Goldmann Gy. tér 3, Budapest, Hungary, fax +36 1-463 3289, E-mail : nagy@mht.bme.hu, Web : http://www.diamond-congress.hu/mow2007

June 2007

VIIth International Symposium on Electromagnetic Compatibility and Electromagnetic Ecology
St. Petersburg, Russia, 26-29 June 2007.
cf. Announcement in the Radio Science Bulletin of September 2006, p. 50.
Contact: Discone-Centre Ltd., St. Petersburg State Electrotechnical University "LETI", Tel: +7 812 234-48-40, Fax: +7 812 234-46-81, E-mail: discone@mail.wplus.net, Website: http://www.eltech.ru/emc.

August 2007

ISAP 2007 - International Symposium on Antennas and Propagation
Niigata, Japan, 20-24 August 2007
Contact : Yoshihiko Konishi (Publicity Chair), Mitsubishi Electric Corporation, 5-1-1 Ofuna, Kamakura, 247-8501 Japan, E-mail : isap-2007@mail.ieice.org, Web : http://www.isap07.org

September 2007

AP-RASC 2007 - Asia-Pacific Radio Science Conference
Perth, Western Australia, 17-20 September 2007
Contact : Dr. Phil Wilkinson, Deputy Director IPS Radio and Space Services, Department of Industry, Tourism and Resources, P O Box 1386, Haymarket, NSW 1240, AUSTRALIA, Tel : +61 2 9213 8003, Fax : +61 2 9213 8060, E-mail: phil@ips.gov.au, Web : http://www.ap-rasc07.org/

October 2007

Metamaterials 2007 - The First International Congress on Advanced Electromagnetic Materials for Microwaves and Optics
Rome, Italy, 22-26 October 2007
Contact : Dr. Said Zouhdi, Electrical Engineering, University Pierre et Marie Curie, Paris, France + Laboratoire de Genie Electrique de Paris LGEP-Supelec, Fax : + 33 1 69 41 83 18, E-mail : sz@ccr.jussieu.fr

December 2007

APMC 2007 - 2007 Asia-Pacific Microwave Conference
Bangkok, Thailand, 11-14 December 2007
cf. Announcement in the Radio Science Bulletin of September 2006, p. 51.

Contact : Dr. Chuwong Phongcharoenpanich, General Secretary of APMC 2007, King Mongkut's Institute of Technology Ladkrabang, Bangkok 10520, Thailand, E-mail:kpchuwon@kmitl.ac.th , Web : http://www.apmc2007.org/

July 2008

EUROEM 2008 - European Electromagnetics
Lausanne, Switzerland, 21-25 July 2008
Contact : EUROEM'08, EPFL-STI- LRE, Station 11, CH-1015 Lausanne, Switzerland, Tel : +41-21-693 26 20, Fax : +41-21-693 46 62, E-mail: information@euroem.org, Web : http://www.euroem.org

August 2008

URSI GA08 - XXIXth URSI General Assembly
Chicago, IL, USA, 9-16 August 2008
Contact : URSI Secretariat, c/o INTEC, Ghent University, Sint-Pietersnieuwstraat 41, B-9000 Ghent, Belgium, Tel. : +32 9 264 3320, Fax : +32 9 264 4288, E-mail : info@ursi.org

News from the URSI Community

NEWS FROM A MEMBER COMMITTEE

BULGARIA

Report on the Bulgarian URSI School and Workshop

Kiten, Bulgaria, 1 - 9 July 2006

A school and workshop on waves and turbulence phenomena in space plasmas, organized by the Bulgarian URSI Committee (Commission H, Waves in Plasmas), was held in the Guest House of the Sofia University at Kiten, Bulgaria, from July 1 to 9, 2006. The number of participants was 36 from 10 countries, as follows: Australia (1), France (1), Germany (1), Italy (2), Japan (1), Rumania (2), Russia (6), UK (4), USA (1), and Bulgaria (17). There were also six accompanying persons; altogether, there were 42 individuals associated with the forum. There were only four students, six PhD students, and five Young Scientists.

The school and workshop were opened in the afternoon of July 1, 2006. After a short opening ceremony, the first talk, entitled "The Solar Zoo," was given by Robert Erdélyi (UK). In the evening, a welcome party got the participants of the event together.

Wave phenomena in the solar atmosphere (linear, nonlinear, shock waves, wave mechanisms of particle accelerations) were exposed in spectacular presentations by Robert Erdélyi (second talk), Yura Taroyan (UK), and Gottfried Mann (Germany). A typical academic talk on the stability of circularly polarized Alfvén waves was given by Michael Ruderman (UK). A logical continuation of that series of lectures was the talk by Ilia Roussev (USA) on the coronal mass ejection and associated solar energetic particle events (interplanetary turbulence and self-generated Alvfén-wave turbulence near shockwave fronts). Close to Roussev's talk was the lecture by Young Scientist Yasuko Honda, entitled "Effects of Mirror Reflection Versus Diffusion Anisotropy on Particle Acceleration in Oblique Shocks." The talk by Massimo Vellante (Italy) on the ULF field-line resonances in the Earth's magnetosphere pointed out how important are the solar wind-magnetosphere interactions.

One of the most discussed phenomena in magnetized plasmas – the magnetic reconnection – was explained in an excellent way by Gunnar Hornig (UK). His two lectures on two- and three-dimensional models of the magnetic reconnection illuminated the latest results in understanding the complex nature of that phenomenon. Another cycle of four lectures, now on stellar plasmas, was delivered by Mark Wardle (Australia). His two lectures were on the problem of missing viscosity (Shakura-Sunyaev phenomenology) and on another debated issue, notably the accretion disks and angular-momentum transport mechanisms (including jets). A natural continuation of Warlde's talks were the lecture by Dmitry Bisikalo (Russia) on waves in accretion disks in binary stars (results of three-dimensional numerical simulations), as well as the presentation by the Young Scientist Pavel Kaygorodov (Russia), on a possible model of Be stars' X-luminosity. The history of the accretion theory of disks was exposed by one of its creators, namely Nikolay Shakura (Russia). The last two lectures by Mark Wardle considered the dynamics

of astrophysical weakly-ionized plasmas and its applications to molecular clouds, star formation and protostellar/ protoplanetary disks. The magneto-rotational supernovae and instability and their numerical simulations were demonstrated by Sergey Moiseenko (Russia).

One of the most mysterious phenomena in plasma physics – the turbulence – was the subject of a series of talks. Alexander Dolgov (Italy) discussed the magnetohydrodynamical turbulence in the early universe and its links with the primordial magnetic fields. The nonlinear effects in charged-particle transport in turbulent magnetic fields were the subject of Madalina Vlad's (Rumania) talk, while the field theoretical methods in the theory of turbulence relaxation were explained in great detail by Florin Spineanu (Romania). A real surprise for the school's participants were the talks by the PhD students Aglika Savchenko (Bulgaria) and Roumyana Mitseva (Bulgaria) on sprites, blue jets, and thunderstorms: two very emotional and very-well-illustrated presentations. One of the most elegant talks (a real joy for the audience) was that by Thierry Dudok de Wit (France) on analysis techniques for characterizing nonlinearity in space plasmas (wavelet analysis versus fast Fourier transforms).

A peculiarity of the School and Workshop in Kiten was the circumstance that graduate and PhD students had the opportunity to give their first talks in a scientific forum. An example of this was the presentation by Yana Maneva (Bulgaria), entitled "Kinetic Equation for the Spectral Density of Alvfén Waves in a Shear Flow: Effective Heating Mechanism of Accreting Turbulent Plasma." The talk by the PhD student Vyacheslav Zhouravlev (Russia), on the instability of laminar compressible axial-symmetric flows, and that of the Young Scientist Yavor Shopov (Bulgaria), on plasma interactions in the far solar corona (last observational data) were received well by the audience.

Although the weather was not too friendly to us during all of the days of the conference (there were rain downpours and gigantic thunderstorms), the excursions to the beautiful city of Sozopol and the Popotamo river (with its famous white water lilies), as well as Kiten's beach, offered some pleasant hours for all the participants.

At a meeting of the International Advisory Committee, it was concluded that the School and Workshop in Kiten was very successful. It should trigger summer schools in Bulgaria on similar items, however with much larger student audiences. All lecturers expressed their willingness to come again to the Black Sea coast, and to participate in a school/ workshop on solar and space plasma physics. Another important conclusion was to put all presentations on a disk or on an Internet site. Later on, they will be published in electronic (Web) format, in order to be accessible to everyone who is interested in various phenomena in solar and space plasmas.

Finally, all organizers of the Bulgarian-URSI School and Workshop in Kiten 2006 would like to sincerely tank the URSI Secretariat (especially Commission H, Waves in Plasmas) for the financial support of 1000 Euro. That money was sufficient to cover the accommodation and meals of the five foreign lecturers: Gunnar Hornig, Mark Wardle, Massimo Vellante, Sergey Moiseenko, and Yasuko Honda. Our thanks also go to the St. Cyril and St. Methodius Foundation (Sofia) for the financial support of the graduate student Lyuba Boundova and the PhD student Borislav Petkov. We are indebted to the Bulgarian Academy of Sciences (in particular, to Academician Nikola Sabotinov, President of the National URSI Committee, and Prof. Dr. Peter Getsov, Director of the Space Research Institute), as well as the Rector of the Sofia University, Prof. Dr. Boyan Biolchev, for their encouragement and financial support.

Ivan Zhelyazkov
Member of Commission H
Faculty of Physics, Sofia University
5 James Boucher Blvd.
BG-1164 Sofia, Bulgaria
Tel: +359 2 816 1641
E-mail: izh@phys.uni-sofia.bg

NEWS FROM A MEMBER COMMITTEE

Microwave Radiometry of Vegetation Canopies

By Alexander A. Chukhlantsev, Springer, ISBN 1-4020-4681-2

Research into microwave radiation from the Earth's surface in the presence of vegetation canopies, as well as the development of algorithms for retrieval of soil and vegetation parameters from microwave radiometric measurements, have been actively conducted for the last thirty years by many scientific groups and organizations all over the world. The capability of the microwave radiometric method to determine soil moisture and vegetation biometric indices was revealed a quarter of a century ago by the author and many of his colleagues. In spite of the fact that the fundamentals and the basic physics of the microwave radiometry of soils and vegetation covers have been well developed, interest in the problem has not decreased but, indeed, has grown significantly in the last decade. This phenomenon has several reasons. The first one is the importance of these objects themselves in the remote

ecological monitoring of land surface. In fact, soil moisture and vegetation covers play a key role in the hydrological cycle, and in water and energy transfer on the border of land surfaces and the atmosphere through evaporation and transpiration. The second reason is increased technical potentialities of microwave radiometric devices by being installed on spacecraft. Accomplishment of large international projects that include global monitoring of the hydrological state of land surface (EOS Aqua, SMOS, and others) shows that microwave radiometry of soil and vegetation more and more has become an instrument of practical application and operational use. In this respect, a systematic account of questions concerning the microwave radiometry of the Earth's surface in the presence of vegetation canopies seems to be useful.

The presence of a vegetation cover on the Earth's surface affects the microwave emission from the surface in two ways. First of all, the vegetation cover screens the microwave emission from the soil surface. Secondly, the microwave emission from the vegetation layer itself is added to the emission from the soil. The vegetation effect depends on the vegetation type and vegetation biometric features, as well as on the measuring configuration (frequency, polarization, observation angle). Assessment of the vegetation impact on the microwave radiometry of surface soil moisture, and examination of feasibilities of the retrieval of biometric parameters from microwave radiometric measurements, are the main objectives of the book.

The book contains nine chapters. In Chapter 1, introductory knowledge on the basics of microwave radiometry is given. Physical and microwave dielectric properties of vegetation and soil are discussed in Chapter 2. In Chapter 3, theoretical models and experimental data on the microwave emission from bare soils are presented. The theory of microwave propagation in vegetation canopies is developed in Chapter 4. Chapter 5 presents a review of experimental research on microwave propagation in vegetation canopies. The theory of microwave emission from vegetation canopies is developed in Chapter 6. An overview of experimental research on microwave emission from vegetation canopies is presented in Chapter 7. Vegetation effects in microwave remote sensing of terrains are considered in Chapter 8. In Chapter 9, the possibility of the assimilation of microwave radiometric remote sensing data into global carbon-cycle models is taken up.

About the Author

Dr. Alexander A. Chukhlantsev is Senior Scientist at the Institute of Radioengineering and Electronics of the Russian Academy of Sciences. He is Professor of General Physics at the Moscow State University of Forest, Moscow. Dr. Chukhlantsev is the official member of URSI Commission F from Russia.

Wireless Networks

The journal of mobile communication, computation and information

Editor-in-Chief:
Imrich Chlamtac
Distinguished Chair in Telecommunications
Professor of Electrical Engineering
The University of Texas at Dallas
P.O. Box 830688, MS EC33
Richardson, TX 75083-0688
email: chlamtac@acm.org

Wireless Networks is a joint publication of the ACM and Baltzer Science Publishers. Officially sponsored by URSI

Aims & Scope:
The wireless communication revolution is bringing fundamental changes to data networking, telecommunication, and is making integrated networks a reality. By freeing the user from the cord, personal communications networks, wireless LAN's, mobile radio networks and cellular systems, harbor the promise of fully distributed mobile computing and communications, any time, anywhere. Numerous wireless services are also maturing and are poised to change the way and scope of communication. WINET focuses on the networking and user aspects of this field. It provides a single common and global forum for archival value contributions documenting these fast growing areas of interest. The journal publishes refereed articles dealing with research, experience and management issues of wireless networks. Its aim is to allow the reader to benefit from experience, problems and solutions described. Regularly addressed issues include: Network architectures for Personal Communications Systems, wireless LAN's, radio , tactical and other wireless networks, design and analysis of protocols, network management and network performance, network services and service integration, nomadic computing, internetworking with cable and other wireless networks, standardization and regulatory issues, specific system descriptions, applications and user interface, and enabling technologies for wireless networks.

For a complete overview on what has been and will be published in Telecommunication Systems please consult our homepage:

BALTZER SCIENCE PUBLISHERSHOMEPAGE
http://www.baltzer.nl/winet

Special Discount for URSI Radioscientists

Euro 62 / US$ 65
(including mailing and handling)

Wireless Networks ISSN 1022-0038
Contact: Mrs. Inge Heleu
Fax +32 9 264 42 88 E-mail ursi@intec.rug.ac.be
Non members/Institutions: contact Baltzer Science Publishers

BALTZER SCIENCE PUBLISHERS
P.O.Box 221, 1400 AE Bussum, The Netherlands
Tel: +31 35 6954250 Fax: +31 35 6954 258 E-mail: publish@baltzer.nl

The Journal of Atmospheric and Solar-Terrestrial Physics

SPECIAL OFFER TO URSI RADIOSCIENTISTS

AIMS AND SCOPE

The *Journal of Atmospheric and Terrestrial Physics* (JASTP) first appeared in print in 1951, at the very start of what is termed the "Space Age". The first papers grappled with such novel subjects as the Earth's ionosphere and photographic studies of the aurora. Since that early, seminal work, the Journal has continuously evolved and expanded its scope in concert with - and in support of - the exciting evolution of a dynamic, rapidly growing field of scientific endeavour: the Earth and Space Sciences. At its Golden Anniversary, the now re-named *Journal of Atmospheric and Solar-Terrestrial Physics* (JASTP) continues its development as the premier international journal dedicated to the physics of the Earth's atmospheric and space environment, especially the highly varied and highly variable physical phenomena that occur in this natural laboratory and the processes that couple them. The *Journal of Atmospheric and Solar-Terrestrial Physics* is an international journal concerned with the inter-disciplinary science of the Sun-Earth connection, defined very broadly. The journal referees and publishes original research papers, using rigorous standards of review, and focusing on the following: The results of experiments and their interpretations, and results of theoretical or modelling studies; Papers dealing with remote sensing carried out from the ground or space and with in situ studies made from rockets or from satellites orbiting the Earth; and, Plans for future research, often carried out within programs of international scope. The Journal also encourages papers involving: large scale collaborations, especially those with an international perspective; rapid communications; papers dealing with novel techniques or methodologies; commissioned review papers on topical subjects; and, special issues arising from chosen scientific symposia or workshops. The journal covers the physical processes operating in the troposphere, stratosphere, mesosphere, thermosphere, ionosphere, magnetosphere, the Sun, interplanetary medium, and heliosphere. Phenomena occurring in other "spheres", solar influences on climate, and supporting laboratory measurements are also considered. The journal deals especially with the coupling between the different regions. Solar flares, coronal mass ejections, and other energetic events on the Sun create interesting and important perturbations in the near-Earth space environment. The physics of this subject, now termed "space weather", is central to the Journal of Atmospheric and Solar-Terrestrial Physics and the journal welcomes papers that lead in the direction of a predictive understanding of the coupled system. Regarding the upper atmosphere, the subjects of aeronomy, geomagnetism and geoelectricity, auroral phenomena, radio wave propagation, and plasma instabilities, are examples within the broad field of solar-terrestrial physics which emphasise the energy exchange between the solar wind, the magnetospheric and ionosphericplasmas, and the neutral gas. In the lower atmosphere, topics covered range from mesoscale to global scale dynamics, to atmospheric electricity, lightning and its effects, and to anthropogenic changes. Helpful, novel schematic diagrams are encouraged. Short animations and ancillary data sets can also be accommodated. Prospective authors should review the *Instructions to Authors* at the back of each issue.

Complimentary Information about this journal:
http://www.elsevier.com/locate/JASTP?
http://earth.elsevier.com/geophysics

Audience:
Atmospheric physicists, geophysicists and astrophysicists.

Abstracted/indexed in:
CAM SCI Abstr
Curr Cont SCISEARCH Data
Curr Cont Sci Cit Ind
Curr Cont/Phys Chem & Sci
INSPEC Data
Meteoro & Geoastrophys Abstr
Res Alert

Editor-in-Chief:
T.L. Killeen, National Centre for Atmospheric Research, Boulder, Colorado, 80307 USA

Editorial Office:
P.O. Box 1930, 1000 BX Amsterdam, The Netherlands

Special Rate for URSI Radioscientists 2003:
Euro 149.00 (US$ 149.00)
Subscription Information
2002: Volume 65 (18 issues)
Subscription price: Euro 2659 (US$ 2975)
ISSN: 1364-6826

CONTENTS DIRECT:
The table of contents for this journal is now available pre-publication, via e-mail, as part of the free ContentsDirect service from Elsevier Science. Please send an e-mail message to cdhelp@elsevier.co.uk for further information about this service.

For ordering information please contact Elsevier Regional Sales Offices:

Asia & Australasia/ e-mail: asiainfo@elsevier.com
Europe, Middle East & Africa: e-mail: nlinfo-f@elsevier.com
Japan: Email: info@elsevier.co.jp
Latin America : e-mail: rsola.info@elsevier.com.br
United States & Canada : e-mail: usinfo-f@elsevier.com

Information for authors

Content

The *Radio Science Bulletin* is published four times per year by the Radio Science Press on behalf of URSI, the International Union of Radio Science. The content of the *Bulletin* falls into three categories: peer-reviewed scientific papers, correspondence items (short technical notes, letters to the editor, reports on meetings, and reviews), and general and administrative information issued by the URSI Secretariat. Scientific papers may be invited (such as papers in the *Reviews of Radio Science* series, from the Commissions of URSI) or contributed. Papers may include original contributions, but should preferably also be of a sufficiently tutorial or review nature to be of interest to a wide range of radio scientists. The *Radio Science Bulletin* is indexed and abstracted by INSPEC.

Scientific papers are subjected to peer review. The content should be original and should not duplicate information or material that has been previously published (if use is made of previously published material, this must be identified to the Editor at the time of submission). Submission of a manuscript constitutes an implicit statement by the author(s) that it has not been submitted, accepted for publication, published, or copyrighted elsewhere, unless stated differently by the author(s) at time of submission. Accepted material will not be returned unless requested by the author(s) at time of submission.

Submissions

Material submitted for publication in the scientific section of the *Bulletin* should be addressed to the Editor, whereas administrative material is handled directly with the Secretariat. Submission in electronic format according to the instructions below is preferred. There are typically no page charges for contributions following the guidelines. No free reprints are provided.

Style and Format

There are no set limits on the length of papers, but they typically range from three to 15 published pages including figures. The official languages of URSI are French and English: contributions in either language are acceptable. No specific style for the manuscript is required as the final layout of the material is done by the URSI Secretariat. Manuscripts should generally be prepared in one column for printing on one side of the paper, with as little use of automatic formatting features of word processors as possible. A complete style guide for the *Reviews of Radio Science* can be downloaded from http://www.ips.gov.au/IPSHosted/NCRS/reviews/. The style instructions in this can be followed for all other *Bulletin* contributions, as well. The name, affiliation, address, telephone and fax numbers, and e-mail address for all authors must be included with all submissions.

All papers accepted for publication are subject to editing to provide uniformity of style and clarity of language. The publication schedule does not usually permit providing galleys to the author.

Figure captions should be on a separate page in proper style; see the above guide or any issue for examples. All lettering on figures must be of sufficient size to be at least 9 pt in size after reduction to column width. Each illustration should be identified on the back or at the bottom of the sheet with the figure number and name of author(s). If possible, the figures should also be provided in electronic format. TIF is preferred, although other formats are possible as well: please contact the Editor. Electronic versions of figures *must* be of sufficient resolution to permit good quality in print. As a rough guideline, when sized to column width, line art should have a minimum resolution of 300 dpi; color photographs should have a minimum resolution of 150 dpi with a color depth of 24 bits. 72 dpi images intended for the Web are generally *not* acceptable. Contact the Editor for further information.

Electronic Submission

A version of Microsoft *Word* is the preferred format for submissions. Submissions in versions of T_EX can be accepted in some circumstances: please contact the Editor before submitting. *A paper copy of all electronic submissions must be mailed to the Editor, including originals of all figures.* Please do *not* include figures in the same file as the text of a contribution. Electronic files can be send to the Editor in three ways: (1) By sending a floppy diskette or CD-R; (2) By attachment to an e-mail message to the Editor (the maximum size for attachments *after* MIME encoding is about 7 MB); (3) By e-mailing the Editor instructions for downloading the material from an ftp site.

Review Process

The review process usually requires about three months. Authors may be asked to modify the manuscript if it is not accepted in its original form. The elapsed time between receipt of a manuscript and publication is usually less than twelve months.

Copyright

Submission of a contribution to the *Radio Science Bulletin* will be interpreted as assignment and release of copyright and any and all other rights to the Radio Science Press, acting as agent and trustee for URSI. Submission for publication implicitly indicates the author(s) agreement with such assignment, and certification that publication will not violate any other copyrights or other rights associated with the submitted material.

APPLICATION FOR AN URSI RADIOSCIENTIST

I have not attended the last URSI General Assembly, and I wish to remain/become an URSI Radioscientist in the 2006-2008 triennium. Subscription to *The Radio Science Bulletin* is included in the fee.
(please type or print in BLOCK LETTERS)

Name: Prof./Dr./Mr./Mrs./Ms. _____
Family Name *First Name* *Middle Initials*

Present job title: _____

Years of professional experience: _____

Professional affiliation: _____

I request that all information, including the bulletin, be sent to my ☐ home ☐ business address, i.e.:

Company name: _____

Department: _____

Street address: _____

City and postal / zip code: _____

Province / State: _____ Country: _____

Phone: _____ ext: _____ Fax: _____

E-mail: _____

Areas of interest (please tick)

☐ A Electromagnetic Metrology
☐ B Fields and Waves
☐ C Signals and Systems
☐ D Electronics and Photonics
☐ E Electromagnetic Noise & Interference
☐ F Wave Propagation & Remote Sensing
☐ G Ionospheric Radio and Propagation
☐ H Waves in Plasmas
☐ J Radio Astronomy
☐ K Electromagnetics in Biology & Medicine

The fee is 50 Euro.
(The URSI Board of Officers will consider waiving of the fee if the case is made to them in writing)

Method of payment: VISA / MASTERCARD (we do not accept cheques)

Credit Card No ☐☐☐☐ ☐☐☐☐ ☐☐☐☐ ☐☐☐☐ Exp. date: _____

Date: _____ Signed _____

Please return this signed form to:

The URSI Secretariat
c /o Ghent University / INTEC
Sint-Pietersnieuwstraat 41
B-9000 GENT, BELGIUM
fax (32) 9-264.42.88